

QUIVERS WITH ADDITIVE LABELINGS: CLASSIFICATION AND ALGEBRAIC ENTROPY

PAVEL GALASHIN AND PAVLO PYLYAVSKYY

ABSTRACT. We show that Zamolodchikov dynamics of a recurrent quiver has zero algebraic entropy only if the quiver has a weakly subadditive labeling, and conjecture the converse. By assigning a pair of generalized Cartan matrices of affine type to each quiver with an additive labeling, we completely classify such quivers, obtaining 40 infinite families and 13 exceptional quivers. This completes the program of classifying Zamolodchikov periodic and integrable quivers.

CONTENTS

Introduction	1
1. Main results	3
2. Preliminaries	6
3. Algebraic entropy	17
4. The general structure of ADE bigraphs	19
5. Many affine \boxtimes affine ADE bigraphs	26
6. The classification of affine \boxtimes affine ADE bigraphs	40
7. Proof of the classification	51
8. Twists	65
9. Conjectures	71
References	75

INTRODUCTION

Given a *bipartite quiver* Q which is just a directed bipartite graph without directed cycles of length 1 and 2, one can define a certain

Date: May 11, 2017.

2010 Mathematics Subject Classification. Primary: 13F60, Secondary: 37K10, 05E99.

Key words and phrases. Cluster algebras, Zamolodchikov periodicity, T-system, Arnold-Liouville integrability, Twisted Dynkin diagrams.

P. P. was partially supported by NSF grants DMS-1148634, DMS-1351590, and Sloan Fellowship.

discrete dynamical system called the T -system associated with Q . It assigns a multivariate rational function $T_v(t)$ to each vertex v of Q and each integer t and satisfies the following recurrence relation

$$(0.1) \quad T_v(t+1)T_v(t-1) = \prod_{u \rightarrow v} T_u(t) + \prod_{v \rightarrow w} T_w(t).$$

In certain cases, this relation specializes to various well studied objects such as the *octahedron recurrence* of Speyer [37].

When a bipartite quiver Q satisfies a certain simple local condition (we call such quivers *recurrent*), the T -system dynamics can be viewed as a special case of a *cluster algebra*, see [7]. Partially because of this connection to cluster algebras, T -systems have received much attention in the past two decades. One particular popular direction of research in this area is the so called *Zamolodchikov periodicity*. It was conjectured by Zamolodchikov [43] that if Q is an orientation of an ADE Dynkin diagram of finite type then the T -system is periodic. This conjecture was later generalized by Kuniba-Nakanishi [25] and Ravanini-Valleriani-Tateo [35] to the case when Q is a *tensor product* of two finite ADE Dynkin diagrams. The conjecture stayed open for around twenty years with various special cases being completed in [8, 16, 25, 26, 35, 40, 42]. It was finally resolved for all pairs of finite ADE Dynkin diagrams by Keller [22].

For the connections of T -systems with thermodynamic Bethe ansatz [43] as well as their other appearances in physics and representation theory, see [10, 23, 24, 26, 31, 32, 36], and see [27] for a survey. Of special note is the work of Hernandez [19], where he studied the occurrence of T -systems in representation theory for simply-laced quivers beyond Dynkin quivers.

This is the third and final paper in the series [12, 13] of works that classify bipartite recurrent quivers for which the T -system satisfies a certain algebraic property. In [12], we have shown that the T -system associated to a bipartite recurrent quiver Q is periodic if and only if Q admits a *strictly subadditive labeling*. Such quivers turn out to exactly correspond to commuting pairs of Cartan matrices which have been classified earlier by Stembridge [39]. In particular, tensor products of finite ADE Dynkin diagrams belong to this family, so the result of [12] is a generalization of the result of [22].

Next, we showed in [13] that the values of the T -system satisfy a linear recurrence only if Q admits a *subadditive labeling*. We gave an analogous classification for quivers admitting a subadditive labeling. In particular, it includes tensor products of an affine ADE Dynkin diagram with a finite ADE Dynkin diagram. This classification allowed

an extensive computational verification of the conjecture that the converse is also true, i.e., for every bipartite recurrent quiver Q admitting a subadditive labeling, the associated T -system satisfies a linear recurrence. We proved this claim for the case when Q has type $\hat{A} \otimes A$ using a combinatorial formula due to Speyer [37] for the octahedron recurrence.

In this text, we classify (Section 6) bipartite recurrent quivers admitting a *weakly subadditive labeling*. We use *algebraic entropy* as a motivating property of the T -system that conjecturally characterizes such quivers. Having zero algebraic entropy is a frequently used criterion for checking integrability of a discrete dynamical system. It was introduced in [6] and further developed in [2, 20]. Roughly speaking, the fact that the algebraic entropy of a discrete dynamical system is nonzero means that its values grow *doubly exponentially*, i.e., as $\exp(\exp(ct))$ for some positive constant c . We show in Section 3 that for any bipartite recurrent quiver that does not admit a weakly subadditive labeling, the T -system has nonzero algebraic entropy. Using our classification again we get rich computational evidence suggesting that for the remaining bipartite recurrent quivers (that is, the ones from our classification), the values of the T -system grow *quadratic exponentially*, i.e. as $\exp(ct^2)$. Thus there seems to be a big gap in the rate of growth that separates the T -systems associated to the quivers in our classification from all other T -systems.

For two special cases (quivers of type $\hat{A} \otimes \hat{A}$ and *twists* $\hat{\Lambda} \times \hat{\Lambda}$ of affine ADE Dynkin diagrams) we prove in Sections 3.1 and 8 respectively that the growth is quadratic exponential. The former again is a consequence of Speyer's formula for the octahedron recurrence. We finish the text (Section 9) by giving some refinements of the rate of growth conjecture. In particular, we conjecture that the Y -systems associated to the quivers from our classification are *Arnold-Liouville integrable*.

1. MAIN RESULTS

Let us start by introducing some notions necessary to formulate our results. As we have mentioned, a *quiver* Q is a directed graph without loops and pairs of arrows forming a directed 2-cycle.

Given a quiver Q with vertex set $\text{Vert}(Q)$, a vertex $v \in \text{Vert}(Q)$, and a family $T_* = (T_u)_{u \in \text{Vert}(Q)}$ of rational functions in some set \mathbf{x} of variables, one can define the *mutation* operation μ_v that produces a new quiver $\mu_v(Q)$ with the same set $\text{Vert}(Q)$ of vertices and a new family $\mu_v(T_*) = (T'_u)_{u \in \text{Vert}(Q)}$ according to a certain set of combinatorial

rules. The definition of the quiver $\mu_v(Q)$ is given in Definition 2.14 and $\mu_v(T_*)$ is defined as follows. For $u \neq v$, we set $T'_u := T_u$, and for $u = v$ we put

$$(1.1) \quad T'_v = \frac{\prod_{u \rightarrow v} T_u + \prod_{v \rightarrow w} T_w}{T_v}.$$

Here the product is taken over all arrows in Q . It follows from the definition that the operations μ_v and μ_w commute when there are no arrows between v and w in Q .

We say that a quiver Q is *bipartite* if there exists a map $\epsilon : \text{Vert}(Q) \rightarrow \{0, 1\}$, $v \mapsto \epsilon_v$ called a *bipartition* such that for every arrow $u \rightarrow v$ of Q we have $\epsilon_u \neq \epsilon_v$. It follows that for a bipartite quiver, the operations

$$(1.2) \quad \mu_0 = \prod_{u: \epsilon_u=0} \mu_u; \quad \mu_1 = \prod_{v: \epsilon_v=1} \mu_v$$

are well defined since the results of products are independent of the order. We are now ready to introduce a crucial notion of a *recurrent* quiver.

Definition 1.1. We say that a bipartite quiver Q is *recurrent* if $\mu_0(Q) = \mu_1(Q) = Q^{\text{op}}$ where Q^{op} is the quiver obtained from Q by reversing all of its arrows.

We give an alternative simpler definition for bipartite recurrent quivers in Corollary 2.15.

Let us now define the T -system. The main part of the definition will be equation (0.1). Note that for each of the terms $T_v(t+1), T_v(t-1), T_u(t), T_w(t)$ involved in (0.1), the numbers

$$\epsilon_v + t + 1, \epsilon_v + t - 1, \epsilon_u + t, \epsilon_w + t$$

all have the same parity. Thus it makes sense to restrict the values of the T -system to only pairs (v, t) such that $t \equiv \epsilon_v \pmod{2}$.

Definition 1.2. Given a bipartite recurrent quiver Q with a bipartition ϵ , the T -system associated with Q is a family $T_v(t)$ of rational functions in variables $\mathbf{x} = \{x_v\}_{v \in \text{Vert}(Q)}$ defined for any $v \in \text{Vert}(Q)$ and any $t \in \mathbb{Z}$ satisfying $t \equiv \epsilon_v \pmod{2}$. For any $v \in \text{Vert}(Q)$ and $t \not\equiv \epsilon_v \pmod{2}$, the values of the T -system are required to satisfy (0.1). Finally, for each $v \in \text{Vert}(Q)$, we impose an initial condition

$$(1.3) \quad T_v(\epsilon_v) = x_v.$$

One easily observes that (1.3) and (0.1) determine $T_v(t)$ uniquely for any $t \equiv \epsilon_v \pmod{2}$.

Since the T -system is defined for only bipartite recurrent quivers, it can be viewed as a composition of mutations $\mu_0\mu_1$, see (1.1) and (1.2).

As a consequence, it follows from the *Laurent phenomenon* property of cluster algebras [7] that for any $t \equiv \epsilon_v \pmod{2}$, the value $T_v(t)$ is actually a *Laurent polynomial* in \mathbf{x} : $T_v(t) \in \mathbb{Z}[\mathbf{x}^{\pm 1}]$.

For $v, u \in \text{Vert}(Q)$ and $t \equiv \epsilon_v \pmod{2}$, define $\deg_{\max}(x_u; T_v(t))$ to be the maximal degree of the variable x_u in the Laurent polynomial $T_v(t)$.

Definition 1.3. We say that Q has *algebraic entropy zero* if for any two vertices $u, v \in \text{Vert}(Q)$ we have

$$(1.4) \quad \lim_{t \rightarrow \infty} \frac{\log(\deg_{\max}(x_u, T_v(\epsilon_v + 2t)))}{t} = 0.$$

Before we state our main results, let us give one more definition.

Definition 1.4. Given a quiver Q , we say that a map $\lambda : \text{Vert}(Q) \rightarrow \mathbb{R}_{>0}$ is a *weakly subadditive labeling* if for any vertex $v \in \text{Vert}(Q)$, we have

$$(1.5) \quad 2\lambda(v) \geq \max \left(\sum_{u \rightarrow v} \lambda(u), \sum_{v \rightarrow w} \lambda(w) \right).$$

This is a generalization of Vinberg's *additive functions* [41]. We recall the analogous definitions of *strictly subadditive* and *subadditive* labelings in Definition 2.19.

Theorem 1.5. *Suppose that Q is a bipartite recurrent quiver. If Q does not admit a weakly subadditive labeling then Q does not have zero algebraic entropy.*

Our second main result is the classification (Theorem 6.1) of bipartite recurrent quivers that admit weakly subadditive labelings.

By Theorem 1.5, every quiver Q that has algebraic entropy zero admits a weakly subadditive labeling and therefore is necessarily one of the quivers in our classification. According to our computer experiments, we give a precise conjecture describing the asymptotics of the T -system.

Definition 1.6. Let $f(0), f(1), \dots$ be a sequence of positive real numbers. We say that f

- (1) is *bounded* if there exists a constant M such that $f(t) < M$ for all $t \geq 0$;
- (2) *grows exponentially* if there exists a positive limit of

$$\frac{\log(f(t))}{t};$$

(3) *grows quadratic exponentially* if there exists a positive limit of

$$\frac{\log(f(t))}{t^2};$$

(4) *grows doubly exponentially* if there exists a positive limit of

$$\frac{\log \log(f(t))}{t}.$$

Conjecture 1.7. Let Q be a bipartite recurrent quiver. Substitute some positive real numbers for each variable in \mathbf{x} . Let $f(t) = T_v(\epsilon_v + 2t), t \geq 0$ be the sequence of values of the T -system at vertex v that we get after such a substitution.

- (1) If Q admits a strictly subadditive labeling then f is bounded (and in fact is periodic);
- (2) otherwise, if Q admits a subadditive labeling then f grows exponentially (and satisfies a linear recurrence);
- (3) otherwise, if Q admits a weakly subadditive labeling then f grows quadratic exponentially;
- (4) otherwise f grows doubly exponentially.

Some parts of this conjecture are already proven. For example, we proved part (1) in [12]. A weaker version of part (2) was shown in [13]. In this paper, we prove part (4) and a weaker version of part (3). When all components of the bigraph associated with Q (see Definition 2.3) are of type A or \hat{A} , we prove all parts of Conjecture 1.7 in full generality. We do the same when Q is a *twist* (see Definition 5.1) of a finite or affine ADE Dynkin diagram.

Remark 1.8. Discrete dynamical systems exhibiting only bounded, linear, quadratic, or exponential growth of the degrees appear in surprisingly many diverse contexts. One example is the analogous result for cluster mutation-periodic quivers with period 1, see [9, Theorem 3.12]. Other instances include [4, 11]. We thank Andrew Hone for bringing these references to our attention.

2. PRELIMINARIES

2.1. Bigraphs. We follow very closely the exposition in [13]. We start by briefly recalling the correspondence between bipartite quivers and *bipartite bigraphs* introduced by Stembridge [39].

Definition 2.1. A *bigraph* is a pair $G = (\Gamma, \Delta)$ of simple undirected graphs on the same vertex set that do not share any edges. A bigraph is called *bipartite* if there is a map $\epsilon : V \rightarrow \{0, 1\}$ such that for every edge (u, v) of Γ or Δ we have $\epsilon_u \neq \epsilon_v$.

The graphs Γ and Δ are allowed to have multiple edges but no loops. Throughout, we assume all bigraphs to be bipartite.

Since our main result is a classification of certain bigraphs, we write down the obvious definition of an isomorphism between two such objects.

Definition 2.2. Two bigraphs $G = (\Gamma, \Delta)$ and $G' = (\Gamma', \Delta')$ are called *isomorphic* if there is a map $\phi : \text{Vert}(G) \rightarrow \text{Vert}(G')$ such that for any $u, v \in \text{Vert}(G)$ we have

- $(u, v) \in \Gamma \Leftrightarrow (\phi(u), \phi(v)) \in \Gamma'$, and
- $(u, v) \in \Delta \Leftrightarrow (\phi(u), \phi(v)) \in \Delta'$.

There is a simple correspondence between bipartite quivers and bipartite bigraphs that we now explain.

Definition 2.3. Given a bipartite quiver Q with bipartition $\epsilon : \text{Vert}(Q) \rightarrow \{0, 1\}$, define the bigraph $G(Q) = (\Gamma(Q), \Delta(Q))$ with the same vertex set as follows:

- For every directed edge $u \rightarrow v$ of Q with $\epsilon_u = 0, \epsilon_v = 1$, $\Gamma(Q)$ contains an undirected edge (u, v) .
- For every directed edge $u \rightarrow v$ of Q with $\epsilon_u = 1, \epsilon_v = 0$, $\Delta(Q)$ contains an undirected edge (u, v) .

Thus every arrow of Q corresponds to precisely one edge of $G(Q)$. Note also that this is a bijection: given a bipartite bigraph G with a bipartition ϵ , one can easily reconstruct the bipartite quiver $Q = Q(G)$ such that $G = G(Q)$.

We represent a bigraph $G = (\Gamma, \Delta)$ as a simple graph with the edges of Γ colored *red* and the edges of Δ colored *blue*.

Let us recall the definition of a *tensor product* of two bipartite graphs:

Definition 2.4. Let S and T be two bipartite undirected graphs. Then their *tensor product* $S \otimes T$ is a bipartite bigraph $G = (\Gamma, \Delta)$ with vertex set $\text{Vert}(S) \times \text{Vert}(T)$ and the following edge sets:

- for each edge $\{u, u'\} \in S$ and each vertex $v \in T$ there is an edge between (u, v) and (u', v) in Γ ;
- for each vertex $u \in S$ and each edge $\{v, v'\} \in T$ there is an edge between (u, v) and (u, v') in Δ ;

An example of a tensor product is given in Figure 1.

2.1.1. *T-systems for bipartite bigraphs.* Just as in [12, 13], we reformulate the definition of the T -system in the language of bigraphs that is more convenient for us to work with.

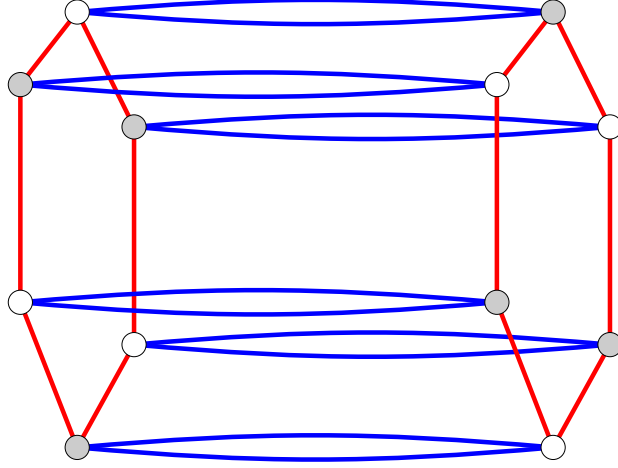


FIGURE 1. A tensor product of a hexagon (type \hat{A}_5) and a 2-cycle (type \hat{A}_1). Tensor products are listed as family #1 in our classification in Section 6.

Name	Finite diagram	$h(\Lambda)$
A_ℓ ($\ell \geq 1$)		$\ell + 1$
D_ℓ ($\ell \geq 4$)		$2\ell - 2$
E_6		12
E_7		18
E_8		30

FIGURE 2. Finite ADE Dynkin diagrams and their Coxeter numbers. Each diagram whose name contains index ℓ has ℓ vertices.

Definition 2.5. Let $G = (\Gamma, \Delta)$ be a bipartite bigraph with vertex set V . Then the associated T -system for G is defined as follows:

$$T_v(t+1)T_v(t-1) = \prod_{(u,v) \in \Gamma} T_u(t) + \prod_{(v,w) \in \Delta} T_w(t);$$

$$T_v(\epsilon_v) = x_v.$$

It is easy to see that we have $T_v(t) = T'_v(t)$ where $T'_v(t)$ is the value of the T -system associated with $Q(G)$ via Definition 1.2.

2.2. Finite and affine ADE Dynkin diagrams.

Name	Affine diagram	$h^{(2)}(\hat{\Lambda})$
$\hat{A}_\ell (\ell \geq 1)$		$\ell + 1$
$\hat{D}_\ell (\ell \geq 4)$		$4(\ell - 2)$
\hat{E}_6		24
\hat{E}_7		48
\hat{E}_8		120

FIGURE 3. Affine ADE Dynkin diagrams together with their additive functions and McKay numbers. Each diagram whose name contains index ℓ has $\ell + 1$ vertices.

Definition 2.6. Given an undirected graph $G = (V, E)$ with possibly multiple edges, we say that a map $\lambda : V \rightarrow \mathbb{R}_{>0}$ is an *additive function* if for all $v \in V$ we have

$$(2.1) \quad 2\lambda(v) = \sum_{(u,v) \in E} \lambda(u).$$

The following characterization of affine ADE Dynkin diagrams is due to Vinberg [41]:

Theorem 2.7. *Let $G = (V, E)$ be an undirected graph with possibly multiple edges. Then G is an affine ADE Dynkin diagram if and only if there exists an additive function for G .*

Finite and affine ADE Dynkin diagrams are given in Figures 2 and 3 respectively. The affine diagrams are drawn together with the values of their additive functions. We scale the values of the additive function so that they are relatively prime positive integers. Note that the only affine ADE Dynkin diagram that is not a bipartite graph is \hat{A}_{2n} for $n \geq 1$.

For each finite ADE Dynkin diagram Λ there is an associated integer $h(\Lambda)$ called the *Coxeter number*, see e.g. [3, Chapter V, §6]. We list

Coxeter numbers of finite *ADE* Dynkin diagrams in Figure 2. If $\hat{\Lambda}$ is an affine *ADE* Dynkin diagram, we set $h(\hat{\Lambda}) = \infty$.

The Coxeter number has various nice interpretations, we list some of them below.

Proposition 2.8.

- If Λ is a finite *ADE* Dynkin diagram then the dominant eigenvalue of its adjacency matrix equals $2 \cos(\pi/h(\Lambda))$;
- if $\hat{\Lambda}$ is an affine *ADE* Dynkin diagram then the dominant eigenvalue of its adjacency matrix equals 2.
- The Coxeter element of the Coxeter group associated with Λ has period $h(\Lambda)$.
- If $\hat{\Lambda}$ is the affine *ADE* Dynkin diagram corresponding to a finite *ADE* Dynkin diagram Λ then $h(\Lambda)$ equals the sum of the values of the additive function for $\hat{\Lambda}$.

□

In particular, the first three claims justify setting $h(\hat{\Lambda}) := \infty$. Motivated by the last claim, we introduce the following affine analog of the Coxeter number that will come into play in the proof of our classification in Section 7.

Definition 2.9. Given an affine *ADE* Dynkin diagram $\hat{\Lambda}$, its *McKay number* $h^{(2)}(\hat{\Lambda})$ is the sum of squares of the values of the additive function for $\hat{\Lambda}$.

The values of $h^{(2)}(\hat{\Lambda})$ are given in Figure 3. The motivation for the name comes from the fact that $h^{(2)}(\hat{\Lambda})$ is the size of the subgroup of $SU(2)$ associated with $\hat{\Lambda}$ via the *McKay correspondence*, see [30] or [38].¹

2.3. Generalized Cartan matrices. In this section, we review Kac's classification [21] of generalized Cartan matrices of affine type. We will however need to consider a slightly more general class of matrices.

Definition 2.10. An $n \times n$ matrix $A = (a_{ij})_{i,j=1}^n$ is called a *weak generalized Cartan matrix* if it satisfies the following axioms:

- (C1) $a_{ii} \in \mathbb{Z}$ and $a_{ii} \leq 2$ for $i = 1, \dots, n$;
- (C2) a_{ij} are non-positive integers for $i \neq j$;
- (C3) $a_{ij} = 0$ implies $a_{ji} = 0$.

¹We thank Christian Gaetz for pointing out this connection to us.

Thus a *generalized Cartan matrix* is a weak generalized Cartan matrix satisfying $a_{ii} = 2$ for all $i \in [n] := \{1, 2, \dots, n\}$. Following [21, §4.7], to each weak generalized Cartan matrix A we associate its *Dynkin diagram* $S(A)$ with vertex set $[n]$ as follows. We connect each vertex i to itself by $2 - a_{ii}$ self-loops. Two vertices $i \neq j \in [n]$ such that $|a_{ij}| \geq |a_{ji}|$ are connected by $|a_{ij}|$ lines in $S(A)$ which are equipped with an arrow pointing toward i if $|a_{ij}| > 1$. We say that A is *indecomposable* if $S(A)$ is a connected graph. For a column vector u with coordinates $u^T = (u_1, u_2, \dots)$, we write $u > 0$ (resp., $u \geq 0$) if all $u_i > 0$ (resp., all $u_i \geq 0$).

Theorem 2.11 ([21, Theorem 4.3]). *Let A be a real $n \times n$ indecomposable weak generalized Cartan matrix. Then exactly one of the following holds:*

- (Fin) *There exists $u > 0$ such that $Au > 0$.*
- (Aff) *There exists $u > 0$ such that $Au = 0$.*
- (Ind) *There exists $u > 0$ such that $Au < 0$.*

In cases (Fin), (Aff), (Ind), we will say that A is of *finite*, *affine*, or *indefinite type*, respectively.

Theorem 2.12.

- (1) *If A is an indecomposable weak generalized Cartan matrix of finite type then $S(A)$ is one of the diagrams in Figure 4.*
- (2) *If A is an indecomposable weak generalized Cartan matrix of affine type then $S(A)$ is one of the diagrams shown in Figure 5.*
- (3) *The labels in Figure 5 are the coordinates of the unique vector $\delta = (\delta_1, \dots, \delta_n)$ such that $A\delta = 0$ and the δ_i are positive relatively prime integers.*

Proof. Most of the statements follow from [21, Theorem 4.8]. The only additional work one needs to do is the case where we have $a_{ii} < 2$ for some $i \in [n]$. Suppose that A is a weak generalized Cartan matrix of finite (resp., affine) type such that $a_{ii} < 2$ for some $i \in [n]$. Introduce a $2n \times 2n$ weak generalized Cartan matrix B with indexing set $[n] \cup [n'] = \{1, 2, \dots, n, 1', 2', \dots, n'\}$ is obtained from A as follows. For $i \neq j \in [n]$, put $b_{ij} = b_{i'j'} = a_{ij}$ and put $b_{ij'} = b_{i'j} = 0$. For $i \in [n]$, set $b_{ii} = b_{i'i'} = 2$ and $b_{ii'} = b_{i'i} = 2 - a_{ii}$. It follows that B is a generalized Cartan matrix of finite (resp., affine) type. Thus $S(A)$ is obtained from $S(B)$ by taking a quotient with respect to a fixed-point-free involutive automorphism of order 2, and it is straightforward to check that the only Dynkin diagrams in Figures 4 and 5 that admit such an automorphism are A_{2n} , $A_{2n+1}^{(1)}$, $C_{2n+1}^{(1)}$, $D_{2n+1}^{(1)}$, and $D_{2n+3}^{(2)}$. We

A_ℓ $\circ - \circ - \dots - \circ - \circ$	B_ℓ $\circ - \circ - \dots - \circ \Rightarrow \circ$
C_ℓ $\circ - \circ - \dots - \circ \Leftarrow \circ$	D_ℓ $\begin{array}{c} \circ \\ \\ \circ - \circ - \dots - \circ - \circ \end{array}$
E_6 $\begin{array}{c} \circ \\ \\ \circ - \circ - \circ - \circ - \circ \end{array}$	E_7 $\begin{array}{c} \circ \\ \\ \circ - \circ - \circ - \circ - \circ - \circ \end{array}$
E_8 $\begin{array}{c} \circ \\ \\ \circ - \circ - \circ - \circ - \circ - \circ - \circ \end{array}$	F_4 $\circ - \circ \Rightarrow \circ - \circ$
G_2 $\circ \Rightarrow \circ$	$\frac{1}{2}A_{2\ell}(\ell \geq 1)$ $\begin{array}{c} \circ \\ \circ - \circ - \dots - \circ - \circ \end{array}$

FIGURE 4. Dynkin diagrams of weak generalized Cartan matrices of finite type. Each diagram whose name contains index ℓ has ℓ vertices.

denote the corresponding diagram $S(A)$ by $\frac{1}{2}A_{2n}$ (Figure 4), $\frac{1}{2}A_{2n+1}^{(1)}$, $\frac{1}{2}C_{2n+1}^{(1)}$, $\frac{1}{2}D_{2n+1}^{(1)}$, and $\frac{1}{2}D_{2n+3}^{(2)}$ (Figure 5) respectively. \square

Note that a 1×1 matrix A with $a_{11} \leq 2$ is an indecomposable weak generalized Cartan matrix for any a_{11} including $a_{11} = 0$. This zero 1×1 matrix corresponds to the diagram $\frac{1}{2}A_{2\ell+1}^{(1)}$ for $\ell = 0$ which is a single vertex with two self-loops. We also denote this diagram by $A_0^{(1)}$.

Remark 2.13. The diagrams in Figure 2 also appear in Figure 4. Similarly, the diagrams in Figure 3 also appear (with slightly different names) in Figure 5. This is done intentionally since we treat diagrams in Figures 2 and 3 as color components of bigraphs (see next section) while we get diagrams in Figures 4 and 5 as component graphs of bigraphs (see Theorem 4.7).

2.4. Bipartite recurrent quivers and bigraphs.

Definition 2.14. Let Q be a quiver. For a vertex v of Q one can define the *quiver mutation* μ_v at v as follows:

- (1) for each pair of arrows $u \rightarrow v$ and $v \rightarrow w$, create an arrow $u \rightarrow w$;
- (2) reverse the direction of all arrows incident to v ;
- (3) if some directed 2-cycle is present, remove both of its arrows; repeat until there are no more directed 2-cycles.

It is straightforward to check that the resulting quiver $\mu_v(Q)$ is well defined. See Figure 6 for an example of each step.

$A_\ell^{(1)} (\ell \geq 2)$	$1 \xrightarrow{\quad} 1 \xrightarrow{\quad} \cdots \xrightarrow{\quad} 1 \xrightarrow{\quad} 1$	$D_\ell^{(1)} (\ell \geq 4)$	$1 \xrightarrow{\quad} 2 \xrightarrow{\quad} 2 \xrightarrow{\quad} \cdots \xrightarrow{\quad} 2 \xrightarrow{\quad} 1$
$E_6^{(1)}$	$1 \xrightarrow{\quad} 2 \xrightarrow{\quad} 3 \xrightarrow{\quad} 2 \xrightarrow{\quad} 1$	$E_7^{(1)}$	$1 \xrightarrow{\quad} 2 \xrightarrow{\quad} 3 \xrightarrow{\quad} 4 \xrightarrow{\quad} 3 \xrightarrow{\quad} 2 \xrightarrow{\quad} 1$
$D_{\ell+1}^{(2)} (\ell \geq 2)$	$1 \leftarrow 1 \xrightarrow{\quad} \cdots \xrightarrow{\quad} 1 \Rightarrow 1$	$E_8^{(1)}$	$2 \xrightarrow{\quad} 4 \xrightarrow{\quad} 6 \xrightarrow{\quad} 5 \xrightarrow{\quad} 4 \xrightarrow{\quad} 3 \xrightarrow{\quad} 2 \xrightarrow{\quad} 1$
$A_1^{(1)}$	$1 \Leftrightarrow 1$	$A_2^{(2)}$	$2 \Leftrightarrow 1$
$G_2^{(1)}$	$1 \xrightarrow{\quad} 2 \Rightarrow 3$	$D_4^{(3)}$	$1 \xrightarrow{\quad} 2 \Leftrightarrow 1$
$B_\ell^{(1)} (\ell \geq 3)$	$1 \xrightarrow{\quad} 2 \xrightarrow{\quad} \cdots \xrightarrow{\quad} 2 \Rightarrow 2$	$A_{2\ell-1}^{(2)} (\ell \geq 3)$	$1 \xrightarrow{\quad} 2 \xrightarrow{\quad} \cdots \xrightarrow{\quad} 2 \Leftarrow 1$
$C_\ell^{(1)} (\ell \geq 2)$	$1 \Rightarrow 2 \xrightarrow{\quad} \cdots \xrightarrow{\quad} 2 \Leftarrow 1$	$A_{2\ell}^{(2)} (\ell \geq 2)$	$2 \Leftarrow 2 \xrightarrow{\quad} \cdots \xrightarrow{\quad} 2 \Leftarrow 1$
$F_4^{(1)}$	$1 \xrightarrow{\quad} 2 \xrightarrow{\quad} 3 \Rightarrow 4 \xrightarrow{\quad} 2$	$E_6^{(2)}$	$1 \xrightarrow{\quad} 2 \xrightarrow{\quad} 3 \Leftarrow 2 \xrightarrow{\quad} 1$
$\frac{1}{2}A_{2\ell+1}^{(1)} (\ell \geq 0)$	$1 \xrightarrow{\quad} 1 \xrightarrow{\quad} \cdots \xrightarrow{\quad} 1 \xrightarrow{\quad} 1$	$\frac{1}{2}C_{2\ell+1}^{(1)} (\ell \geq 1)$	$1 \Rightarrow 2 \xrightarrow{\quad} \cdots \xrightarrow{\quad} 2 \xrightarrow{\quad} 2$
$\frac{1}{2}D_{2\ell+1}^{(1)} (\ell \geq 2)$	$1 \xrightarrow{\quad} 2 \xrightarrow{\quad} \cdots \xrightarrow{\quad} 2 \xrightarrow{\quad} 2$	$\frac{1}{2}D_{2\ell+3}^{(2)} (\ell \geq 1)$	$1 \Leftarrow 1 \xrightarrow{\quad} \cdots \xrightarrow{\quad} 1 \xrightarrow{\quad} 1$

FIGURE 5. Dynkin diagrams of weak generalized Cartan matrices of affine type. Each diagram whose name contains index ℓ has $\ell + 1$ vertices. The names of the diagrams are taken from [21].

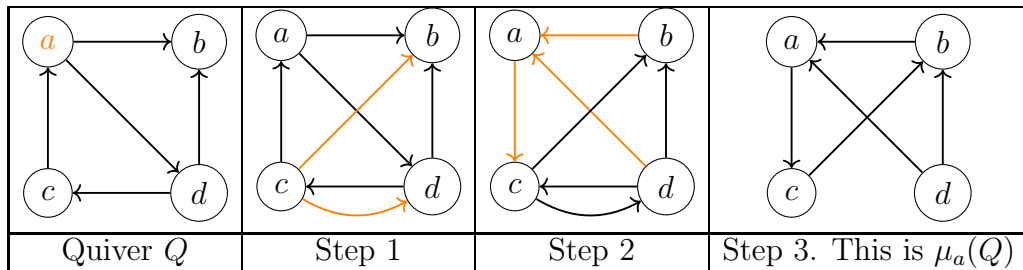


FIGURE 6. Mutating a quiver Q at vertex a . The edges changed at the corresponding step are highlighted in orange.

Now, let Q be a bipartite quiver. Recall that μ_0 (resp., μ_1) is the simultaneous mutation at all white (resp., all black) vertices of Q , and that Q is *recurrent* if $\mu_0(Q) = \mu_1(Q) = Q^{\text{op}}$, see Definition 1.1.

Corollary 2.15. *A bipartite quiver Q is recurrent if and only if the associated bipartite bigraph $G(Q)$ has commuting adjacency matrices A_Γ, A_Δ .*

Equivalently, this means that for any two vertices $u, w \in \text{Vert}(Q)$, the number of directed 2-paths $u \rightarrow v \rightarrow w$ in Q equals the number of directed 2-paths $w \rightarrow v \rightarrow u$ in Q . In other words, the number of *red-blue paths* $(u, v) \in \Gamma, (v, w) \in \Delta$ in G equals the number of *blue-red paths* $(u, v) \in \Delta, (v, w) \in \Gamma$ in G .

Let us now recall a few facts from [13].

Lemma 2.16 ([13, Lemma 1.1.8]). *Let $G = (\Gamma, \Delta)$ be a connected bigraph and assume that the adjacency matrices A_Γ, A_Δ commute. Then the dominant eigenvalues of all components of Γ are equal to the same value $\mu_\Gamma > 0$, and the dominant eigenvalues of all components of Δ are equal to the same value $\mu_\Delta > 0$. Matrices A_Γ and A_Δ have a common dominant eigenvector $\mathbf{v} > 0$ such that*

$$A_\Gamma \mathbf{v} = \mu_\Gamma \mathbf{v}; \quad A_\Delta \mathbf{v} = \mu_\Delta \mathbf{v}.$$

□

Applying the well known characterization of affine and finite ADE Dynkin diagrams by their eigenvalues (see Proposition 2.8), we get the following:

Corollary 2.17. *Suppose that a bipartite bigraph $G = (\Gamma, \Delta)$ has commuting adjacency matrices. Then exactly one of the following is true:*

- (i) *all components of Γ are finite ADE Dynkin diagrams;*
- (ii) *all components of Γ are affine ADE Dynkin diagrams;*
- (iii) *every component of Γ is neither a finite nor an affine ADE Dynkin diagram.*

A similar claim holds for the components of Δ .

This motivates us to define three families of bipartite bigraphs that will be of the most importance to us.

Definition 2.18 ([13, Definition 1.1.7]). Let $G = (\Gamma, \Delta)$ be a bipartite bigraph with commuting adjacency matrices. We say that:

- (1) G is a *finite \boxtimes finite ADE bigraph* if both Γ and Δ satisfy (i);
- (2) G is an *affine \boxtimes finite ADE bigraph* if Γ satisfies (ii) and Δ satisfies (i);

- (3) G is an *affine \boxtimes affine ADE bigraph* if both Γ and Δ satisfy (ii).

The finite \boxtimes finite ADE bigraphs have been introduced by Stembridge [39] under the name *admissible ADE bigraphs*.

Let $G = (\Gamma, \Delta)$ be a bipartite bigraph on vertex set V . A *labeling* of its vertices is a function $\nu : V \rightarrow \mathbb{R}_{>0}$, which assigns a positive real number $\nu(v)$ to each vertex v of G .

Definition 2.19 ([13, Definition 1.1.4]). A labeling $\nu : V \rightarrow \mathbb{R}_{>0}$ is called

- *strictly subadditive* if for any vertex $v \in V$,

$$2\nu(v) > \sum_{(u,v) \in \Gamma} \nu(u), \quad \text{and} \quad 2\nu(v) > \sum_{(v,w) \in \Delta} \nu(w).$$

- *subadditive* if for any vertex $v \in V$,

$$2\nu(v) \geq \sum_{(u,v) \in \Gamma} \nu(u), \quad \text{and} \quad 2\nu(v) > \sum_{(v,w) \in \Delta} \nu(w).$$

- *weakly subadditive* if for any vertex $v \in V$,

$$2\nu(v) \geq \sum_{(u,v) \in \Gamma} \nu(u), \quad \text{and} \quad 2\nu(v) \geq \sum_{(v,w) \in \Delta} \nu(w).$$

- *additive* if for any vertex $v \in V$,

$$2\nu(v) = \sum_{(u,v) \in \Gamma} \nu(u), \quad \text{and} \quad 2\nu(v) = \sum_{(v,w) \in \Delta} \nu(w).$$

Examples of each type can be found in Figure 7.

Thus any additive labeling is not subadditive but is weakly subadditive. As we will see later, the converse is also true: additive labelings are precisely the weakly subadditive labelings that are not subadditive.

Strictly subadditive, subadditive and weakly subadditive labelings of quivers have been introduced by the second author in [34].

The connection between Definitions 2.18 and 2.19 is as follows.

Proposition 2.20 ([13, Proposition 1.1.10]). *Let Q be a bipartite recurrent quiver Q and $G(Q) = (\Gamma, \Delta)$ be the corresponding bipartite bigraph. Then*

- (1) Q admits a strictly subadditive labeling if and only if $G(Q)$ is a finite \boxtimes finite ADE bigraph;
- (2) Q admits a subadditive labeling which is not strictly subadditive if and only if $G(Q)$ is an affine \boxtimes finite ADE bigraph;
- (3) Q admits a weakly subadditive labeling which is not subadditive if and only if $G(Q)$ is an affine \boxtimes affine ADE bigraph, in which case Q admits an additive labeling. \square

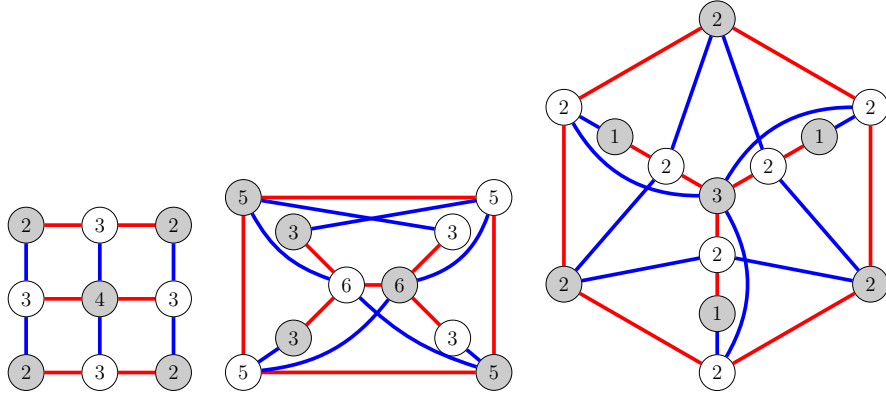


FIGURE 7. A strictly subadditive labeling (left). A subadditive labeling (middle). A weakly subadditive labeling which is also an additive labeling (right).

2.5. Tropical T -systems. In this section, we recall how to *tropicalize* the T -system. We again follow the exposition of [13].

Given a bipartite recurrent quiver Q , we call the associated T -system from Definition 1.2 *the birational T -system* associated with Q in order to distinguish it from another discrete dynamical system which we introduce in this section.

Definition 2.21. Let Q be a bipartite recurrent quiver, and let $\lambda : \text{Vert}(Q) \rightarrow \mathbb{R}$ be any assignment of real numbers to the vertices of Q . Then the *tropical T -system* associated with Q and λ is a family of real numbers $\mathfrak{t}_v^\lambda(t) \in \mathbb{R}$ defined for every $v \in \text{Vert}(Q), t \in \mathbb{Z}$ with $t \equiv \epsilon_v \pmod{2}$ satisfying the following relations:

$$(2.2) \quad \mathfrak{t}_v^\lambda(t+1) + \mathfrak{t}_v^\lambda(t-1) = \max \left(\sum_{u \rightarrow v} \mathfrak{t}_u^\lambda(t), \sum_{v \rightarrow w} \mathfrak{t}_w^\lambda(t) \right);$$

$$\mathfrak{t}_v^\lambda(\epsilon_v) = \lambda(v).$$

The defining recurrence (2.2) can be translated into the language of bigraphs in a similar way: if $G = (\Gamma, \Delta)$ is a bipartite recurrent bigraph then the relation becomes

$$\mathfrak{t}_v^\lambda(t+1) + \mathfrak{t}_v^\lambda(t-1) = \max \left(\sum_{(u,v) \in \Gamma} \mathfrak{t}_u^\lambda(t), \sum_{(v,w) \in \Delta} \mathfrak{t}_w^\lambda(t) \right).$$

Let $P(\mathbf{x}) \in \mathbb{Z}[\mathbf{x}^{\pm 1}]$ be a multivariate Laurent polynomial in variables $\mathbf{x} = (x_v)_{v \in \text{Vert}(Q)}$. Define $P|_{\mathbf{x}=q^\lambda} \in \mathbb{Z}[q^{\pm 1}]$ to be the (univariate) Laurent polynomial in q obtained from P by substituting $x_v = q^{\lambda(v)}$ for all

$v \in \text{Vert}(Q)$. Further, define $\deg_{\max}(q, P|_{\mathbf{x}=q^\lambda})$ to be the maximal degree of q in $P|_{\mathbf{x}=q^\lambda}$. The following claim gives a connection between the birational and tropical T -systems:

Proposition 2.22 ([12, Lemma 6.3]). *For every $v \in \text{Vert}(Q)$, $t \in \mathbb{Z}$ with $t + \epsilon_v$ even and any $\lambda : \text{Vert}(Q) \rightarrow \mathbb{R}$, we have*

$$\mathfrak{t}_v^\lambda(t) = \deg_{\max}(q, T_v(t)|_{\mathbf{x}=q^\lambda}).$$

Thus the fact that Q has algebraic entropy zero can be deduced from the limiting behavior of the tropical T -system associated with Q .

3. ALGEBRAIC ENTROPY

In this section, we prove Theorem 1.5 that motivates us to classify affine \boxtimes affine ADE bigraphs.

Proof of Theorem 1.5. Let $G = (\Gamma(Q), \Delta(Q))$ be the bigraph associated to Q . By Lemma 2.16, there exist positive real numbers μ_Γ, μ_Δ and a map $\lambda : \text{Vert}(Q) \rightarrow \mathbb{R}_{>0}$ given by $\lambda(v) = \mathbf{v}_v$ for any vertex v of Q such that for any vertex $v \in \text{Vert}(Q)$ we have

$$(3.1) \quad \sum_{(u,v) \in \Gamma} \lambda(u) = \mu_\Gamma \lambda(v), \quad \sum_{(v,w) \in \Delta} \lambda(w) = \mu_\Delta \lambda(v).$$

By symmetry we may assume that $\mu_\Gamma \geq \mu_\Delta$. We claim that $\mu_\Gamma > 2$. Suppose that this is not the case: $2 \geq \mu_\Gamma \geq \mu_\Delta > 0$. Then λ is a weakly subadditive function for Q which contradicts the assumption of the theorem. Thus we have $\mu_\Gamma > 2$. Now consider the tropical T -system \mathfrak{t}^λ . Combining (2.2) with (3.1) yields

$$\mathfrak{t}_v^\lambda(t+1) + \mathfrak{t}_v^\lambda(t-1) = \max(\mu_\Gamma \mathfrak{t}_v^\lambda(t-1), \mu_\Delta \mathfrak{t}_v^\lambda(t-1)) = \mu_\Gamma \mathfrak{t}_v^\lambda(t-1).$$

Here we are using the fact that $\mathfrak{t}_v^\lambda(t-1) > 0$ which easily follows by induction as well as the fact that

$$\sum_{(u,v) \in \Gamma} \mathfrak{t}_u^\lambda(t) = \mu_\Gamma \mathfrak{t}_v^\lambda(t-1), \quad \sum_{(v,w) \in \Delta} \mathfrak{t}_w^\lambda(t) = \mu_\Delta \mathfrak{t}_v^\lambda(t-1).$$

Therefore the values of the tropical T -system $\mathfrak{t}_v^\lambda(t)$ for this special choice of λ are given by

$$\mathfrak{t}_v^\lambda(\epsilon_v + 2t) = \lambda(v)(\mu_\Gamma - 1)^t.$$

Since $\mu_\Gamma > 2$, it follows that

$$\lim_{t \rightarrow \infty} \frac{\log(\mathfrak{t}_v^\lambda(\epsilon_v + 2t))}{t} = \log(\mu_\Gamma - 1) > 0.$$

Now it remains to note that any point $\mathbf{p} = (p_u)_{u \in \text{Vert}(Q)}$ of the *Newton polytope* (see [12, Section 6.1]) of $T_v(\epsilon_v + 2t)$ satisfies $p_u \leq \deg_{\max}(x_u, T_v(\epsilon_v +$

$2t$). Since $\mathfrak{t}_v^\lambda(\epsilon_v + 2t)$ is just the maximum of the dot product $\langle \mathbf{p}, \lambda \rangle$ over all points \mathbf{p} of the Newton polytope and since $\lambda(u) > 0$ for all $u \in \text{Vert}(Q)$, it follows by the Cauchy-Schwartz inequality that

$$\mathfrak{t}_v^\lambda(\epsilon_v + 2t) \leq |\lambda| \cdot \sqrt{\sum_{u \in \text{Vert}(Q)} (\deg_{\max}(x_u, T_v(\epsilon_v + 2t)))^2},$$

where $|\lambda| = \sqrt{\sum_{u \in \text{Vert}(Q)} \lambda(u)^2}$ does not depend on t . In particular,

$$\mathfrak{t}_v^\lambda(\epsilon_v + 2t) \leq |\lambda| \sqrt{|\text{Vert}(Q)|} \max_{u \in \text{Vert}(Q)} |\deg_{\max}(x_u, T_v(\epsilon_v + 2t))|.$$

Taking the logarithm of both sides and dividing by t yields that for at least one $u \in \text{Vert}(Q)$, (1.4) must fail. We are done with the proof of the theorem. \square

3.1. Algebraic entropy for quivers of type $\hat{A} \otimes \hat{A}$. It turns out that the statement of Conjecture 1.7 applied to the quivers of type $\hat{A} \otimes \hat{A}$ can be easily proven using Speyer's formula [37] for the *octahedron recurrence*. Let us first give a quick background before actually stating the result.

Definition 3.1. The *octahedron recurrence* is a family $T_{i,j,k}$ of rational functions in some set of variables \mathbf{x} indexed by all triples $(i, j, k) \in \mathbb{Z}^3$ of integers. The values $T_{i,j,k}$ are required to satisfy

$$T_{i,j,k+1}T_{i,j,k-1} = T_{i,j+1,k}T_{i,j-1,k} + T_{i+1,j,k}T_{i-1,j,k}.$$

Again, the parity of $i + j + k$ in each term is the same so the system splits into two independent parts. One imposes various initial conditions that define the values $T_{i,j,k}$ uniquely for all triples (i, j, k) , and we will be interested in assigning $T_{i,j,0} = T_{i,j,1} = x_{i,j}$ for some family $\mathbf{x} = (x_{i,j})_{i,j \in \mathbb{Z}}$ of variables.

Theorem 3.2 ([37]). *For $k > 1$, the value $T_{i,j,k}$ is a Laurent polynomial in \mathbf{x} . More specifically, it is a sum of $2^{\binom{k}{2}}$ monomials, and the power of every variable $x_{i',j'}$ in every monomial belongs to the set $\{-1, 0, 1\}$.*

Consider an infinite quiver Q_∞ with vertex set \mathbb{Z}^2 such that for each vertex (i, j) with $i + j$ even, we have arrows

$$(i-1, j) \rightarrow (i, j), \quad (i+1, j) \rightarrow (i, j), \quad (i, j) \rightarrow (i, j-1), \quad (i, j) \rightarrow (i, j+1).$$

For each vertex with (i, j) odd we therefore have the reverses of the above arrows in Q_∞ .

Fix two linearly independent vectors $A = (a_1, a_2)$ and $B = (b_1, b_2)$ in \mathbb{Z}^2 such that $a_1 + a_2$ and $b_1 + b_2$ are even. Suppose that the variables $x_{i,j}$ satisfy

$$(3.2) \quad x_{i,j} = x_{i+a_1, j+a_2} = x_{i+b_1, i+b_2}$$

One can take a factor of Q_∞ by the lattice generated by A and B , we denote the resulting quiver by $Q_{A,B}$. Thus the vertices of $Q_{A,B}$ correspond to equivalence classes $(i, j) + \mathbb{Z}A + \mathbb{Z}B$ and there is an arrow from one such class to another in $Q_{A,B}$ if there is an arrow from a vertex of the first class to a vertex of the second class in Q_∞ . It is clear that $Q_{A,B}$ is a bipartite recurrent affine \boxtimes affine quiver since all components of both $\Gamma(Q)$ and $\Delta(Q)$ are of type \hat{A} . In particular, if $A = (2n, 0)$ and $B = (0, 2m)$ then $Q_{A,B}$ has type $\hat{A}_{2n-1} \otimes \hat{A}_{2m-1}$. We will consider these quivers more closely in Section 5.2.1.

One easily observes that if the initial conditions of the octahedron recurrence satisfy (3.2) then the values of the octahedron recurrence coincide with the values of the T -system associated with the quiver $Q_{A,B}$ that we have just constructed. Substituting the values into Theorem 3.2 yields the following:

Corollary 3.3. *The T -system associated with $Q_{A,B}$ grows quadratic exponentially.²*

Proof. Indeed, the number of terms grows quadratic exponentially, and since we have substituted periodic variables into Theorem 3.2, the degree of a variable in a monomial now grows quadratically as well. \square

4. THE GENERAL STRUCTURE OF ADE BIGRAPHS

In this section, we prove some general properties of affine \boxtimes affine and affine \boxtimes finite ADE bigraphs. The main result of this section will be the construction of a weak generalized Cartan matrix $A(G)$ associated to G which will later help us with the classification. We assume that the red components of G are affine ADE Dynkin diagrams while the blue components of G are either affine or finite ADE Dynkin diagrams. If G has one red connected component then we say that G is a *self binding*. If G has two red connected components then we say that G is a *double binding*.

²As it was pointed out to us by Andrew Hone, the quadratic growth for the octahedron recurrence has been shown recently by Mase [29, Theorem 6.8].

4.1. The structure of self bindings.

Proposition 4.1. *Let G be a self binding. If G is an affine \boxtimes finite ADE bigraph, set $\text{mult}(G) := 1$, and if G is an affine \boxtimes affine ADE bigraph, set $\text{mult}(G) = 2$. Let \mathbf{v} be the additive function for the unique red connected component of G . Then we have*

$$(4.1) \quad \text{mult}(G)\mathbf{v}(v) = \sum_{(u,v) \in \Delta} \mathbf{v}(u).$$

Proof. It follows that \mathbf{v} is the common eigenvector for A_Γ and A_Δ from Lemma 2.16. Thus for any v we have

$$\sum_{(u,v) \in \Delta} \mathbf{v}(u) = \mu_\Delta \mathbf{v}(v),$$

which shows that μ_Δ is an integer and therefore is either equal to 1 (in which case all components of Δ are of type A_2) or to 2 (in which case all components of Δ are affine ADE Dynkin diagrams). \square

4.2. Double bindings: scaling factor. Throughout this section, we assume that $G = (\Gamma, \Delta)$ is a double binding, and that $\text{Vert}(G) = X \sqcup Y$, where X and Y are the two connected components of Γ , and recall that they are affine ADE Dynkin diagrams. We also assume that every edge of Δ connects a vertex of X to a vertex of Y . Again, we do not assume here that $h(\Gamma) = \infty$.

A *parallel binding* is a bigraph of type $\hat{\Lambda} \otimes A_2$. We let \mathbf{v} be the common eigenvector for A_Γ and A_Δ from Lemma 2.16, and we denote by \mathbf{v}_X and \mathbf{v}_Y the additive functions for $\Gamma(X)$ and $\Gamma(Y)$ from Figure 3.

Proposition 4.2. *There exist two integers $\text{scf}_X(G)$ and $\text{scf}_Y(G)$ such that*

$$(4.2) \quad \sum_{(v,w) \in \Delta} \mathbf{v}_Y(w) = \text{scf}_X(G)\mathbf{v}_X(v), \quad \forall v \in X;$$

$$(4.3) \quad \sum_{(v,w) \in \Delta} \mathbf{v}_X(v) = \text{scf}_Y(G)\mathbf{v}_Y(w), \quad \forall w \in Y.$$

The pair $(\text{scf}_X(G), \text{scf}_Y(G))$ is denoted $\text{scf}(G)$ and is called the scaling factor of G . Exactly one of the following holds:

- $\text{scf}(G) = (1, 1)$ and connected components of Δ are of type A_2 ;
- $\text{scf}(G) = (2, 1)$ or $\text{scf}(G) = (1, 2)$ and connected components of Δ are of type A_3 ;
- $\text{scf}(G) = (3, 1)$ or $\text{scf}(G) = (1, 3)$ and connected components of Δ are either of type A_5 or of type D_4 ;

- $\text{scf}(G) = (4, 1)$ or $\text{scf}(G) = (1, 4)$ and connected components of Δ are affine ADE Dynkin diagrams;
- $\text{scf}(G) = (2, 2)$ and connected components of Δ are affine ADE Dynkin diagrams.

Proof. We copy the proof of [13, Proposition 2.1.4] with slight modifications. We view maps $\tau : \text{Vert}(G) \rightarrow \mathbb{R}$ as pairs $\begin{pmatrix} \tau_X \\ \tau_Y \end{pmatrix}$ where $\tau_X : \text{Vert}(X) \rightarrow \mathbb{R}$ and $\tau_Y : \text{Vert}(Y) \rightarrow \mathbb{R}$ are restrictions of τ to the corresponding subsets. Let $\tau = \begin{pmatrix} \tau_X \\ \tau_Y \end{pmatrix}$ be the common dominant eigenvector for A_Γ and A_Δ from Lemma 2.16, thus $\tau(v) = \mathbf{v}(v)$ for all $v \in \text{Vert}(G)$.³ We may rescale it so that $\tau_X = \alpha \mathbf{v}_X$ and $\tau_Y = \mathbf{v}_Y$ for some $\alpha \in \mathbb{R}$. Since the entries of the dominant eigenvector are positive, we may assume $\alpha > 0$. Now, let $\mu_\Delta := 2 \cos(\pi/h(\Delta))$ be the dominant eigenvalue for A_Δ , including the case $h(\Delta) = \infty$. Since $A_\Delta \tau = \mu_\Delta \tau$, we have

$$\begin{aligned} \sum_{(v,w) \in \Delta} \mathbf{v}_Y(w) &= \mu_\Delta \alpha \mathbf{v}_X(v), \quad \forall v \in X; \\ \sum_{(v,w) \in \Delta} \alpha \mathbf{v}_X(v) &= \mu_\Delta \mathbf{v}_Y(w), \quad \forall w \in Y. \end{aligned}$$

In particular, the second equation can be rewritten as

$$\sum_{(v,w) \in \Delta} \mathbf{v}_X(v) = \frac{\mu_\Delta}{\alpha} \mathbf{v}_Y(w), \quad \forall w \in Y.$$

If we substitute $v \in X$ such that $\mathbf{v}_X(v) = 1$ in the first equation, we will get that $\mu_\Delta \alpha \in \mathbb{Z}_{>0}$. Similarly, if we substitute $w \in Y$ such that $\mathbf{v}_Y(w) = 1$ in the second equation, we will get that $\mu_\Delta/\alpha \in \mathbb{Z}_{>0}$. Therefore their product μ_Δ^2 belongs to $\mathbb{Z}_{>0}$ as well. This proves the first part of the proposition: we have $\text{scf}_X(G) = \mu_\Delta \alpha$ and $\text{scf}_Y(G) = \mu_\Delta/\alpha$.

In particular, their product $\text{scf}_X(G) \text{scf}_Y(G) = \mu_\Delta^2$ is an integer which can only happen when $h(\Delta) = 3, 4, 6$, or ∞ corresponding to $\mu_\Delta^2 = 1, 2, 3$, or 4 . This makes the second part of the proposition obvious. \square

Definition 4.3. When X is an affine ADE Dynkin diagram of type $\hat{\Lambda}$ and Y is an affine ADE Dynkin diagram of type $\hat{\Lambda}'$ then we say that G is a double binding of type $\hat{\Lambda} * \hat{\Lambda}'$.

Note that Proposition 4.2 is not symmetric in X and Y , so if G is a double binding of type $\hat{\Lambda} * \hat{\Lambda}'$ then necessarily X has type $\hat{\Lambda}$, Y has type

³Recall that \mathbf{v}_X denotes the additive function for $\Gamma(X)$ from Figure 3. On the other hand τ_X denote the restriction of $\tau = \mathbf{v}$ to X .

$\hat{\Lambda}'$ and (4.2) and (4.3) hold. In other words, we treat double bindings of types $\hat{\Lambda} * \hat{\Lambda}'$ and $\hat{\Lambda}' * \hat{\Lambda}$ differently.

We now show how the McKay number defined in Section 2.2 comes into play.

Proposition 4.4. *Suppose G is a double binding of type $\hat{\Lambda} * \hat{\Lambda}'$ and scaling factor (a, b) . Then we have*

$$(4.4) \quad \frac{a}{b} = \frac{h^{(2)}(\hat{\Lambda}')}{h^{(2)}(\hat{\Lambda})}.$$

Proof. Recall that $a = \text{scf}_X(G)$ and $b = \text{scf}_Y(G)$. By Equations (4.2) and (4.3), we have

$$\begin{aligned} \text{scf}_X(G)h^{(2)}(\hat{\Lambda}) &= \sum_{v \in X} \text{scf}_X(G)\mathbf{v}_X(v)^2 = \sum_{v \in X} \mathbf{v}_X(v) \sum_{(v,w) \in \Delta} \mathbf{v}_Y(w) \\ &= \sum_{(v,w) \in \Delta} \mathbf{v}_X(v)\mathbf{v}_Y(w) = \sum_{w \in Y} \mathbf{v}_Y(w) \sum_{(v,w) \in \Delta} \mathbf{v}_X(v) \\ &= \sum_{w \in Y} \text{scf}_Y(G)\mathbf{v}_Y(w)^2 = \text{scf}_Y(G)h^{(2)}(\hat{\Lambda}'). \end{aligned}$$

□

This simple double counting argument dramatically reduces the number of options one needs to consider in the proof of the classification in Section 7.

4.3. The weak generalized Cartan matrix of an ADE bigraph.

We are now ready to define the matrix $A(G)$ for an arbitrary affine \boxtimes affine or affine \boxtimes finite ADE bigraph G . Given a subset C of vertices of G , denote by $G(C)$ the restriction (induced subgraph) of G to C . Denote by G° the bigraph obtained from G by removing all blue edges that connect two vertices from the same red connected component (thus G° is obtained from G by removing all self bindings). It is easy to see that if G is an affine \boxtimes affine or affine \boxtimes finite ADE bigraph then the same is true for G° .

Definition 4.5. Let G be an affine \boxtimes affine or affine \boxtimes finite ADE bigraph, and let C_1, C_2, \dots, C_n be its red connected components. Define an $n \times n$ matrix $A(G) = (a_{ij})$ as follows.

- For $i \in [n]$, set $a_{ii} = 2 - \text{mult}(G(C_i))$.
- For $i \neq j \in [n]$, set $a_{ij} = 0$ if there is no blue edge in G connecting a vertex of C_i to a vertex of C_j .
- For all other pairs of $i \neq j \in [n]$, let $\text{scf}(G^\circ(C_i \cup C_j)) = (p, q)$ and we set $a_{ij} = -p$, $a_{ji} = -q$.

Thus, given two connected components C_i and C_j that form a double binding with scaling factor $(1, 1)$, $(1, 2)$, $(1, 3)$, $(1, 4)$, or $(2, 2)$, we connect i and j in $S(A(G))$ by an edge of the form $i-j$, $i \Rightarrow j$, $i \Rrightarrow j$, $i \Lrightarrow j$, or $i \Leftrightarrow j$ respectively.

Let \mathbf{v} be the common eigenvector for A_Γ and A_Δ from Lemma 2.16, and let \mathbf{v}_{C_i} be the additive function for $\Gamma(C_i)$ from Figure 3.

Lemma 4.6. *For each $i \in [n]$, there exists a positive real number δ_i such that for any $v \in C_i$ we have*

$$\delta_i = \frac{\mathbf{v}(v)}{\mathbf{v}_{C_i}(v)}.$$

Proof. Since \mathbf{v} is the common eigenvector for A_Γ and A_Δ , it must be proportional to \mathbf{v}_{C_i} on C_i . \square

Theorem 4.7. *For an affine \boxtimes finite (resp., affine \boxtimes affine) ADE bigraph G , the matrix $A = A(G)$ is a weak generalized Cartan matrix of finite (resp., affine) type. The vector $\delta = (\delta_1, \dots, \delta_n)$ from Lemma 4.6 satisfies $A\delta > 0$ (resp., $A\delta = 0$).*

Proof. Since the matrix A is clearly indecomposable, by Theorems 2.11 and 2.12, we only need to show that $A\delta > 0$ (resp., $A\delta = 0$).

Recall that \mathbf{v} is an eigenvector for A_Δ with eigenvalue μ_Δ which is either less than 2 (if $h(\Delta) < \infty$) or equal to 2 (if $h(\Delta) = \infty$). Now let $v \in C_i$ be a vertex. Using (4.1), (4.2), and (4.3), we get

$$\mu_\Delta \mathbf{v}(v) = \sum_{(u,v) \in \Delta} \mathbf{v}(u) = - \sum_{j \neq i} a_{ij} \delta_j \mathbf{v}_{C_j}(v) + (2 - a_{ii}) \delta_i \mathbf{v}_{C_i}(v).$$

Using the fact that $\mu_\Delta < 2$ (resp., $\mu_\Delta = 2$) and $\mathbf{v}(v) = \delta_i \mathbf{v}_{C_i}(v)$, we get $A\delta > 0$ (resp., $A\delta = 0$), as desired. \square

We let $S(G) := S(A(G))$ be the Dynkin diagram of $A(G)$ from Figure 5.

Let us now introduce a convenient way to encode G that often determines G uniquely.

Definition 4.8. Let G be an affine \boxtimes finite or an affine \boxtimes affine ADE bigraph. The *description* $\text{descr}(G)$ of G is the Dynkin diagram $S(G)$ of $A(G)$ with each vertex $i \in [n]$ labeled by $\text{type}(\Gamma(C_i))$. Here $\text{type}(\Gamma(C_i))$ is the *type* of $\Gamma(C_i)$ as an affine ADE Dynkin diagram, in other words, $\text{type}(\Gamma(C_i))$ belongs to the set

$$\{\hat{A}_{2m-1}, \hat{D}_m, \hat{E}_6, \hat{E}_7, \hat{E}_8\}.$$

For example, for the bigraph $G = \hat{D}_5 \otimes \hat{A}_2$, $\text{descr}(G)$ is equal to $\hat{D}_5 \Leftrightarrow \hat{D}_5$.

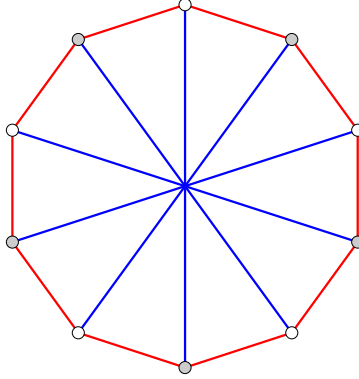


FIGURE 8. An affine \boxtimes finite self-binding \mathcal{S}_{4n+1} for $n = 2$.

4.4. Affine \boxtimes finite self and double bindings. In this section, we review some of our results from [13].

For $n \geq 1$, the bigraph \mathcal{S}_{4n+1} is defined as follows. Its unique red connected component is a $(4n + 2)$ -gon and the blue edges of \mathcal{S}_{4n+1} connect pairs of opposite vertices of this $(4n + 2)$ -gon. See Figure 8.

Theorem 4.9 ([13]).

- *The only possible affine \boxtimes finite self bindings are \mathcal{S}_{4n+1} for $n \geq 1$. We have*

$$\text{descr}(\mathcal{S}_{4n+1}) = \hat{A}_{4n+1} \ .$$

- *all the double bindings with scaling factor $(1, 2)$ are listed in Figure 9;*
- *all the double bindings with scaling factor $(1, 3)$ are listed in Figure 10;*
- *the only other affine \boxtimes finite double bindings are parallel bindings $\hat{\Lambda} - \hat{\Lambda}$.*

Definition 4.10. We say that a Dynkin diagram of a weak generalized Cartan matrix of affine type (see Figure 5) is *ambiguous* if it either has at most two vertices (with the exception of $\frac{1}{2}A_1^{(1)}$) or it is a path with two double arrows at the ends. Otherwise, we call it *unambiguous*. The set of ambiguous diagrams is equal to

$$\{A_1^{(1)}, A_\ell^{(1)} (\ell \geq 2), A_2^{(2)}, \frac{1}{2}A_1^{(1)}\} \cup \{D_{\ell+1}^{(2)}, C_\ell^{(1)}, A_{2\ell}^{(2)}\}.$$

The terminology is motivated by the following proposition which is a variation on [39, Remark 2.1].

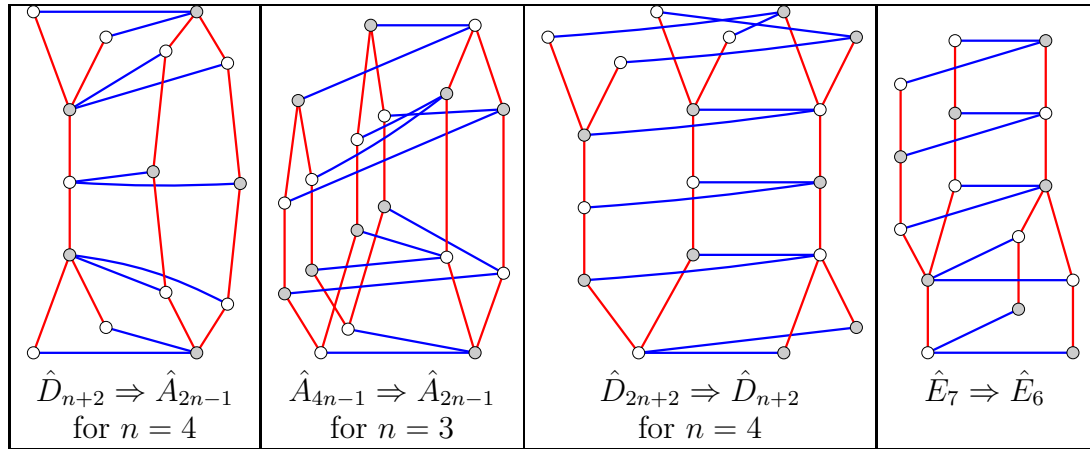


FIGURE 9. Three infinite and one exceptional family of double bindings with scaling factor $(1, 2)$. All blue components have type A_3 .

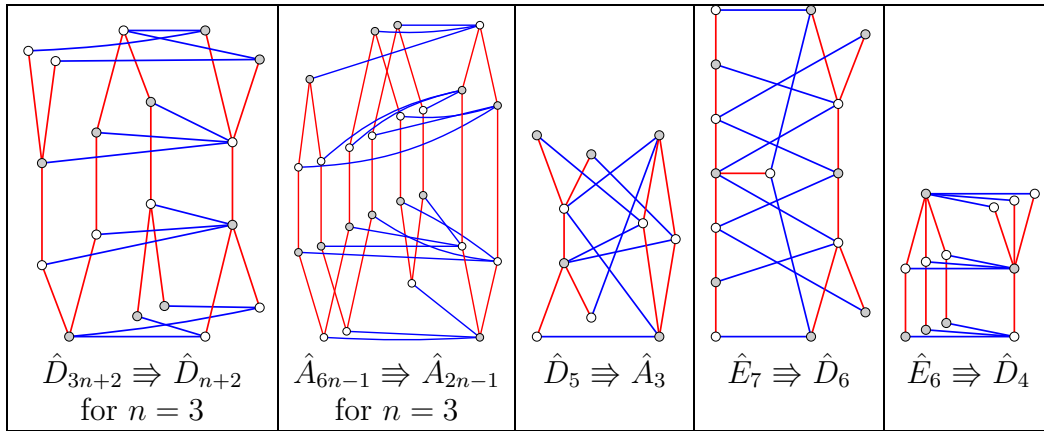


FIGURE 10. Two infinite and three exceptional families of double bindings with scaling factor $(1, 3)$. All blue components have types A_5 or D_4 .

Proposition 4.11. *Let G be an affine \boxtimes finite or an affine \boxtimes affine ADE bigraph and suppose that its Dynkin diagram $S(G)$ is unambiguous. Then G is uniquely determined by $\text{descr}(G)$.*

Proof. This is easy to see because if $S(G)$ is not one of the ambiguous Dynkin diagrams then $S(G)$ is a tree (with possibly some loops) and at most one affine \boxtimes finite double binding. As it follows from Theorem 4.9, each of them is uniquely determined by its description, and the result follows since an automorphism of the double binding always induces

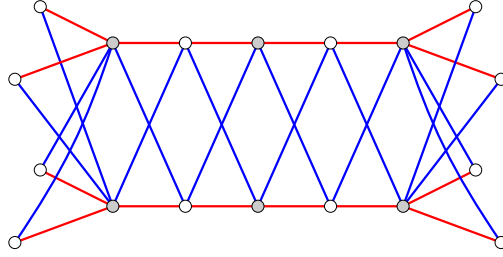


FIGURE 11. A twist $\hat{D}_8 \times \hat{D}_8$. Twists are listed as family #2 in the classification.

an automorphism of the rest of G . This is slightly non-trivial to see when G has a loop but in this case the result easily follows from our considerations in Section 5.3.1. \square

5. MANY AFFINE \boxtimes AFFINE ADE BIGRAPHS

In this section we give several constructions that produce affine \boxtimes affine ADE bigraphs. As we will see in the next section, they will be sufficient for us to state our classification theorem which is the main result of this paper.

5.1. Twists. The following construction is due to Stembridge [39].

Definition 5.1. Given a bipartite undirected graph H with vertex set V , we define the *twist* $H \times H = (\Gamma, \Delta)$ to be a bipartite bigraph with vertex set $V' \cup V''$ and edge sets defined as follows.

- For any edge (u, v) of H , Γ contains edges (u', v') and (u'', v'') .
- For any edge (u, v) of H , Δ contains edges (u', v'') and (u'', v') .

In particular, if H is a bipartite affine ADE Dynkin diagram $\hat{\Lambda}$ then $H \times H$ is an affine \boxtimes affine ADE bigraph (see Corollary 8.4) which is called a *twist of type* $\hat{\Lambda} \times \hat{\Lambda}$. For $G = \hat{\Lambda} \times \hat{\Lambda}$, we have $\text{descr}(G) = \text{descr}(G^{\text{op}}) = \hat{\Lambda} \Leftrightarrow \hat{\Lambda}$ thus by Proposition 4.11, twists may not be uniquely determined by their description. See Figure 11 (or Figure 21) for an example.

5.2. Toric bigraphs. Let $\hat{\Lambda}$ be a bipartite affine ADE Dynkin diagram and let η be its automorphism (not necessarily of order two or color-preserving). For an integer $n \geq 1$, we define a *toric bigraph* $\mathcal{T}(\hat{\Lambda}, \eta, n) = (\Gamma, \Delta)$ as follows. The red connected components of $\mathcal{T}(\hat{\Lambda}, \eta, n)$ are C_1, C_2, \dots, C_n , and the restriction of Γ on each C_i has type $\hat{\Lambda}$. In particular, for each $i \in [n]$, let us fix a map $\phi_i : \text{Vert}(\hat{\Lambda}) \rightarrow C_i$

that induces an isomorphism between $\hat{\Lambda}$ and $\Gamma(C_i)$. Now, for every $i = 1, 2, \dots, n - 1$ and every vertex v of $\hat{\Lambda}$, Δ contains an edge $(\phi_i(v), \phi_{i+1}(v))$. Also, for every $v \in \text{Vert}(\hat{\Lambda})$, Δ contains an edge $(\phi_n(v), \phi_1(\eta(v)))$. Thus if one starts at some vertex $v \in C_1$ and follows the blue path that traverses the components $C_1, C_2, C_3, \dots, C_n, C_1$, one arrives at $\eta(v)$.

Lemma 5.2. *In the following cases, $\mathcal{T}(\hat{\Lambda}, \eta, n)$ is an affine \boxtimes affine ADE bigraph:*

- (1) η is color-reversing and $n \geq 3$ is odd;
- (2) η is color-preserving and $n \geq 2$ is even;
- (3) $n = 1$, η is color-reversing and does not send any vertex to one of its neighbors.

Proof. The fact that $\mathcal{T}(\hat{\Lambda}, \eta, n)$ is always recurrent is trivial to check, thus we only need to make sure that it is bipartite and that Γ and Δ do not share edges. This is easy to see and the result follows since the components of Γ and Δ are affine ADE Dynkin diagrams by construction. \square

If $G = \mathcal{T}(\hat{\Lambda}, \eta, n)$ is an affine \boxtimes affine ADE bigraph and $n > 1$ then $S(G) = A_{n-1}^{(1)}$ and $\text{descr}(G)$ equals

$$\hat{\Lambda} \text{ --- } \hat{\Lambda} \text{ --- } \cdots \text{ --- } \hat{\Lambda} \text{ --- } \hat{\Lambda} \text{ ,}$$

where the number of components is n . If $n = 1$ then $S(G) = \frac{1}{2}A_1^{(1)}$ and $\text{descr}(G)$ equals

$$\begin{array}{c} \cap \cap \\ \hat{\Lambda} \end{array} .$$

Even though the main purpose of this section is to produce many affine \boxtimes affine ADE bigraphs and not worry about which of them are isomorphic, we give a simple criterion for when two toric bigraphs are isomorphic.

Proposition 5.3. *Let $\hat{\Lambda}$ be an affine ADE Dynkin diagram and let $\text{Aut}(\hat{\Lambda})$ be the automorphism group of $\hat{\Lambda}$. Let $\eta, \eta' \in \text{Aut}(\hat{\Lambda})$ be two automorphisms of $\hat{\Lambda}$. Then the bigraphs $G = \mathcal{T}(\hat{\Lambda}, \eta, n)$ and $G' = \mathcal{T}(\hat{\Lambda}, \eta', n)$ are isomorphic if and only if η is conjugate to either η' or its inverse in $\text{Aut}(\hat{\Lambda})$.*

Proof. Suppose that there exists $g \in \text{Aut}(\hat{\Lambda})$ such that $\eta' = g\eta g^{-1}$. Consider a map from G to G' that applies g to each red connected

component of G . It is clear that this map provides an isomorphism between G and G' .

Suppose now that η and η' are inverses of each other. Then consider a map from G to G' that reverses the order of the red connected components. Again, this map clearly gives an isomorphism between G and G' .

Conversely, suppose that there is an isomorphism ψ between G and G' . Then it must either preserve or reverse the cyclic ordering of the red connected components C_1, C_2, \dots, C_n . But note that reversing their ordering just corresponds to replacing η with its inverse, and cyclically permuting the components does not change η , so we may assume that ψ sends C_i to C'_i for all $i \in [n]$. It follows that $(\phi'_i)^{-1} \circ \psi \circ \phi_i$ is the same element of $\text{Aut}(\hat{\Lambda})$ for all $i \in [n]$ where ϕ_i and ϕ'_i are the maps used in the definitions of $\mathcal{T}(\hat{\Lambda}, \eta, n)$ and $\mathcal{T}(\hat{\Lambda}, \eta', n)$. The result follows since conjugating by this element takes η to η' . \square

Let us say that a *weak conjugacy class* of an element g in a group H is the union of the conjugacy class of g with the conjugacy class of g^{-1} .

Thus in order to classify affine \boxtimes affine toric *ADE* bigraphs it suffices to list representatives of weak conjugacy classes in $\text{Aut}(\hat{\Lambda})$ for each affine *ADE* Dynkin diagram $\hat{\Lambda}$. Since for any even n we have $\mathcal{T}(\hat{\Lambda}, \text{id}, n) = \hat{\Lambda} \otimes \hat{A}_{n-1}$, we only list *non-identity weak conjugacy classes* of $\text{Aut}(\hat{\Lambda})$ in each case. Thus *we do not consider the case $\eta = \text{id}$ to be a toric bigraph in what follows*.

Remark 5.4. Whenever $\hat{\Lambda}$ is a diagram from Figure 4 and $\eta \in \text{Aut}(\hat{\Lambda})$, there is another diagram in Figure 4 which we denote $\hat{\Lambda}/\eta$. It is obtained from $\hat{\Lambda}$ by *folding via η* . This notion is standard but we do not define it rigorously here. Note that if $G = \mathcal{T}(\hat{\Lambda}, \eta, n)$ then $S(G^*)$ is exactly $\hat{\Lambda}/\eta$, and the label of a vertex v of $\hat{\Lambda}/\eta$ in $\text{descr}(G^*)$ is $A_{r_{n-1}}$ where r is the size of the preimage of v in $\hat{\Lambda}$ (i.e. v corresponds to an orbit of some vertex of $\hat{\Lambda}$ under η and r is the size of this orbit).

5.2.1. *The case $\hat{\Lambda} = \hat{A}_{2m-1}$.* In this case, $\text{Aut}(\hat{\Lambda})$ is isomorphic to $\text{Dih}(4m)$, the dihedral group of the $2m$ -gon with $4m$ elements. It contains a subgroup $\mathbb{Z}/2m\mathbb{Z}$ whose elements we represent by $\exp(\pi ik/m)$ for every residue k modulo $2m$ (that is, for every $k = 0, 1, \dots, 2m - 1$). There are $m + 2$ non-identity weak conjugacy classes in $\text{Aut}(\hat{\Lambda})$. The representatives of the first m of them are $\exp(\pi ik/m)$ for $k =$

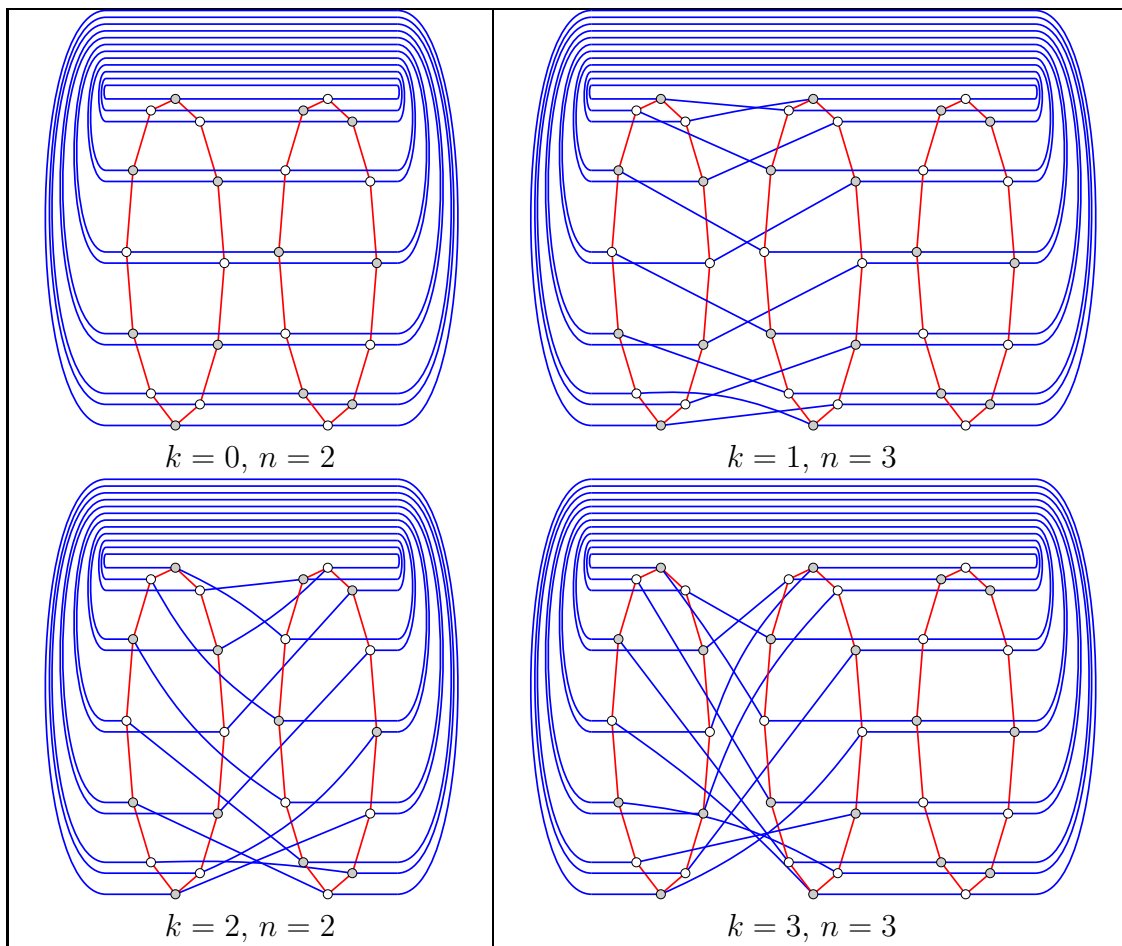


FIGURE 12. The family $\mathcal{T}(\hat{A}_{2m-1}, \exp(\pi ik/m), n)$ for $m = 6$, $k = 0, 1, 2, 3$, and $n = 2$ or $n = 3$ depending on the parity of k . In the classification in Section 6, this is family #3.

$1, 2, \dots, m$, see Figure 12. The other two are a *reflection about a diagonal* (denoted $\eta^{(1)}$) and a *reflection about a line joining the midpoints of two opposite edges* (denoted $\eta^{(2)}$), see Figure 13. For $k \in [m]$, $\exp(\pi ik/m)$ is color-preserving if and only if k is even. Additionally, $\eta^{(1)}$ is color-preserving while $\eta^{(2)}$ is color-reversing.

5.2.2. *The case $\hat{\Lambda} = \hat{D}_{m+2}$, $m \geq 3$.* Let us describe the group $\text{Aut}(\hat{\Lambda})$ in this case. Let u^+, u^- be two leaves of $\hat{\Lambda}$ that have a common neighbor, and let v^+, v^- be the other two leaves of $\hat{\Lambda}$. Let σ be the automorphism of $\hat{\Lambda}$ that switches u^+ and u^- and fixes the rest of $\hat{\Lambda}$. Similarly, let τ

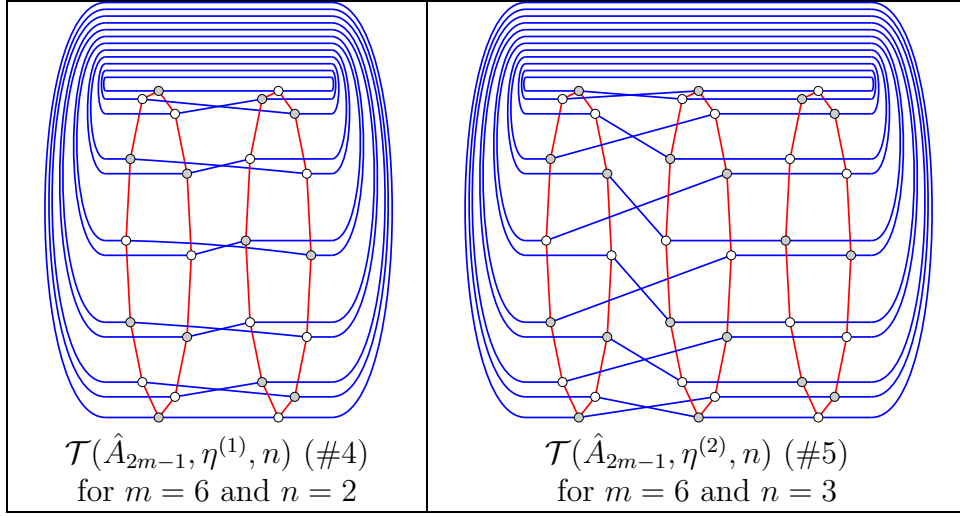


FIGURE 13. The other two families of toric bigraphs of type \hat{A} .

be the automorphism of $\hat{\Lambda}$ that switches u^+ with v^+ and u^- with v^- . It is non-trivial to see that $\text{Aut}(\hat{\Lambda})$ is isomorphic to the group $\text{Dih}(8)$ of symmetries of the square.⁴ It is clear that $\text{Aut}(\hat{\Lambda})$ is generated by σ and τ . There are four non-identity weak conjugacy classes in $\text{Aut}(\hat{\Lambda})$, and their representatives are

$$\sigma, \quad \sigma\tau\sigma\tau, \quad \tau, \quad \sigma\tau.$$

The first three elements have order 2 and the last element has order 4. The first two elements are always color-preserving while the last two elements are color-preserving if and only if m is even. If m is odd, the last two elements send some vertex to its neighbor. See Figure 14 for some examples.

5.2.3. *The case $\hat{\Lambda} = \hat{D}_4$.* In this case $\text{Aut}(\hat{\Lambda}) = \mathfrak{S}_4$, the symmetric group on four elements. Two permutations belong to the same (weak) conjugacy class if and only if they have the same cycle type, thus the weak conjugacy classes are in bijection with partitions λ of 4 which we denote by

$$(1 + 1 + 1 + 1), \quad (2 + 1 + 1), \quad (2 + 2), \quad (4), \quad (3 + 1).$$

Since $(1 + 1 + 1 + 1)$ corresponds to the identity permutation, we only need to consider the other four cases. The only case that we have not considered in the previous section is $(3 + 1)$, however, note that

⁴The vertices of the square are u^+, v^+, u^-, v^- in this cyclic order.

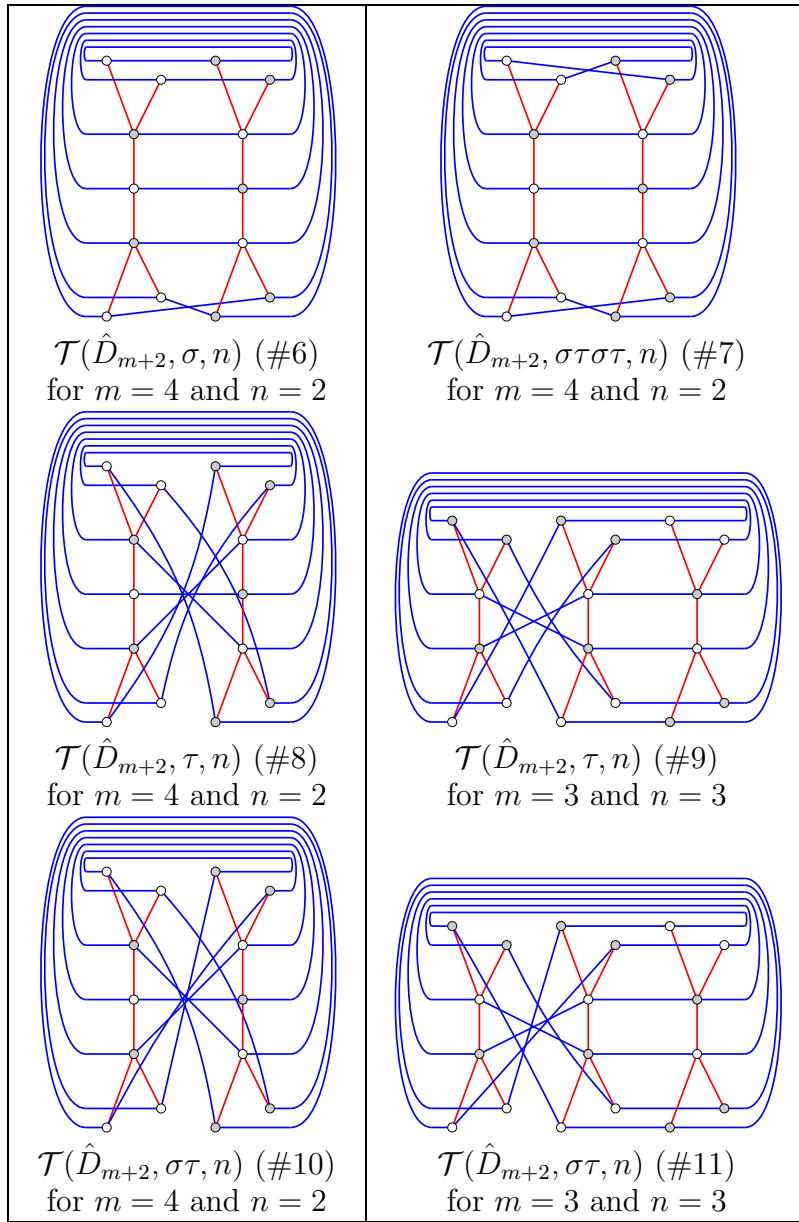
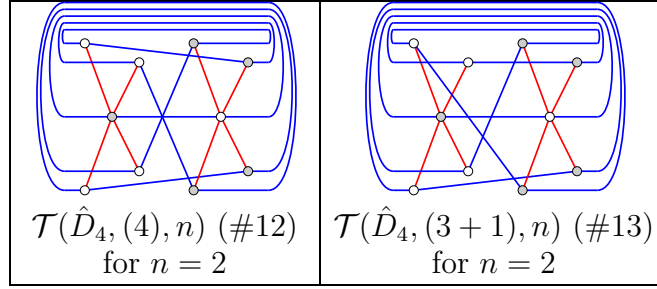
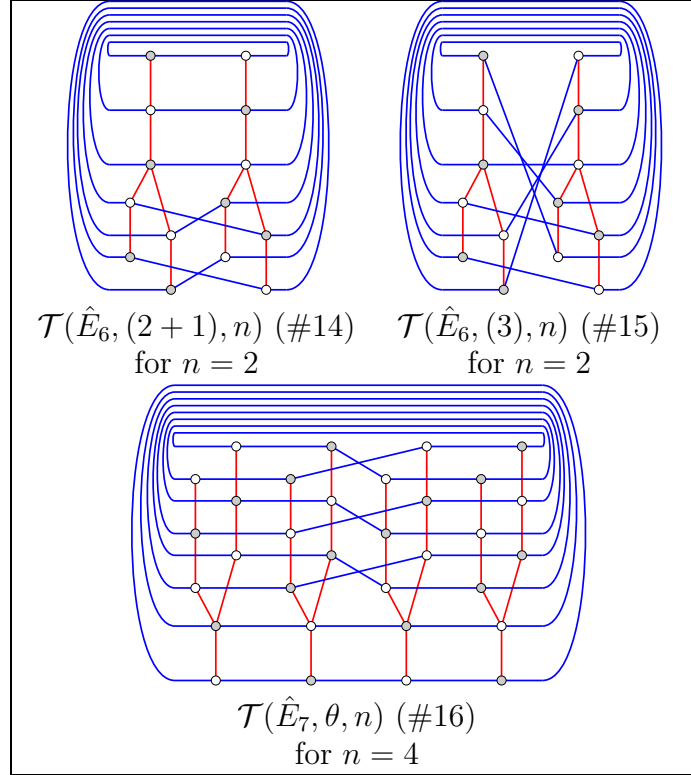


FIGURE 14. Toric bigraphs of type \hat{D}_{m+2} .

the permutations $\sigma\tau\sigma\tau$ and τ were not conjugate for $m \geq 3$ but are conjugate for $m = 2$ since they both have cycle type $(2+2)$. In the classification, we treat σ as a representative of $(2+1+1)$ and $\sigma\tau\sigma\tau$ as a representative of $(2+2)$ which naturally includes \hat{D}_4 as a special $m = 2$ case of \hat{D}_{m+2} . The cases (4) and $(3+1)$ are listed in the classification as separate items, see also Figure 15.

FIGURE 15. Additional toric bigraphs of type \hat{D}_4 .FIGURE 16. Toric bigraphs of type \hat{E} .

5.2.4. *The case $\hat{\Lambda} = \hat{E}_6$.* In this case $\text{Aut}(\hat{\Lambda}) = \mathfrak{S}_3$ so the non-identity weak conjugacy classes correspond precisely to partitions $(2 + 1)$ and (3) , see Figure 16 (top).

5.2.5. *The case $\hat{\Lambda} = \hat{E}_7$.* The only non-trivial automorphism θ of $\hat{\Lambda}$ has order 2 and thus the only affine \boxtimes affine toric ADE bigraphs of

the form $\mathcal{T}(\hat{E}_7, \eta, n)$ have n even and coincide with $G = \mathcal{T}(\hat{E}_7, \theta, n)$, see Figure 16 (bottom).

5.2.6. *The case $\hat{\Lambda} = \hat{E}_8$.* In this case $\text{Aut}(\hat{\Lambda}) = \{\text{id}\}$ so there are no non-identity conjugacy classes.

5.3. Path bigraphs. In this section, we would like to give a list of bigraphs G with $S(G)$ being a path with two double arrows at the ends, that is,

$$S(G) \in \{D_{\ell+1}^{(2)}, C_{\ell}^{(1)}, A_{2\ell}^{(2)}\}.$$

Let us revisit the classification of affine \boxtimes finite double bindings with $\text{scf} = (2, 1)$ classified in Figure 9. Consider such a double binding G with red components X of type $\hat{\Lambda}$ and Y of type $\hat{\Lambda}'$ so that $\text{descr}(G)$ equals $\hat{\Lambda} \Rightarrow \hat{\Lambda}'$. Thus every blue component of G has type A_3 , in particular, every vertex v of X either has blue degree 2 (in which case we set $v' := v$) or there exists a unique other vertex $v' \in X$ that belongs to the same blue connected component of v . One easily checks that this construction defines a color-preserving involution $\alpha \in \text{Aut}(\hat{\Lambda})$ via $\alpha(v) = v'$. Similarly, we define a color-preserving involution $\beta \in \text{Aut}(\hat{\Lambda}')$.

One easily checks that for every affine ADE Dynkin diagram $\hat{\Lambda}$ and every color-preserving involution $\alpha \in \text{Aut}(\hat{\Lambda})$ (except for the identity in types \hat{D} and \hat{E}), the pair $(\hat{\Lambda}, \alpha)$ appears in Figure 9 exactly once in this way. Here we consider α up to conjugation. In particular, let us rewrite for each double binding in Figure 9 the corresponding pairs $(\hat{\Lambda}, \alpha)$ that it involves (we use the description of conjugacy classes from the previous section):

$$(5.1) \quad \begin{aligned} (\hat{D}_{m+2}, \sigma\tau\sigma\tau) &\Rightarrow (\hat{A}_{2m-1}, \eta^{(1)}); & (\hat{D}_{2m+2}, \tau) &\Rightarrow (\hat{D}_{m+2}, \sigma); \\ (\hat{A}_{4m-1}, \exp(\pi i)) &\Rightarrow (\hat{A}_{2m-1}, \text{id}); & (\hat{E}_7, \theta) &\Rightarrow (\hat{E}_6, (2+1)). \end{aligned}$$

Definition 5.5. Let $\hat{\Lambda}$ be an affine ADE Dynkin diagram and consider two color-preserving non-identity involutions $\alpha, \beta \in \text{Aut}(\hat{\Lambda})$. Given a positive integer $n \geq 2$, The *path bigraph* $\mathcal{P}(\hat{\Lambda}, \alpha, \beta, n)$ is an affine \boxtimes affine ADE bigraph G obtained from the tensor product $\hat{\Lambda} \otimes A_{n-1}$ by attaching on the left a double binding from (5.1) involving $(\hat{\Lambda}, \alpha)$ and attaching on the right a double binding from (5.1) involving $(\hat{\Lambda}, \beta)$.

See Figures 17–20 for examples. It is clear that any path bigraph is always an affine \boxtimes affine ADE bigraph since all the blue components are of types \hat{A} or \hat{D} . Just as in the previous section, we give a simple criterion for when two path bigraphs are isomorphic.

Proposition 5.6. *Two path bigraphs $G = \mathcal{P}(\hat{\Lambda}, \alpha, \beta, n)$ and $G' = \mathcal{P}(\hat{\Lambda}', \alpha', \beta', n')$ are isomorphic if and only if $\hat{\Lambda} = \hat{\Lambda}'$, $n = n'$, and there exists an element $g \in \text{Aut}(\hat{\Lambda})$ such that at least one of the following holds:*

- $g\alpha g^{-1} = \alpha'$ and $g\beta g^{-1} = \beta'$, or
- $g\alpha g^{-1} = \beta'$ and $g\beta g^{-1} = \alpha'$.

Proof. Let C_1, \dots, C_{n+1} be the red components of G and C'_1, \dots, C'_{n+1} be the red components of G' . Since the red component graph of G is a path, an isomorphism $\phi : \text{Vert}(G) \rightarrow \text{Vert}(G')$ either flips it or preserves it. In the former case, ϕ sends C_i to C'_i and in the former case ϕ sends C_i to C'_{n+2-i} isomorphically in both cases. Suppose that ϕ sends C_i to C'_i for all $i \in [n+1]$. Consider a vertex $v \in C_2$. If $\alpha(v) = v$ then v has blue degree 2 in $G(C_1, C_2)$ so $\phi(v)$ must have blue degree 2 in $G(C'_1, C'_2)$ and thus $\alpha'(\phi(v)) = \phi(v)$. Similarly, if there is a blue path of length 2 from v to $u = \alpha(v) \in C_2$ through C_1 then there must be a blue path of length 2 from $\phi(v)$ to $\phi(u)$ in C'_2 through C'_1 . The conclusion is that $\phi \circ \alpha = \alpha' \circ \phi$. Similarly we get that $\phi \circ \beta = \beta' \circ \phi$ so we can just put g to be the restriction of ϕ to C_2 or C_m (they have to coincide). The case when ϕ sends C_i to C'_{n+2-i} is completely analogous. This shows one direction of the proposition. The converse direction is shown in a way similar to the proof of Proposition 5.3 and we leave it as an exercise for the reader. \square

Thus isomorphism classes of path bigraphs correspond to (unordered) pairs of color-preserving involutions modulo simultaneous conjugation. Let us say that two pairs (α, β) and (α', β') related by these transformations are *equivalent*. Note that we can always conjugate α to be a specific fixed representative of a conjugacy class from the previous section, and after that β will be determined up to conjugation by an element from the *centralizer* of α , that is, by an element $g \in \text{Aut}(\hat{\Lambda})$ (not necessarily color-preserving) that commutes with α . We are ready to list all pairs of involutions from (5.1) that give non-isomorphic path bigraphs.

Remark 5.7. We list $\text{descr}(G)$ and $\text{descr}(G^*)$ for path bigraphs in Section 6. We give the following informal explanation on how to quickly compute $\text{descr}(G^*)$ when $G = \mathcal{P}(\hat{\Lambda}, \alpha, \beta, n)$. Since α and β are involutions, they define a matching on $\text{Vert}(\hat{\Lambda})$. Superimposing these matchings yields several cycles and paths. Each path with r vertices corresponds to a node labeled \hat{D}_{rn+2} in $\text{descr}(G^*)$. Each cycle with r vertices corresponds to a node labeled \hat{A}_{rn-1} in $\text{descr}(G^*)$. The Dynkin

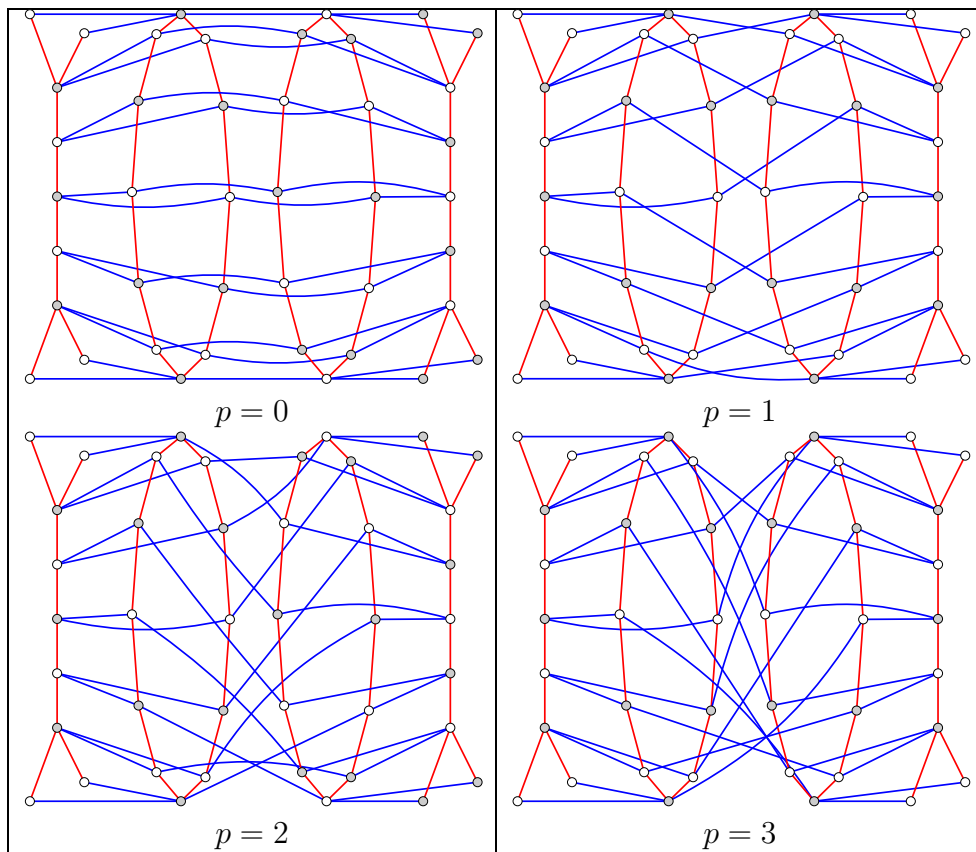


FIGURE 17. Path bigraphs of the form $\mathcal{P}(\hat{A}_{2m-1}, \eta^{(1)}, \eta_p, n)$ for $m = 6$, $n = 3$, and $p = 0, 1, 2, 3$. The case $p = 1$ belongs to family #18, the remaining cases $p = 0, 2, 3$ belong to family #17.

diagram $S(G^*)$ is obtained from $\hat{\Lambda}$ by *folding* via the subgroup generated by α and β .

5.3.1. *The case $\hat{\Lambda} = \hat{A}_{2m-1}$.* There are three color-preserving involutions in (5.1) for type \hat{A}_{2m-1} :

- a reflection about a diagonal $\eta^{(1)}$ for $m \geq 2$,
- a 180° rotation $\exp(\pi i)$ for even m , and
- the identity id for $m \geq 1$.

Note that for the last two cases, the size of the conjugacy class is equal to 1. For the case $\eta^{(1)}$, the conjugacy class consists of m reflections which we denote $\eta_0 = \eta^{(1)}, \eta_1, \dots, \eta_{m-1}$ in the cyclic order. The elements that commute with $\eta^{(1)}$ are $\text{id}, \eta^{(1)}, \exp(\pi i)$, and a reflection η_0^\perp that switches the two fixed points of $\eta^{(1)}$. Conjugating η_p for $p \in [m-1]$

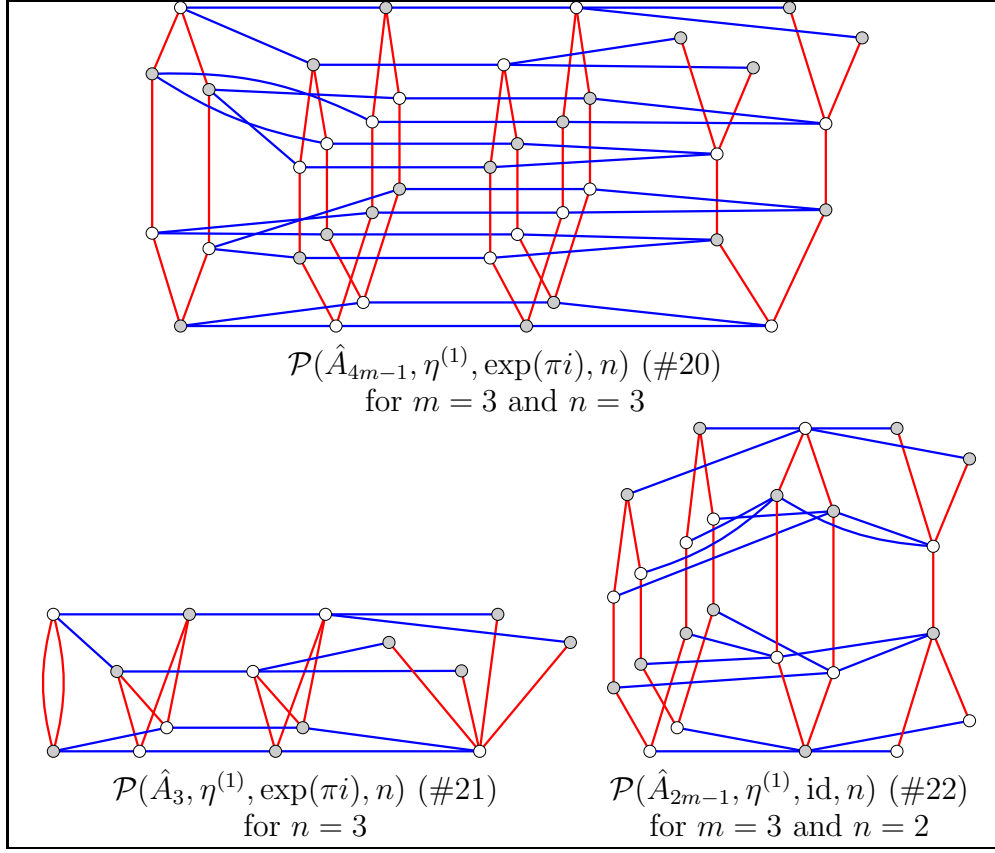


FIGURE 18. The remaining (non-toric) path bigraphs of type \hat{A} .

by $\eta^{(1)}$ or by η_0^\perp produces the reflection η_{m-p} . Thus the list of all the non-equivalent pairs in this case is:

- $(\eta^{(1)}, \eta_p)$ for $1 \leq p \leq m/2$;
- $(\eta^{(1)}, \exp(\pi i))$ when m is even;
- $(\eta^{(1)}, \text{id})$;
- $(\exp(\pi i), \exp(\pi i))$ when m is even;
- $(\exp(\pi i), \text{id})$ when m is even;
- (id, id) .

All the cases are possible for $m \geq 2$ except for the last case which is possible for $m \geq 1$. For the last three cases, G^* is a toric bigraph and thus G will not be listed as a path bigraph in the classification. The first case is shown in Figure 17, and the second and third cases are shown in Figure 18.

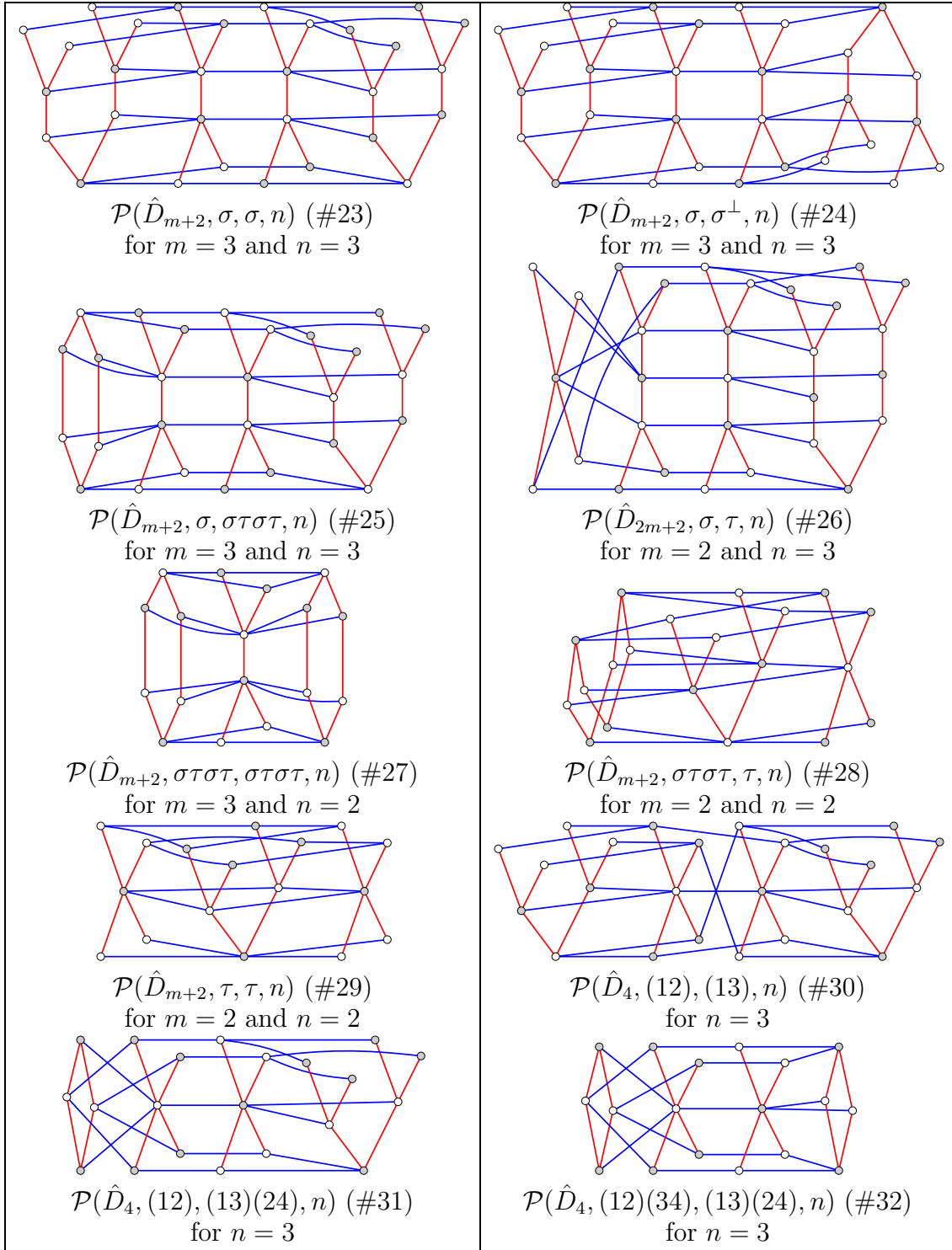


FIGURE 19. Path bigraphs of type \hat{D} .

5.3.2. *The case $\hat{\Lambda} = \hat{D}_{m+2}$, $m \geq 3$.* The three involutions from (5.1) in this case are σ , $\sigma\tau\sigma\tau$, and τ when m is even. We see that σ has conjugacy class $\{\sigma, \sigma^\perp\}$ of size 2, $\sigma\tau\sigma\tau$ has conjugacy class of size 1, and τ has conjugacy class τ, τ^\perp of size 2. Conjugating τ by σ gives τ^\perp . Thus in this case the list of all non-equivalent pairs is as follows:

- (σ, σ) ;
- (σ, σ^\perp) ;
- $(\sigma, \sigma\tau\sigma\tau)$;
- (σ, τ) when m is even;
- $(\sigma\tau\sigma\tau, \sigma\tau\sigma\tau)$;
- $(\sigma\tau\sigma\tau, \tau)$ when m is even;
- (τ, τ) when m is even.
- (τ, τ^\perp) when m is even.

The last case will not appear in the classification as the bigraph $\mathcal{P}(\hat{D}_{2m+2}, \tau, \tau^\perp, n)$ is dual to $\mathcal{P}(\hat{A}_{2n-1}, \eta^{(1)}, \text{id}, m)$. The rest of the cases are shown in Figure 19.

5.3.3. *The case $\hat{\Lambda} = \hat{D}_4$.* In this case, $\text{Aut}(\hat{D}_4)$ is the symmetric group \mathfrak{S}_4 so we write elements in the cycle notation. For example, the permutation (12) is the transposition of 1 and 2. The involutions from (5.1) now split into two conjugacy classes: $(2+1+1)$ of size 6 and $(2+2)$ of size 3 with respective representatives (12) and (12)(34). The centralizer of each of the permutations is generated by the transpositions (12) and (34). Therefore we get the following list of non-equivalent pairs:

- $((12), (12))$;
- $((12), (34))$;
- $((12), (13))$;
- $((12), (12)(34))$;
- $((12), (13)(24))$;
- $((12)(34), (12)(34))$;
- $((12)(34), (13)(24))$.

Just as for toric bigraphs, the case of \hat{D}_4 naturally becomes a special case of \hat{D}_{m+2} when all the permutations involved belong to the set

$$\{\sigma = (12), \sigma^\perp = (34), \sigma\tau\sigma\tau = (12)(34)\}.$$

See Figure 19 for examples.

5.3.4. *The case $\hat{\Lambda} = \hat{E}_6$.* In this case $\text{Aut}(\hat{\Lambda}) = \mathfrak{S}_3$ so there is just one conjugacy class $(2+1)$ from (5.1) with three permutations (12), (13), and (23). The centralizer of (12) is just $\{\text{id}, (12)\}$ and conjugating (13) by (12) produces (23). Thus we get only two non-equivalent pairs:

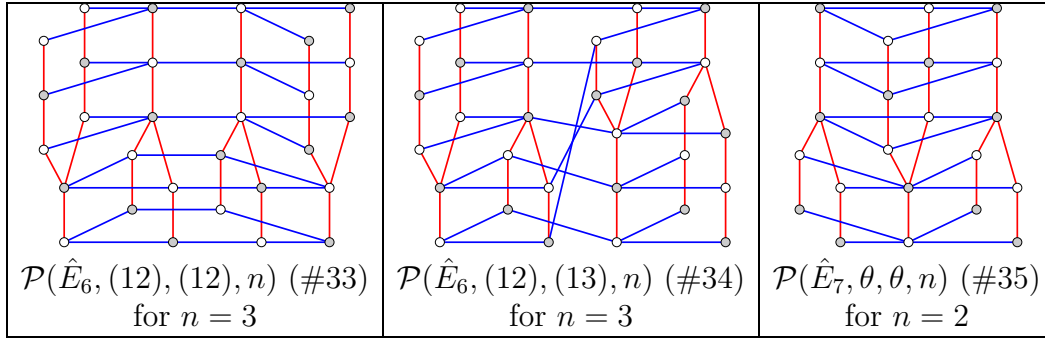


FIGURE 20. Path bigraphs of type \hat{E} .

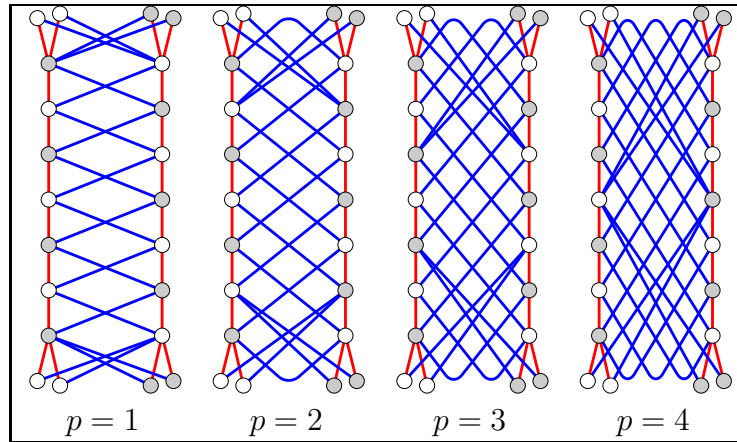


FIGURE 21. Pseudo twists $\hat{D}_{m+2} \times_p \hat{D}_{m+2}$ for $m = 8$ and $p = 1, 2, 3, 4$. The cases $p = 1, 3$ belong to family #19 while the cases $p = 2, 4$ belong to family #18.

- $((12), (12))$;
- $((12), (13))$.

See Figure 20.

5.3.5. *The case $\hat{\Lambda} = \hat{E}_7$.* The only involution in (5.1) is θ so the only pair that we can have here is (θ, θ) , see Figure 20.

5.4. **Pseudo twists of type $\hat{D}_{m+2} \times_p \hat{D}_{m+2}$.** Let X and Y be two red components of type \hat{D}_{m+2} . Label the vertices of X by

$$u_0^+, u_0^-, u_1, u_2, \dots, u_{m-1}, u_m^+, u_m^-$$

so that the leaves u_0^+ and u_0^- are connected to u_1 and the leaves u_m^+ and u_m^- are connected to u_{m-1} . Let $p \in [m - 1]$ be an integer. We denote

by $X_0, X_1, X_2, \dots, X_{m+p}$ a sequence of subsets of X defined as follows:

$$\begin{aligned} X_0 &= \{u_0^+, u_0^-\}, X_1 = \{u_1\}, \dots, X_{m-1} = \{u_{m-1}\}, X_m = \{u_m^+, u_m^-\}, \\ X_{m+1} &= X_{m-1}, X_{m+2} = X_{m-2}, \dots, X_{m+p} = X_{m-p}. \end{aligned}$$

We similarly label the vertices of Y by

$$v_0^+, v_0^-, v_1, v_2, \dots, v_{m-1}, v_m^+, v_m^-$$

and introduce the subsets $Y_0, Y_1, Y_2, \dots, Y_{m+p}$.

Definition 5.8. The bigraph $\hat{D}_{m+2} \times_p \hat{D}_{m+2} = (\Gamma, \Delta)$ is a double binding with two red components X and Y as above and blue edges as follows: for every $i \in \{0, 1, \dots, m\}$, connect every vertex in X_i with every vertex in Y_{i+p} and every vertex in Y_i with every vertex in X_{i+p} by an edge of Δ .

An example is given in Figure 21. It is easy to see that for every $p \in [m-1]$, $G = \hat{D}_{m+2} \times_p \hat{D}_{m+2}$ is an affine \boxtimes affine ADE bigraph with $S(G) = A_1^{(1)}$ and

$$\text{descr}(G) = \hat{D}_{m+2} \Leftrightarrow \hat{D}_{m+2} .$$

Note that the case $p = 1$ recovers the twist $\hat{D}_{m+2} \times \hat{D}_{m+2}$.

5.5. Five exceptional affine \boxtimes affine double bindings. In this section we list five affine \boxtimes affine ADE bigraphs G such that both $S(G)$ and $S(G^*)$ are equal to either $A_1^{(1)}$ or $A_2^{(2)}$. This is equivalent to saying that both G and G^* are affine \boxtimes affine double bindings. As we will see later in Section 7, these five bigraphs are the only affine \boxtimes affine ADE bigraphs with this property that do not belong to any of the infinite families that we have already constructed in the previous sections. The five bigraphs are shown in Figure 22.

6. THE CLASSIFICATION OF AFFINE \boxtimes AFFINE ADE BIGRAPHS

Theorem 6.1. *Let G be an affine \boxtimes affine ADE bigraph. Then either of the following is true.*

- *Both G and G^* appear exactly once in the below list. They are members of the same self-dual family.*
- *The below list contains a unique bigraph that is isomorphic to either G or G^* .*

Here we say that a *self-dual family of bigraphs* is a collection of bigraphs that is closed under taking duals. In the below list, such families are marked with [SD].

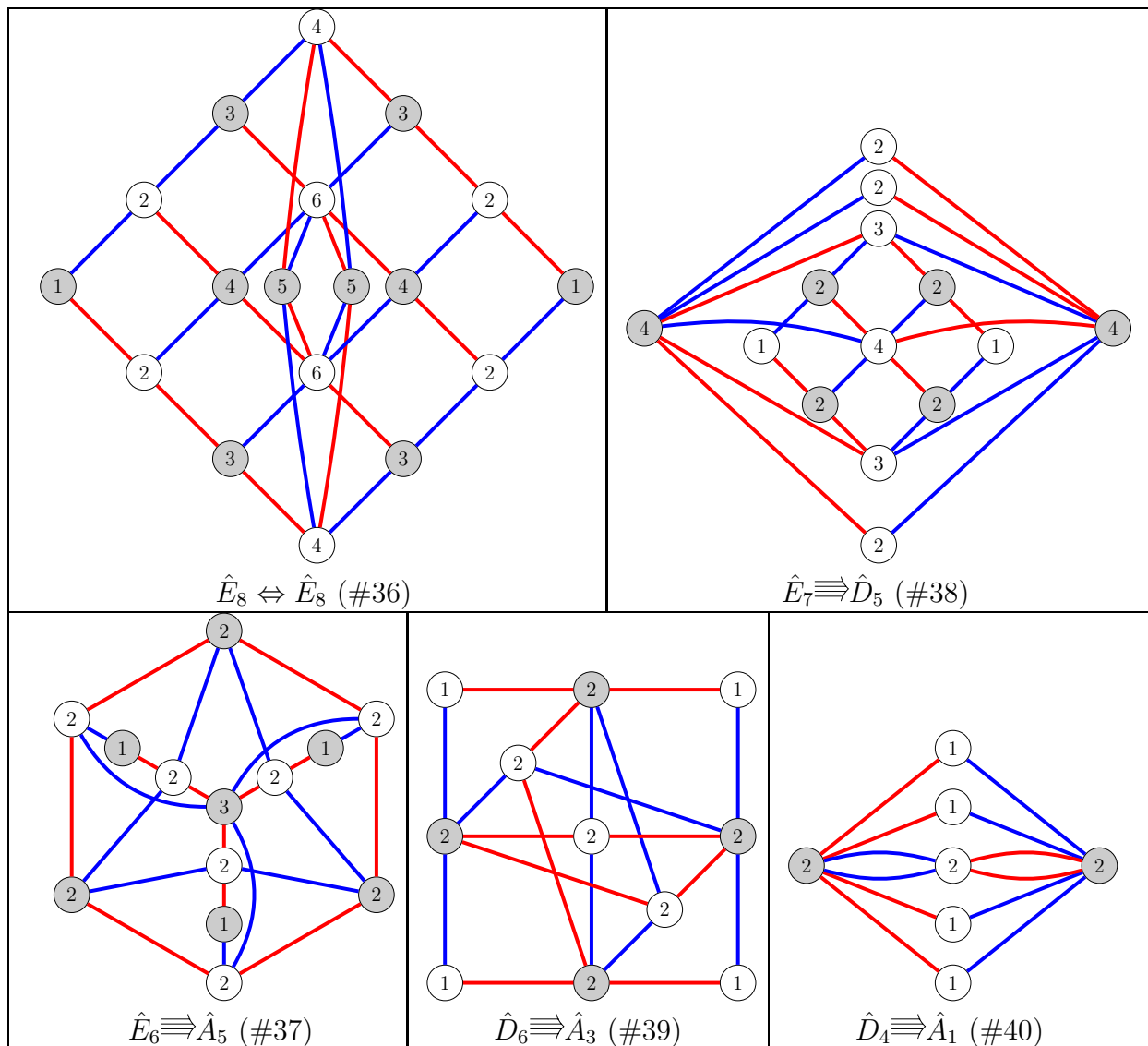


FIGURE 22. Five exceptional affine \boxtimes affine double bindings given together with their subadditive functions. Each double binding G is *self-dual*, i.e., is isomorphic to G^* .

For each affine \boxtimes affine ADE bigraph G , define the *Kac quadruple* of G to be one of the following tables:

$S(G)$	$\text{descr}(G)$
$S(G^*)$	$\text{descr}(G^*)$

OR

$S(G)$	$\text{descr}(G)$	$S(G^*)$	$\text{descr}(G^*)$
--------	-------------------	----------	---------------------

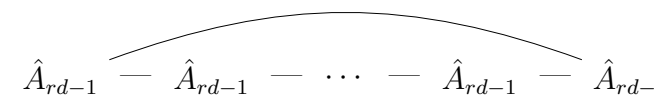
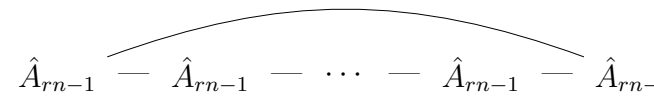
We list each family of affine \boxtimes affine *ADE* bigraphs together with its parameters and the corresponding Kac quadruples, except that we do not list the Kac quadruples for tensor products. For exceptional families, we just give Kac quadruples (KQ for short) and omit the name and parameters.

#1. [SD] (Fig. 1) **Name:** a tensor product $\hat{\Lambda} \otimes \hat{\Lambda}'$. **Parameters:** $\hat{\Lambda}$, $\hat{\Lambda}'$ — two bipartite affine *ADE* Dynkin diagrams.

#2. [SD] (Fig. 11) **Name:** a twist $\hat{\Lambda} \times \hat{\Lambda}$. **Parameters:** a bipartite affine *ADE* Dynkin diagram $\hat{\Lambda}$. **KQ:**

$A_1^{(1)}$	$\hat{\Lambda} \Leftrightarrow \hat{\Lambda}$	$A_1^{(1)}$	$\hat{\Lambda} \Leftrightarrow \hat{\Lambda}$
-------------	---	-------------	---

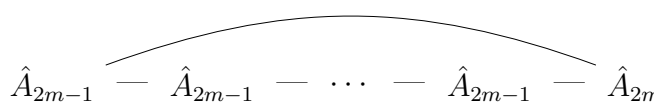
#3. [SD] (Fig. 12) **Name:** $\mathcal{T}(\hat{A}_{rd-1}, \exp(2\pi ip/r), n)$. **Parameters:** $r \geq 1$ and $1 \leq p \leq r/2$ coprime with r ; $n, d \geq 1$ such that either n, d are both even or n, d, p are odd and r is even. The forbidden cases are $n = d = p = 1$, r even (in which case Γ and Δ share edges) and $n = d = 2, p = 1, r \geq 1$ (in which case G is a twist $\hat{A}_{2r-1} \times \hat{A}_{2r-1}$). **KQ:**

$A_{n-1}^{(1)}$	$\hat{A}_{rd-1} \text{ --- } \hat{A}_{rd-1} \text{ --- } \cdots \text{ --- } \hat{A}_{rd-1} \text{ --- } \hat{A}_{rd-1}$ 
$A_{d-1}^{(1)}$	$\hat{A}_{rn-1} \text{ --- } \hat{A}_{rn-1} \text{ --- } \cdots \text{ --- } \hat{A}_{rn-1} \text{ --- } \hat{A}_{rn-1}$ 

The dual bigraph is $\mathcal{T}(\hat{A}_{rn-1}, \exp(2\pi iq/r), d)$, where $1 \leq q \leq r/2$ is the unique integer satisfying $pq \equiv \pm 1 \pmod{r}$. For the case $n = 1$ (resp., $d = 1$), we have

$$\text{descr}(G) = \hat{A}_{rd-1}^{\cap \cap}, \quad \text{resp.}, \quad \text{descr}(G^*) = \hat{A}_{rn-1}^{\cap \cap}.$$

#4. (Fig. 13) **Name:** $\mathcal{T}(\hat{A}_{2m-1}, \eta^{(1)}, n)$. **Parameters:** $m \geq 2$; $n \geq 2$ even. **KQ:**

$A_{n-1}^{(1)}$	$\hat{A}_{2m-1} \text{ --- } \hat{A}_{2m-1} \text{ --- } \cdots \text{ --- } \hat{A}_{2m-1} \text{ --- } \hat{A}_{2m-1}$ 
$D_{m+1}^{(2)}$	$\hat{A}_{n-1} \Leftarrow \hat{A}_{2n-1} \text{ --- } \cdots \text{ --- } \hat{A}_{2n-1} \Rightarrow \hat{A}_{n-1}$

The dual bigraph is $\mathcal{P}(\hat{A}_{2n-1}, \exp(\pi i), \exp(\pi i), m)$.

- #5. (Fig. 13) **Name:** $\mathcal{T}(\hat{A}_{2m-1}, \eta^{(2)}, n)$. **Parameters:** $m \geq 2; n \geq 3$ odd. **KQ:**

$A_{n-1}^{(1)}$	$\hat{A}_{2m-1} \text{ --- } \hat{A}_{2m-1} \text{ --- } \cdots \text{ --- } \hat{A}_{2m-1} \text{ --- } \hat{A}_{2m-1}$
$\frac{1}{2}A_{2m-1}^{(1)}$	$\hat{A}_{2n-1} \text{ --- } \hat{A}_{2n-1} \text{ --- } \cdots \text{ --- } \hat{A}_{2n-1} \text{ --- } \hat{A}_{2n-1}$

- #6. (Fig. 14) **Name:** $\mathcal{T}(\hat{D}_{m+2}, \sigma, n)$. **Parameters:** $m \geq 2; n \geq 2$ even. **KQ:**

$A_{n-1}^{(1)}$	$\hat{D}_{m+2} \text{ --- } \hat{D}_{m+2} \text{ --- } \cdots \text{ --- } \hat{D}_{m+2} \text{ --- } \hat{D}_{m+2}$
$A_{2m+1}^{(2)}$	$\hat{A}_{n-1} \text{ --- } \hat{A}_{n-1} \text{ --- } \cdots \text{ --- } \hat{A}_{n-1} \Leftarrow \hat{A}_{2n-1}$

- #7. (Fig. 14) **Name:** $\mathcal{T}(\hat{D}_{m+2}, \sigma\tau\sigma\tau, n)$. **Parameters:** $m \geq 2; n \geq 2$ even. **KQ:**

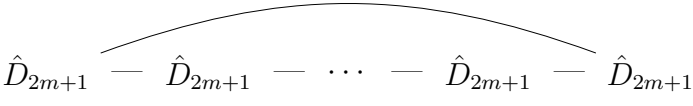

$A_{n-1}^{(1)}$	$\hat{D}_{m+2} \text{ --- } \hat{D}_{m+2} \text{ --- } \cdots \text{ --- } \hat{D}_{m+2} \text{ --- } \hat{D}_{m+2}$
$C_m^{(1)}$	$\hat{A}_{2n-1} \Rightarrow \hat{A}_{n-1} \text{ --- } \cdots \text{ --- } \hat{A}_{n-1} \Leftarrow \hat{A}_{2n-1}$

The dual bigraph is $\mathcal{P}(\hat{A}_{n-1}, \text{id}, \text{id}, m)$.

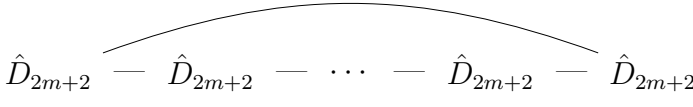
- #8. (Fig. 14) **Name:** $\mathcal{T}(\hat{D}_{2m+2}, \tau, n)$. **Parameters:** $m \geq 2; n \geq 2$ even. **KQ:**

$A_{n-1}^{(1)}$	$\hat{D}_{2m+2} \text{ --- } \hat{D}_{2m+2} \text{ --- } \cdots \text{ --- } \hat{D}_{2m+2} \text{ --- } \hat{D}_{2m+2}$
$B_{m+1}^{(1)}$	$\hat{A}_{2n-1} \text{ --- } \hat{A}_{2n-1} \text{ --- } \cdots \text{ --- } \hat{A}_{2n-1} \Rightarrow \hat{A}_{n-1}$

- #9. (Fig. 14) **Name:** $\mathcal{T}(\hat{D}_{2m+1}, \tau, n)$. **Parameters:** $m \geq 2; n \geq 3$ odd. **KQ:**

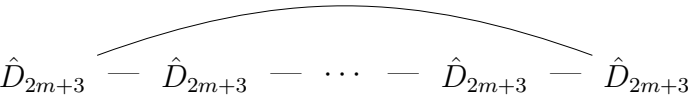
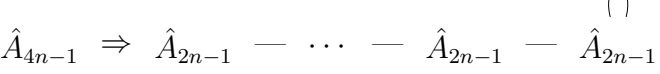
$A_{n-1}^{(1)}$	$\hat{D}_{2m+1} \text{ --- } \hat{D}_{2m+1} \text{ --- } \cdots \text{ --- } \hat{D}_{2m+1} \text{ --- } \hat{D}_{2m+1}$ 
$\frac{1}{2}D_{2m+1}^{(1)}$	\hat{A}_{2n-1} 

#10. (Fig. 14) **Name:** $\mathcal{T}(\hat{D}_{2m+2}, \sigma\tau, n)$. **Parameters:** $m \geq 2$; $n \geq 2$ even. **KQ:**


$A_{n-1}^{(1)}$	$\hat{D}_{2m+2} \text{ --- } \hat{D}_{2m+2} \text{ --- } \cdots \text{ --- } \hat{D}_{2m+2} \text{ --- } \hat{D}_{2m+2}$ 
$A_{2m}^{(2)}$	$\hat{A}_{n-1} \Leftarrow \hat{A}_{2n-1} \text{ --- } \cdots \text{ --- } \hat{A}_{2n-1} \Leftarrow \hat{A}_{4n-1}$

The dual bigraph is $\mathcal{P}(\hat{A}_{2n-1}, \exp(\pi i), \text{id}, m)$.


#11. (Fig. 14) **Name:** $\mathcal{T}(\hat{D}_{2m+3}, \sigma\tau, n)$. **Parameters:** $m \geq 1$; $n \geq 3$ odd. **KQ:**

$A_{n-1}^{(1)}$	$\hat{D}_{2m+3} \text{ --- } \hat{D}_{2m+3} \text{ --- } \cdots \text{ --- } \hat{D}_{2m+3} \text{ --- } \hat{D}_{2m+3}$ 
$\frac{1}{2}C_{2m+1}^{(1)}$	$\hat{A}_{4n-1} \Rightarrow \hat{A}_{2n-1} \text{ --- } \cdots \text{ --- } \hat{A}_{2n-1} \text{ --- } \hat{A}_{2n-1}$ 

#12. (Fig. 15) **Name:** $\mathcal{T}(\hat{D}_4, (4), n)$. **Parameters:** $n \geq 2$ even. **KQ:**

$A_{n-1}^{(1)}$	$\hat{D}_4 \text{ --- } \hat{D}_4 \text{ --- } \cdots \text{ --- } \hat{D}_4 \text{ --- } \hat{D}_4$ 
$A_2^{(2)}$	$\hat{A}_{n-1} \Leftarrow \hat{A}_{4n-1}$

#13. (Fig. 15) **Name:** $\mathcal{T}(\hat{D}_4, (3+1), n)$. **Parameters:** $n \geq 2$ even. **KQ:**

$A_{n-1}^{(1)}$	$\hat{D}_4 \text{ --- } \hat{D}_4 \text{ --- } \cdots \text{ --- } \hat{D}_4 \text{ --- } \hat{D}_4$ 
$D_4^{(3)}$	$\hat{A}_{n-1} \text{ --- } \hat{A}_{n-1} \Leftarrow \hat{A}_{3n-1}$

- #14. (Fig. 16) **Name:** $\mathcal{T}(\hat{E}_6, (2+1), n)$. **Parameters:** $n \geq 2$ even. **KQ:**

$A_{n-1}^{(1)}$	$\hat{E}_6 \text{ --- } \hat{E}_6 \text{ --- } \cdots \text{ --- } \hat{E}_6 \text{ --- } \hat{E}_6$
$E_6^{(2)}$	$\hat{A}_{n-1} \text{ --- } \hat{A}_{n-1} \text{ --- } \hat{A}_{n-1} \Leftrightarrow \hat{A}_{2n-1} \text{ --- } \hat{A}_{2n-1}$

- #15. (Fig. 16) **Name:** $\mathcal{T}(\hat{E}_6, (3), n)$. **Parameters:** $n \geq 2$ even. **KQ:**

$A_{n-1}^{(1)}$	$\hat{E}_6 \text{ --- } \hat{E}_6 \text{ --- } \cdots \text{ --- } \hat{E}_6 \text{ --- } \hat{E}_6$
$G_2^{(1)}$	$\hat{A}_{3n-1} \text{ --- } \hat{A}_{3n-1} \Rightarrow \hat{A}_{n-1}$

- #16. (Fig. 16) **Name:** $\mathcal{T}(\hat{E}_7, \theta, n)$. **Parameters:** $n \geq 2$ even. **KQ:**

$A_{n-1}^{(1)}$	$\hat{E}_7 \text{ --- } \hat{E}_7 \text{ --- } \cdots \text{ --- } \hat{E}_7 \text{ --- } \hat{E}_7$
$F_4^{(1)}$	$\hat{A}_{2n-1} \text{ --- } \hat{A}_{2n-1} \text{ --- } \hat{A}_{2n-1} \Rightarrow \hat{A}_{n-1} \text{ --- } \hat{A}_{n-1}$

- #17. [SD] (Fig. 17) **Name:** $\mathcal{P}(\hat{A}_{2rd-1}, \eta^{(1)}, \eta_{pd}, n)$. **Parameters:** $n, d \geq 2$; $r \geq 1$; $1 \leq p \leq r/2$ coprime with $r \geq 2$ or $p = 0$ if $r = 1$. **KQ:**

$C_n^{(1)}$	$\hat{D}_{rd+2} \Rightarrow \hat{A}_{2rd-1} \text{ --- } \cdots \text{ --- } \hat{A}_{2rd-1} \Leftarrow \hat{D}_{rd+2}$
$C_d^{(1)}$	$\hat{D}_{rn+2} \Rightarrow \hat{A}_{2rn-1} \text{ --- } \cdots \text{ --- } \hat{A}_{2rn-1} \Leftarrow \hat{D}_{rn+2}$

The dual bigraph is $\mathcal{P}(\hat{A}_{2rn-1}, \eta^{(1)}, \eta_{qn}, d)$, where $1 \leq q \leq r/2$ is defined by $pq \equiv \pm 1 \pmod{r}$.

- #18. (Fig. 17) **Name:** $\mathcal{P}(\hat{A}_{2r-1}, \eta^{(1)}, \eta_p, n)$. **Parameters:** $n \geq 2$; $r \geq 1$; $1 \leq p \leq r/2$ coprime with r . **KQ:**

$C_n^{(1)}$	$\hat{D}_{r+2} \Rightarrow \hat{A}_{2r-1} \text{ --- } \cdots \text{ --- } \hat{A}_{2r-1} \Leftarrow \hat{D}_{r+2}$
$A_1^{(1)}$	$\hat{D}_{rn+2} \Leftrightarrow \hat{D}_{rn+2}$

The dual bigraph is $\hat{D}_{rn+2} \rtimes_{qn} \hat{D}_{rn+2}$, where $1 \leq q \leq r/2$ is defined by $pq \equiv \pm 1 \pmod{r}$.

- #19. [SD] (Fig. 21) **Name:** $\hat{D}_{m+2} \rtimes_p \hat{D}_{m+2}$. **Parameters:** $m \geq 2$; $2 \leq p \leq m/2$ coprime with m . **KQ:**

$A_1^{(1)}$	$\hat{D}_{m+2} \Leftrightarrow \hat{D}_{m+2}$	$A_1^{(1)}$	$\hat{D}_{m+2} \Leftrightarrow \hat{D}_{m+2}$
-------------	---	-------------	---

The dual bigraph is $\hat{D}_{m+2} \times_q \hat{D}_{m+2}$ where $2 \leq q \leq m/2$ is the unique integer such that $pq \equiv \pm 1 \pmod{m}$. The case $p = q = 1$ is not included here as it corresponds to the twist $\hat{D}_{m+2} \times \hat{D}_{m+2}$.

#20. [SD] (Fig. 18) **Name:** $\mathcal{P}(\hat{A}_{4m-1}, \eta^{(1)}, \exp(\pi i), n)$. **Parameters:** $n, m \geq 2$. **KQ:**

$A_{2n}^{(2)}$	$\hat{A}_{2m-1} \Leftarrow \hat{A}_{4m-1} - \cdots - \hat{A}_{4m-1} \Leftarrow \hat{D}_{2m+2}$
$A_{2m}^{(2)}$	$\hat{A}_{2n-1} \Leftarrow \hat{A}_{4n-1} - \cdots - \hat{A}_{4n-1} \Leftarrow \hat{D}_{2n+2}$

The dual bigraph is $\mathcal{P}(\hat{A}_{4n-1}, \eta^{(1)}, \exp(\pi i), m)$.

#21. (Fig. 18) **Name:** $\mathcal{P}(\hat{A}_3, \eta^{(1)}, \exp(\pi i), n)$. **Parameters:** $n \geq 2$. **KQ:**

$A_{2n}^{(2)}$	$\hat{A}_1 \Leftarrow \hat{A}_3 - \cdots - \hat{A}_3 \Leftarrow \hat{D}_4$
$A_2^{(2)}$	$\hat{A}_{2n-1} \Leftarrow \hat{D}_{2n+2}$

#22. (Fig. 18) **Name:** $\mathcal{P}(\hat{A}_{2m-1}, \eta^{(1)}, \text{id}, n)$. **Parameters:** $n, m \geq 2$. **KQ:**

$C_n^{(1)}$	$\hat{A}_{4m-1} \Rightarrow \hat{A}_{2m-1} - \cdots - \hat{A}_{2m-1} \Leftarrow \hat{D}_{m+2}$
$D_{m+1}^{(2)}$	$\hat{D}_{n+2} \Leftarrow \hat{D}_{2n+2} - \cdots - \hat{D}_{2n+2} \Rightarrow \hat{D}_{n+2}$

The dual bigraph is $\mathcal{P}(\hat{D}_{2n+2}, \tau, \tau^\perp, m)$.

#23. (Fig. 19) **Name:** $\mathcal{P}(\hat{D}_{m+2}, \sigma, \sigma^\perp, n)$. **Parameters:** $n, m \geq 2$. **KQ:**

$C_n^{(1)}$	$\hat{D}_{2m+2} \Rightarrow \hat{D}_{m+2} - \cdots - \hat{D}_{m+2} \Leftarrow \hat{D}_{2m+2}$
$B_{m+1}^{(1)}$	$\begin{array}{c} \hat{D}_{n+2} \\ \\ \hat{D}_{n+2} - \hat{D}_{n+2} - \cdots - \hat{D}_{n+2} \Rightarrow \hat{A}_{2n-1} \end{array}$

#24. [SD] (Fig. 19) **Name:** $\mathcal{P}(\hat{D}_{m+2}, \sigma, \sigma^\perp, n)$. **Parameters:** $n, m \geq 2$. **KQ:**

$C_n^{(1)}$	$\hat{D}_{2m+2} \Rightarrow \hat{D}_{m+2} - \cdots - \hat{D}_{m+2} \Leftarrow \hat{D}_{2m+2}$
$C_m^{(1)}$	$\hat{D}_{2n+2} \Rightarrow \hat{D}_{n+2} - \cdots - \hat{D}_{n+2} \Leftarrow \hat{D}_{2n+2}$

The dual bigraph is $\mathcal{P}(\hat{D}_{n+2}, \sigma, \sigma^\perp, m)$.

- #25. [SD] (Fig. 19) **Name:** $\mathcal{P}(\hat{D}_{m+2}, \sigma, \sigma\tau\sigma\tau, n)$. **Parameters:** $n, m \geq 2$. **KQ:**

$A_{2n}^{(2)}$	$\hat{A}_{2m-1} \leftarrow \hat{D}_{m+2} - \cdots - \hat{D}_{m+2} \leftarrow \hat{D}_{2m+2}$
$A_{2m}^{(2)}$	$\hat{A}_{2n-1} \leftarrow \hat{D}_{n+2} - \cdots - \hat{D}_{n+2} \leftarrow \hat{D}_{2n+2}$

The dual bigraph is $\mathcal{P}(\hat{D}_{n+2}, \sigma, \sigma\tau\sigma\tau, m)$.

- #26. [SD] (Fig. 19) **Name:** $\mathcal{P}(\hat{D}_{2m+2}, \sigma, \tau, n)$. **Parameters:** $n, m \geq 2$. **KQ:**

$A_{2n}^{(2)}$	$\hat{D}_{m+2} \leftarrow \hat{D}_{2m+2} - \cdots - \hat{D}_{2m+2} \leftarrow \hat{D}_{4m+2}$
$A_{2m}^{(2)}$	$\hat{D}_{n+2} \leftarrow \hat{D}_{2n+2} - \cdots - \hat{D}_{2n+2} \leftarrow \hat{D}_{4n+2}$

The dual bigraph is $\mathcal{P}(\hat{D}_{2n+2}, \sigma, \tau, m)$.

- #27. [SD] (Fig. 19) **Name:** $\mathcal{P}(\hat{D}_{m+2}, \sigma\tau\sigma\tau, \sigma\tau\sigma\tau, n)$. **Parameters:** $n, m \geq 2$. **KQ:**

$D_{n+1}^{(2)}$	$\hat{A}_{2m-1} \leftarrow \hat{D}_{m+2} - \cdots - \hat{D}_{m+2} \Rightarrow \hat{A}_{2m-1}$
$D_{m+1}^{(2)}$	$\hat{A}_{2n-1} \leftarrow \hat{D}_{n+2} - \cdots - \hat{D}_{n+2} \Rightarrow \hat{A}_{2n-1}$

The dual bigraph is $\mathcal{P}(\hat{D}_{n+2}, \sigma\tau\sigma\tau, \sigma\tau\sigma\tau, m)$.

- #28. [SD] (Fig. 19) **Name:** $\mathcal{P}(\hat{D}_{2m+2}, \sigma\tau\sigma\tau, \tau, n)$. **Parameters:** $n, m \geq 2$. **KQ:**

$D_{n+1}^{(2)}$	$\hat{A}_{4m-1} \leftarrow \hat{D}_{2m+2} - \cdots - \hat{D}_{2m+2} \Rightarrow \hat{D}_{m+2}$
$D_{m+1}^{(2)}$	$\hat{A}_{4n-1} \leftarrow \hat{D}_{2n+2} - \cdots - \hat{D}_{2n+2} \Rightarrow \hat{D}_{n+2}$

The dual bigraph is $\mathcal{P}(\hat{D}_{2n+2}, \sigma\tau\sigma\tau, \tau, m)$.

- #29. (Fig. 19) **Name:** $\mathcal{P}(\hat{D}_{2m+2}, \tau, \tau, n)$. **Parameters:** $n, m \geq 2$. **KQ:**

$D_{n+1}^{(2)}$	$\hat{D}_{m+2} \leftarrow \hat{D}_{2m+2} - \cdots - \hat{D}_{2m+2} \Rightarrow \hat{D}_{m+2}$
$A_{2m+1}^{(2)}$	$\begin{array}{c} \hat{A}_{2n-1} \\ \\ \hat{A}_{2n-1} - \hat{A}_{2n-1} - \cdots - \hat{A}_{2n-1} \leftarrow \hat{D}_{n+2} \end{array}$

- #30. (Fig. 19) **Name:** $\mathcal{P}(\hat{D}_4, (12), (13), n)$. **Parameters:** $n \geq 2$. **KQ:**

$C_n^{(1)}$	$\hat{D}_6 \Rightarrow \hat{D}_4 - \cdots - \hat{D}_4 \Leftarrow \hat{D}_6$
$D_4^{(3)}$	$\hat{D}_{n+2} - \hat{D}_{n+2} \Leftarrow \hat{D}_{3n+2}$

#31. (Fig. 19) **Name:** $\mathcal{P}(\hat{D}_4, (12), (13)(24), n)$. **Parameters:** $n \geq 2$.
KQ:

$A_{2n}^{(2)}$	$\hat{A}_3 \Leftarrow \hat{D}_4 - \cdots - \hat{D}_4 \Leftarrow \hat{D}_6$
$A_2^{(2)}$	$\hat{D}_{n+2} \Leftarrow \hat{D}_{4n+2}$

#32. (Fig. 19) **Name:** $\mathcal{P}(\hat{D}_4, (12)(34), (13)(24), n)$. **Parameters:** $n \geq 2$. **KQ:**

$D_{n+1}^{(2)}$	$\hat{A}_3 \Leftarrow \hat{D}_4 - \cdots - \hat{D}_4 \Rightarrow \hat{A}_3$
$A_1^{(1)}$	$A_{4n-1} \Leftrightarrow D_{n+2}$

#33. (Fig. 20) **Name:** $\mathcal{P}(\hat{E}_6, (12), (12), n)$. **Parameters:** $n \geq 2$. **KQ:**

$C_n^{(1)}$	$\hat{E}_7 \Rightarrow \hat{E}_6 - \cdots - \hat{E}_6 \Leftarrow \hat{E}_7$
$F_4^{(1)}$	$\hat{D}_{n+2} - \hat{D}_{n+2} - \hat{D}_{n+2} \Rightarrow \hat{A}_{2n-1} - \hat{A}_{2n-1}$

#34. (Fig. 20) **Name:** $\mathcal{P}(\hat{E}_6, (12), (13), n)$. **Parameters:** $n \geq 2$. **KQ:**

$C_n^{(1)}$	$\hat{E}_7 \Rightarrow \hat{E}_6 - \cdots - \hat{E}_6 \Leftarrow \hat{E}_7$
$G_2^{(1)}$	$\hat{D}_{3n+2} - \hat{D}_{3n+2} \Rightarrow \hat{D}_{n+2}$

#35. (Fig. 20) **Name:** $\mathcal{P}(\hat{E}_7, \theta, \theta, n)$. **Parameters:** $n \geq 2$. **KQ:**

$D_{n+1}^{(2)}$	$\hat{E}_6 \Leftarrow \hat{E}_7 - \cdots - \hat{E}_7 \Rightarrow \hat{E}_6$
$E_6^{(2)}$	$\hat{A}_{2n-1} - \hat{A}_{2n-1} - \hat{A}_{2n-1} \Leftarrow \hat{D}_{n+2} - \hat{D}_{n+2}$

#36. [SD] (Fig. 22) **KQ:**

$A_1^{(1)}$	$\hat{E}_8 \Leftrightarrow \hat{E}_8$	$A_1^{(1)}$	$\hat{E}_8 \Leftrightarrow \hat{E}_8$
-------------	---------------------------------------	-------------	---------------------------------------

#37. [SD] (Fig. 22) **KQ:**

$A_2^{(2)}$	$\hat{A}_5 \Leftarrow \hat{E}_6$	$A_2^{(2)}$	$\hat{A}_5 \Leftarrow \hat{E}_6$
-------------	----------------------------------	-------------	----------------------------------

#38. [SD] (Fig. 22) **KQ:**

$A_2^{(2)}$	$\hat{D}_5 \Leftarrow \hat{E}_7$	$A_2^{(2)}$	$\hat{D}_5 \Leftarrow \hat{E}_7$
-------------	----------------------------------	-------------	----------------------------------

#39. [SD] (Fig. 22) **KQ:**

$A_2^{(2)}$	$\hat{A}_3 \Leftarrow \hat{D}_6$	$A_2^{(2)}$	$\hat{A}_3 \Leftarrow \hat{D}_6$
-------------	----------------------------------	-------------	----------------------------------

#40. [SD] (Fig. 22) **KQ:**

$A_2^{(2)}$	$\hat{A}_1 \Leftarrow \hat{D}_4$	$A_2^{(2)}$	$\hat{A}_1 \Leftarrow \hat{D}_4$
-------------	----------------------------------	-------------	----------------------------------

#41. (Fig. 23) **KQ:**

$D_4^{(3)}$	$\hat{A}_3 - \hat{A}_3 \Leftarrow \hat{D}_5$	$A_1^{(1)}$	$\hat{D}_6 \Leftrightarrow \hat{D}_6$
-------------	--	-------------	---------------------------------------

#42. (Fig. 23) **KQ:**

$G_2^{(1)}$	$\hat{D}_5 - \hat{D}_5 \Rightarrow \hat{A}_3$	$A_1^{(1)}$	$\hat{E}_7 \Leftrightarrow \hat{E}_7$
-------------	---	-------------	---------------------------------------

#43. [SD] (Fig. 23) **KQ:**

$D_4^{(3)}$	$\hat{D}_6 - \hat{D}_6 \Leftarrow \hat{E}_7$	$D_4^{(3)}$	$\hat{D}_6 - \hat{D}_6 \Leftarrow \hat{E}_7$
-------------	--	-------------	--

#44. [SD] (Fig. 23) **KQ:**

$G_2^{(1)}$	$\hat{E}_7 - \hat{E}_7 \Rightarrow \hat{D}_6$	$G_2^{(1)}$	$\hat{E}_7 - \hat{E}_7 \Rightarrow \hat{D}_6$
-------------	---	-------------	---

#45. [SD] (Fig. 23) **KQ:**

$D_4^{(3)}$	$\hat{D}_4 - \hat{D}_4 \Leftarrow \hat{E}_6$	$D_4^{(3)}$	$\hat{D}_4 - \hat{D}_4 \Leftarrow \hat{E}_6$
-------------	--	-------------	--

#46. [SD] (Fig. 23) **KQ:**

$G_2^{(1)}$	$\hat{E}_6 - \hat{E}_6 \Rightarrow \hat{D}_4$	$G_2^{(1)}$	$\hat{E}_6 - \hat{E}_6 \Rightarrow \hat{D}_4$
-------------	---	-------------	---

#47. [SD] (Fig. 24) **Name:** $(\hat{D}_{2m+2})^{n+1} \hat{D}_{m+2}$. **Parameters:** $n, m \geq 2$.

KQ:

	\hat{D}_{2m+2}
$B_{n+1}^{(1)}$	$\hat{D}_{2m+2} - \hat{D}_{2m+2} - \cdots - \hat{D}_{2m+2} \Rightarrow \hat{D}_{m+2}$
	\hat{D}_{2n+2}
$B_{m+1}^{(1)}$	$\hat{D}_{2n+2} - \hat{D}_{2n+2} - \cdots - \hat{D}_{2n+2} \Rightarrow \hat{D}_{n+2}$

The dual bigraph is $(\hat{D}_{2n+2})^{m+1}\hat{D}_{n+2}$.

#48. [SD] (Fig. 24) **Name:** $(\hat{D}_{m+2})^{n+1}\hat{D}_{2m+2}$. **Parameters:** $n, m \geq 2$.

KQ:

	\hat{D}_{m+2}
$A_{2n+1}^{(2)}$	$\hat{D}_{m+2} - \hat{D}_{m+2} - \dots - \hat{D}_{m+2} \Leftarrow \hat{D}_{2m+2}$
	\hat{D}_{n+2}
$A_{2m+1}^{(2)}$	$\hat{D}_{n+2} - \hat{D}_{n+2} - \dots - \hat{D}_{n+2} \Leftarrow \hat{D}_{2n+2}$

The dual bigraph is $(\hat{D}_{n+2})^{m+1}\hat{D}_{2n+2}$.

#49. (Fig. 24) **Name:** $(\hat{E}_7)^{n+1}\hat{E}_6$. **Parameters:** $n \geq 2$. **KQ:**

	\hat{E}_7
$B_{n+1}^{(1)}$	$\hat{E}_7 - \hat{E}_7 - \dots - \hat{E}_7 \Rightarrow \hat{E}_6$
$F_4^{(1)}$	$\hat{D}_{2n+2} - \hat{D}_{2n+2} - \hat{D}_{2n+2} \Rightarrow \hat{D}_{n+2} - \hat{D}_{n+2}$

#50. (Fig. 24) **Name:** $(\hat{E}_6)^{n+1}\hat{E}_7$. **Parameters:** $n \geq 2$. **KQ:**

	\hat{E}_6
$A_{2n+1}^{(2)}$	$\hat{E}_6 - \hat{E}_6 - \dots - \hat{E}_6 \Leftarrow \hat{E}_7$
$E_6^{(2)}$	$\hat{D}_{n+2} - \hat{D}_{n+2} - \hat{D}_{n+2} \Leftarrow \hat{D}_{2n+2} - \hat{D}_{2n+2}$

#51. [SD] (Fig. 25) **KQ:**

$F_4^{(1)}$	$\hat{E}_7 - \hat{E}_7 - \hat{E}_7 \Rightarrow \hat{E}_6 - \hat{E}_6$
$F_4^{(1)}$	$\hat{E}_7 - \hat{E}_7 - \hat{E}_7 \Rightarrow \hat{E}_6 - \hat{E}_6$

#52. [SD] (Fig. 25) **KQ:**

$E_6^{(2)}$	$\hat{E}_6 - \hat{E}_6 - \hat{E}_6 \Leftarrow \hat{E}_7 - \hat{E}_7$
$E_6^{(2)}$	$\hat{E}_6 - \hat{E}_6 - \hat{E}_6 \Leftarrow \hat{E}_7 - \hat{E}_7$

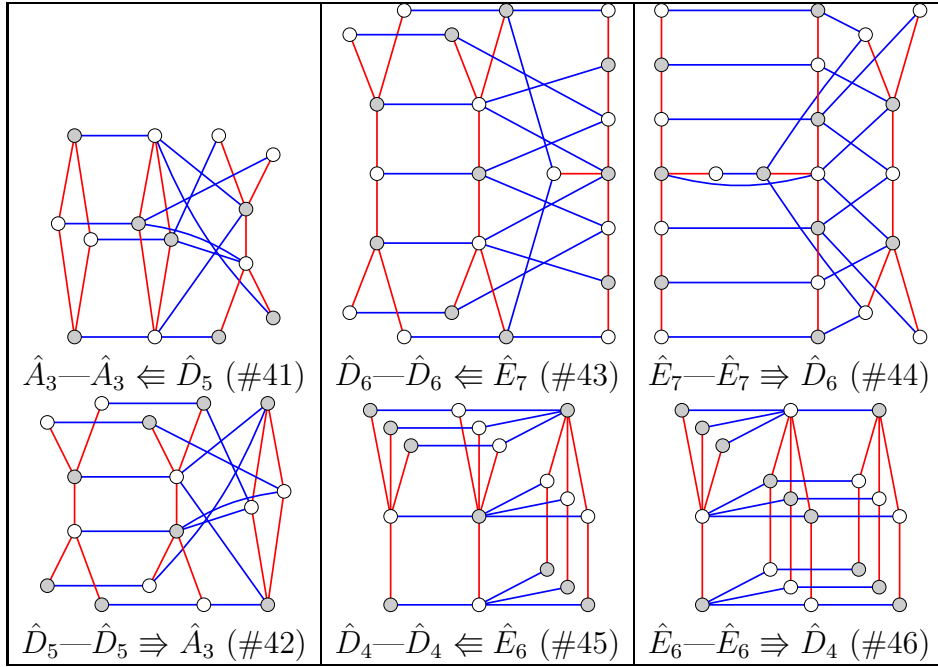


FIGURE 23. Bigraphs G such that $S(G)$ contains a triple arrow.

#53. [SD] (Fig. 26) **Name:** $\hat{D}_{2m+3}(\hat{A}_{4m+1})^n$. **Parameters:** $n, m \geq 1$.
KQ:

$\frac{1}{2}C_{2n+1}^{(1)}$	$\hat{D}_{2m+3} \Rightarrow \hat{A}_{4m+1} - \cdots - \hat{A}_{4m+1} - \hat{A}_{4m+1}$ $\binom{\quad}{\quad}$
$\frac{1}{2}C_{2m+1}^{(1)}$	$\hat{D}_{2n+3} \Rightarrow \hat{A}_{4n+1} - \cdots - \hat{A}_{4n+1} - \hat{A}_{4n+1}$ $\binom{\quad}{\quad}$

The dual bigraph is $\hat{D}_{2n+3}(\hat{A}_{4n+1})^m$.

Note that for families #1–#40, the illustrations have been given in Section 5 (and in Figure 1). The rest of the families are shown in Figures 23–26. The exceptional bigraphs are #36–#46, #51, and #52. Thus there are 13 of them, and the rest 40 items in the classification are infinite families (including two 3-parameter families #3 and #17).

7. PROOF OF THE CLASSIFICATION

First, it is straightforward to check that each of #1–#53 is an affine \boxtimes affine ADE bigraph. One helpful result [39, Lemma 2.4] of Stembridge states that G has commuting adjacency matrices if and only if

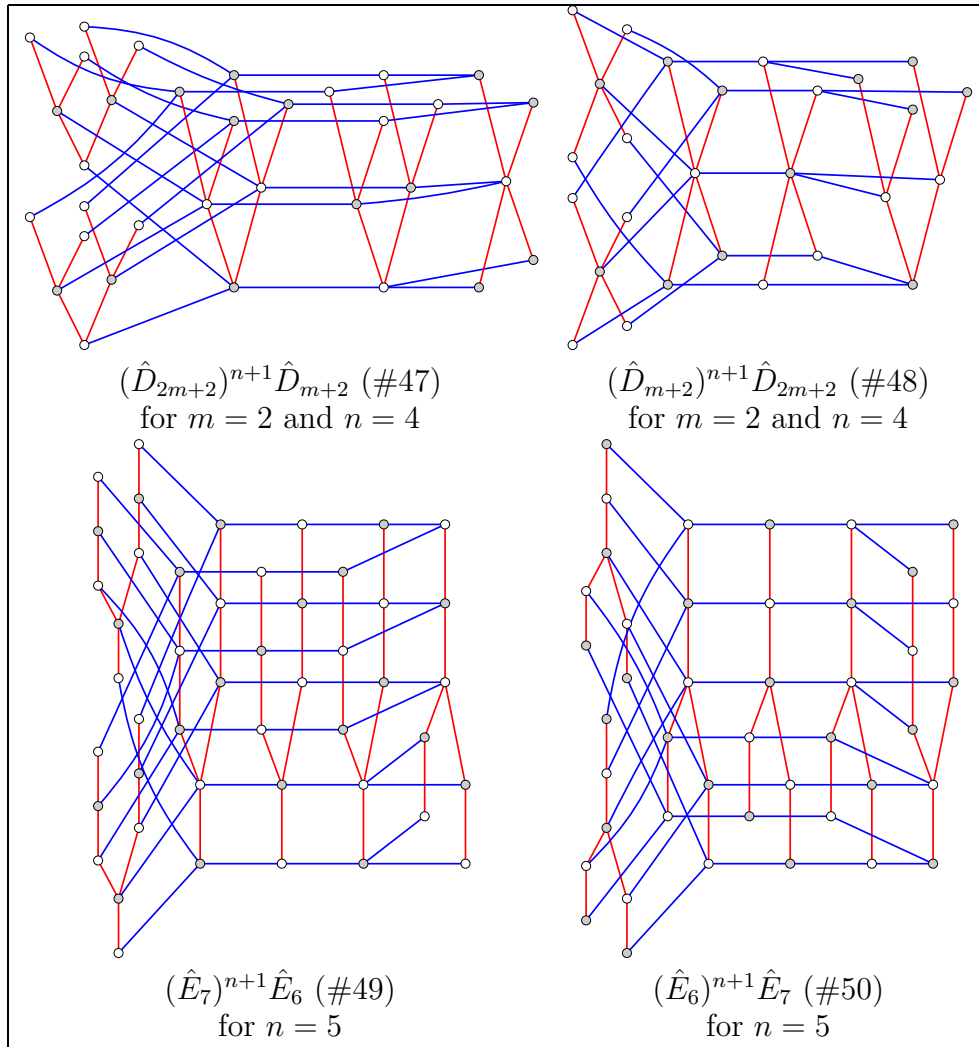


FIGURE 24. Bigraphs G such that $S(G)$ is of type D with a double arrow at the end.

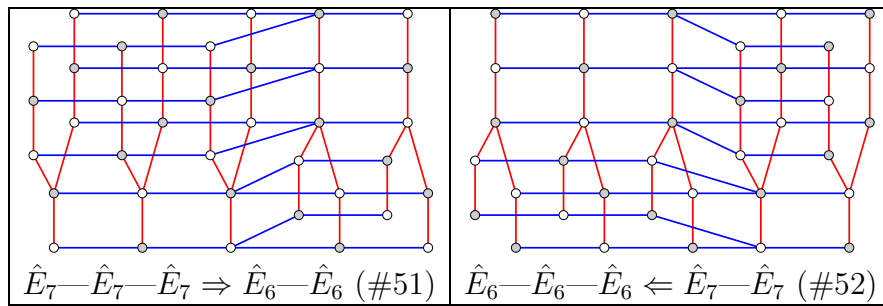


FIGURE 25. Bigraphs #51 and #52.

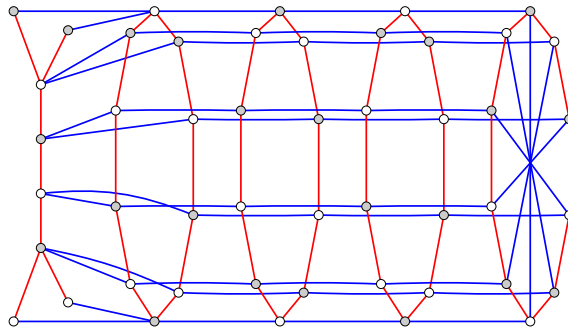


FIGURE 26. The family $\hat{D}_{2m+3}(\hat{A}_{4m+1})^n$ (#53) for $m = 2$ and $n = 4$.

all of the self and double bindings involved have commuting adjacency matrices. From this it follows almost immediately that each of #1–#53 has commuting adjacency matrices; one needs to check this fact separately for affine \boxtimes affine and affine \boxtimes finite self and double bindings. The fact that all red and blue components are affine *ADE* Dynkin diagrams is clear from looking at $\text{descr}(G)$ and $\text{descr}(G^*)$.

Second, it is easy to verify that no two of the bigraphs #1–#53 are isomorphic. Indeed, the only cases where we can have both $\text{descr}(G_1) = \text{descr}(G_2)$ and $\text{descr}(G_1^*) = \text{descr}(G_2^*)$ without G_1 and G_2 being isomorphic arise when both G_1 and G_2 belong to one of the following families: #2, #3, #17, #18, #19, and in each case the fact that they are not isomorphic follows from the results of Section 5.

Thus it remains to prove that we listed *all* possible affine \boxtimes affine *ADE* bigraphs.

Suppose that G is an affine \boxtimes affine *ADE* bigraph and consider the diagram $S(G)$ which by Theorem 4.7 is a diagram from Figure 5. According to whether $S(G)$ is *ambiguous* (see Proposition 4.11), we will consider the following disjoint cases:

- (i) $S(G) = A_\ell^{(1)}$ for $\ell \geq 2$;
- (ii) $S(G)$ is either one of $D_{\ell+1}^{(2)}$, $C_\ell^{(1)}$, or $A_{2\ell}^{(2)}$ for $\ell \geq 2$;
- (iii) $S(G)$ is either one of $A_1^{(1)}$, $A_2^{(2)}$, or $\frac{1}{2}A_1^{(1)}$;
- (iv) $S(G)$ is none of the above, i.e. is unambiguous.

For the case (i), we showed in Section 5.2 that such graphs are classified by weak conjugacy classes of automorphisms of diagrams in Figure 5. One can verify directly that these graphs are exactly the ones listed in families #3–#16 together with tensor products $\hat{A} \otimes \hat{A}$ from #1.

Similarly, for the case (ii), we showed in Section 5.3 that such graphs are classified by pairs of color-preserving involutions of affine *ADE*

Dynkin diagrams up to simultaneous conjugation. Since we have listed all such pairs in Section 5.3, it is straightforward to check that these graphs are exactly the ones listed in families #17, #18, #20–#35, together with the duals of #4, #7, #10, and #22.

Suppose now that (iv) holds. By Proposition 4.11 then G is uniquely determined by $\text{descr}(G)$. It remains to go through all the possible unambiguous diagrams S in Figure 5 and for each of them list all possible assignments of double bindings with $\text{scf} = (2, 1)$, double bindings with $\text{scf} = (3, 1)$, and self bindings to double arrows, triple arrows, and loops in $S(G)$ respectively that yield affine ADE Dynkin diagrams as blue components. This can be done in a straightforward way producing the families #41–#53 and their duals, together with the duals of some toric and path bigraphs. Note also that family #1 of tensor products falls into this category as well.

Similarly, if G^* falls into categories (i), (ii), or (iv) then G^* appears in the list.

It remains to consider the case when both G and G^* satisfy (iii).

7.1. Affine \boxtimes affine self bindings. In this section, we consider the case $S(G) = \frac{1}{2}A_1^{(1)}$ which means that G is an affine \boxtimes affine self binding.

Let $\mathbf{v} : \text{Vert}(G) \rightarrow \mathbb{R}$ be the common eigenvector for A_Γ and A_Δ from Lemma 2.16. Thus $A_\Gamma \mathbf{v} = 2\mathbf{v}$ and $A_\Delta \mathbf{v} = 2\mathbf{v}$. Since Γ has just one connected component, we may rescale \mathbf{v} so that it is equal to \mathbf{v}_Γ . By Proposition 4.1, we have that for every $v \in \text{Vert}(G)$,

$$(7.1) \quad \sum_{(v,w) \in \Delta} \mathbf{v}(w) = \sum_{(v,w) \in \Gamma} \mathbf{v}(w) = 2\mathbf{v}(v).$$

Theorem 7.1. *The only possible affine \boxtimes affine self bindings are*

$$\mathcal{T}(\hat{A}_{2n-1}, \exp(\pi i(2m-1)/n), 1), \quad \text{for } n \geq 2 \text{ and } 1 < 2m-1 \leq n,$$

and any two such bigraphs are non-isomorphic.

Proof. Let G be an affine \boxtimes affine self binding, thus Γ is an affine ADE Dynkin diagram. We are first going to eliminate the cases when Γ has type \hat{E}_6, \hat{E}_7 , or \hat{E}_8 . Suppose Γ is of one of these exceptional types. Consider the vertex $u \in \text{Vert}(G)$ with the maximum value of \mathbf{v}_u . Thus $\mathbf{v}_u = 3$ for \hat{E}_6 , $\mathbf{v}_u = 4$ for \hat{E}_7 , and $\mathbf{v}_u = 6$ for \hat{E}_8 , see Figure 3. Note that since G is a bigraph, Γ and Δ do not share edges. In particular, the neighbors of u in Γ cannot be the neighbors of u in Δ . It remains to note that the sum of \mathbf{v}_w over $w \in \text{Vert}(G)$ with $\epsilon_w \neq \epsilon_u$ and $(u, w) \notin \Gamma$ is less than $2\mathbf{v}_u$ so (7.1) cannot hold even if u is connected to all available vertices of G .

Let us now assume that Γ is of type \hat{D}_{n+2} for $n \geq 2$. Thus G has $n + 3$ vertices which we denote $v_0^+, v_0^-, v_1, \dots, v_{n-1}, v_n^+, v_n^-$. Here Γ consists of edges (v_i, v_{i+1}) for $i \in [n - 2]$ together with four edges $(v_0^\pm, v_1), (v_{n-1}, v_n^\pm)$.

Suppose Δ contains an edge (v_k, v_{k+m}) for $k, k+m \in [n-1]$. Among all such edges, choose the one with the minimal value of m . Since v_k and v_{k+m} are not neighbors in Γ , we have $m \geq 2$. There is a red-blue path from v_{k+1} to v_{k+m} so there must be a blue-red path as well by Corollary 2.15. Since v_{k+1} cannot be connected to v_{k+m-1} by a blue edge, we have either $k+m = n-1$ or $(v_{k+1}, v_{k+m+1}) \in \Delta$. Similarly, we have either $k = 1$ or $(v_{k-1}, v_{k+m-1}) \in \Delta$. Thus for every $i = 1, 2, \dots, n-m-1$, we have an edge $(v_i, v_{i+m}) \in \Delta$. Consider the blue edge (v_1, v_{1+m}) . There is a red-blue path from v_m to v_1 so without loss of generality we may assume that $(v_0^+, v_m) \in \Delta$. But then there is a blue-red path from v_0 to v_{m-1} so there must be a red-blue path which necessarily passes through v_1 , the only red neighbor of v_0^+ . Thus $(v_1, v_{m-1}) \in \Delta$, a contradiction. This shows that Δ has no edges of the form (v_k, v_{k+m}) for $k, k+m \in [n-1]$. Now, consider any vertex v_k for $k \in [n-1]$. It can only be connected by a blue edge to v_0^\pm and v_n^\pm , and by (7.1), it is connected to all these four vertices. This holds for any $k \in [n-1]$ but by (7.1) applied to v_0^+ , there can be only one such vertex. It follows that $n = 2$ in which case the edge (v_0^+, v_1) belongs to both Γ and Δ which is impossible. Thus there are no self bindings with Γ being of type \hat{D}_{n+2} .

Finally, suppose Γ is of type \hat{A}_{2n-1} . Let v_1, \dots, v_{2n} be the vertices of Γ , and we label them cyclically so that $v_{2n+1} = v_1$, etc. Let $(v_k, v_{k+2m-1}) \in \Delta$ be an edge with the minimal positive value of m , where again $m \geq 1$ (in fact, $m \geq 2$ because (v_k, v_{k+1}) is already an edge of Γ). Then by the above reasoning, we have $(v_i, v_{i+2m-1}) \in \Delta$ for every $i \in [2n]$. By (7.1), there are no other edges in Δ . We get precisely the bigraph $\mathcal{T}(\hat{A}_{2n-1}, \exp(\pi i(2m-1)/n), 1)$. The fact that any two of these bigraphs are not isomorphic follows from Proposition 5.3. \square

Thus every affine \boxtimes affine self binding appears as a special case for $n = 1$ in family #3.

7.2. Affine \boxtimes affine double bindings: preliminaries. We are left with the case (iii) where both $S(G)$ and $S(G^*)$ belong to the set $\{A_1^{(1)}, A_2^{(2)}\}$. This implies that each of G and G^* is an affine \boxtimes affine double binding. Proving Theorem 6.1 reduces to showing the following.

Theorem 7.2. *Suppose that both $S(G)$ and $S(G^*)$ belong to the set $\{A_1^{(1)}, A_2^{(2)}\}$. Then either G or G^* belongs to one of the families #1, #2, #3, #12, #19, or #36–#40.*

Proof. We use the notation of Section 4.2: let X and Y be the two red connected components of G , every edge of Δ connects a vertex of X to a vertex of Y . We let \mathbf{v} be the common eigenvector for A_Γ and A_Δ from Lemma 2.16, and we denote by \mathbf{v}_X and \mathbf{v}_Y the additive functions for $\Gamma(X)$ and $\Gamma(Y)$ from Figure 3.

Recall that G is a double binding of type $\hat{\Lambda} * \hat{\Lambda}'$ if X has type $\hat{\Lambda}$ and Y has type $\hat{\Lambda}'$.

Definition 7.3. We say that G is a double binding of type $\hat{\Lambda} \Leftrightarrow \hat{\Lambda}'$ if X has type $\hat{\Lambda}$ and Y has type $\hat{\Lambda}'$ and $\text{scf}(G) = (2, 2)$. We similarly introduce double bindings of type $\hat{\Lambda} \Leftarrow \hat{\Lambda}'$ and of type $\hat{\Lambda} \Rightarrow \hat{\Lambda}'$ for the cases $\text{scf}(G) = (1, 4)$ and $\text{scf}(G) = (4, 1)$ respectively.

As it follows from (4.4), the values of \mathbf{v} , \mathbf{v}_X , and \mathbf{v}_Y are related as follows. For any $u \in X$ and $v \in Y$, we have

- $\mathbf{v}(u) = \mathbf{v}_X(u)$, $\mathbf{v}(v) = \mathbf{v}_Y(v)$ if G is of type $\hat{\Lambda} \Leftrightarrow \hat{\Lambda}'$;
- $\mathbf{v}(u) = 2\mathbf{v}_X(u)$, $\mathbf{v}(v) = \mathbf{v}_Y(v)$ if G is of type $\hat{\Lambda} \Leftarrow \hat{\Lambda}'$;
- $\mathbf{v}(u) = \mathbf{v}_X(u)$, $\mathbf{v}(v) = 2\mathbf{v}_Y(v)$ if G is of type $\hat{\Lambda} \Rightarrow \hat{\Lambda}'$.

Thus if we know $\text{descr}(G)$ then we know \mathbf{v} .

Definition 7.4. Given an affine ADE Dynkin diagram $\hat{\Lambda}$, denote by $M(\hat{\Lambda})$ the *multiset of values* of $\mathbf{v}_{\hat{\Lambda}}$. We also define $M_0(\hat{\Lambda})$ and $M_1(\hat{\Lambda})$ to be the multisets of values of $\mathbf{v}_{\hat{\Lambda}}$ restricted to the set of black (resp., white) vertices of $\hat{\Lambda}$. For example, $M(\hat{E}_6) = \{1, 1, 1, 2, 2, 2, 3\}$ which splits into $M_0(\hat{E}_6) = \{1, 1, 1, 3\}$ and $M_1(\hat{E}_6) = \{2, 2, 2\}$.

We denote $X = X_0 \sqcup X_1$ and $Y = Y_0 \sqcup Y_1$ the partitions of X and Y into sets of vertices that have the same color. Thus either of the following is true:

- every edge of Δ connects a vertex of X_i to a vertex of Y_{1-i} for $i = 0, 1$;
- every edge of Δ connects a vertex of X_i to a vertex of Y_i for $i = 0, 1$.

We denote by $M(X_0)$ the multiset of values of \mathbf{v} restricted to X_0 . We similarly define $M(X_1)$, $M(Y_0)$, $M(Y_1)$. We identify two multisets if one of them is obtained from another one via rescaling every element by a positive real number. The following lemma is immediate.

Lemma 7.5. *Suppose that G and G^* are both double bindings and suppose that G^* has type $\hat{\Lambda} * \hat{\Lambda}'$. Then after a possible swapping of $\hat{\Lambda}$ with $\hat{\Lambda}'$, one of the following holds:*

- $M(X_0) = M_i(\hat{\Lambda})$ and $M(Y_0) = M_{1-i}(\hat{\Lambda})$ for some $i \in \{0, 1\}$;
- $M(X_0) = M_i(\hat{\Lambda})$ and $M(Y_1) = M_{1-i}(\hat{\Lambda})$ for some $i \in \{0, 1\}$.

Let us sum up these observations. Suppose that both G and G^* are double bindings and let G^* have type $\hat{\Lambda} * \hat{\Lambda}'$. If we know $\text{descr}(G)$ then we know \mathbf{v} and this gives us the multisets $M(X_0), M(X_1), M(Y_0), M(Y_1)$. There are two options for the components $\hat{\Lambda}$ and $\hat{\Lambda}'$ of Δ described in the above lemma. Since an affine ADE Dynkin diagram can be recovered from its additive function, we get that knowing $\text{descr}(G)$ gives two possibilities for the types of its blue components. In each case, we recover $\text{descr}(G^*)$.

We now finish the proof with a simple case analysis according to the types of X and Y .

7.3. Affine \boxtimes affine double bindings involving type \hat{E} .

7.3.1. *The case $\hat{E} * \hat{E}$.* Applying (4.4), we get that there are the following possibilities for $\text{descr}(G)$:

- (a) $\hat{E}_6 \Leftrightarrow \hat{E}_6$;
- (b) $\hat{E}_7 \Leftrightarrow \hat{E}_7$;
- (c) $\hat{E}_8 \Leftrightarrow \hat{E}_8$.

Indeed, all the other cases are impossible since the ratio of any pair of numbers from $\{24, 48, 120\}$ is not equal to 4.

From looking at the multisets of values, it follows that for each case we have $\text{descr}(G) = \text{descr}(G^*)$. This actually implies that in the first two cases, G is a twist. For example, in case (a), take a vertex v_1 of X with $\mathbf{v}_X(v_1) = 1$. It must be connected to a vertex u_2 of Y with $\mathbf{v}_Y(u_2) = 2$ which in turn must be connected to a vertex v_3 of X with $\mathbf{v}_X(v_3) = 3$. Thus u_2 is not connected to anything else in Δ . We can now consider another leaf $v'_1 \in X$ with $\mathbf{v}_X(v'_1) = 1$. It must be connected to a vertex $u'_2 \in Y$ with $\mathbf{v}_Y(u'_2) = 2$ and by the above observation, $u'_2 \neq u_2$. Continuing in this fashion, we get that G is a twist $\hat{E}_6 \times \hat{E}_6$.

Let us now give a similar but a bit more complicated argument for \hat{E}_7 . Let v_4 and u_4 be the vertices of X and Y respectively with $\mathbf{v}_X(v_4) = \mathbf{v}_Y(u_4) = 4$. Then they must be of the same color since v_4 must be connected to the neighbors u_3 and u'_3 of u_4 with $\mathbf{v}_Y(u_3) = \mathbf{v}_Y(u'_3) = 3$. This implies that u_3 is connected to a vertex v_2 of X with $\mathbf{v}_X(v_2) = 2$

that has the same color as v_4 and now we this argument is finished in the same way as our proof for \hat{E}_6 .

For the third case, we actually get something besides twists, namely, the bigraph #36. Label the vertices of the two copies of \hat{E}_8 with v_1 through v_9 and with u_1 through u_9 as shown in Figure 27.

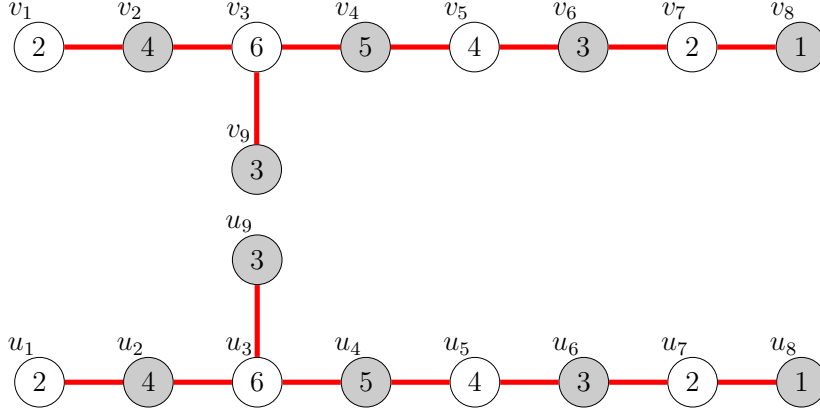


FIGURE 27. Labeling the nodes of X and Y .

From looking at the multisets of values, we get that the vertices v_3 and u_3 have the same color. We see that there are **two cases** to consider: v_3 is connected to either u_2, u_4, u_9 or to u_2, u_4, u_6 .

Assume v_3 is connected to u_2, u_4, u_6 . The same consideration as for v_3 can be applied to u_3 , with the only possible choice now of u_3 being connected to v_2, v_4, v_6 . Since u_2 is connected to v_3 , its only other blue neighbor has to be a vertex v with $\mathbf{v}_X(v) = 2$ so either $v = v_1$ or $v = v_7$. Counting the red-blue and blue-red paths⁵ between u_2 and u_6 , we conclude that u_2 is connected to $v = v_7$. Since u_8 is connected to either v_7 or v_1 , it follows that u_8 is connected to v_1 . Since the vertex u_6 is already connected to v_3 , it cannot be connected to v_1 , and now it follows that Δ contains a path with vertices

$$u_8, v_1, u_9, v_5, u_4, v_3, u_2, v_7$$

which determines the graph uniquely and we see that it is exactly the bigraph #36.

Assume v_3 is connected to u_2, u_4, u_9 . The same consideration as for v_3 can be applied to u_3 , with the only possible choice now of u_3 being connected to v_2, v_4, v_9 . We know that v_2 is connected to either u_1 or u_7 and counting the red-blue and blue-red paths between u_1 and u_3 we

⁵Throughout the text, the phrase *counting the red-blue and blue-red paths* refers to Corollary 2.15 and the discussion after it.

conclude v_2 is connected to u_1 . We now have enough information to conclude that Δ contains a path with vertices

$$u_1, v_2, u_3, v_4, u_5, v_6, u_7, v_8$$

which implies that G is a twist $\hat{E}_8 \times \hat{E}_8$.

7.3.2. *The case $\hat{E}_6 * \hat{A}$.* The component X of type \hat{E}_6 has a vertex v_3 with $\mathbf{v}_X(v_3) = 3$ and therefore it cannot be connected to anything by an edge of Δ unless $\text{scf}(G) = (1, 4)$. Thus we only need to find all double bindings of type $\hat{E}_6 \rightleftharpoons \hat{A}_5$.

It follows from looking at the multisets of values that $\text{descr}(G^*) = \text{descr}(G)$ in this case, and because of the symmetries of X and Y , there is essentially one way to connect the vertices v_2, v'_2, v''_2 of X with $\mathbf{v}_X(v_2) = \mathbf{v}_X(v'_2) = \mathbf{v}_X(v''_2) = 2$ to the vertices u_2, u_4, u_6 of Y to form a 6-cycle in Δ . The rest of the edges are reconstructed uniquely and we get the bigraph #37.

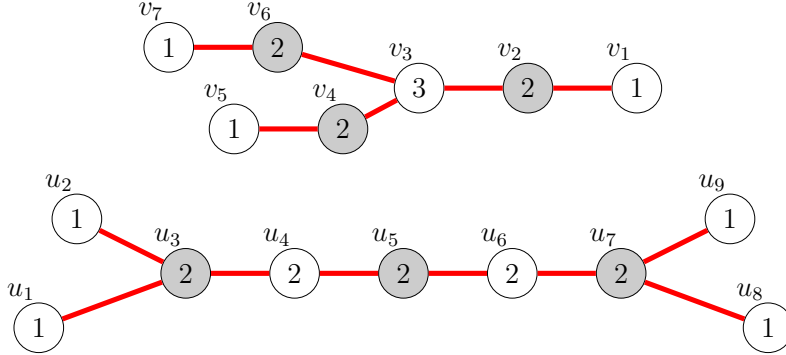
7.3.3. *The case $\hat{E}_7 * \hat{A}$.* The component X of type \hat{E}_7 has a vertex v_4 with $\mathbf{v}_X(v_4) = 4$ and therefore it cannot be connected to anything by an edge of Δ unless $\text{scf}(G) = (1, 4)$. Thus we only need to find all double bindings of type $\hat{E}_7 \rightleftharpoons \hat{A}_{11}$. We get an immediate contradiction from looking at the multisets of values since there is no affine ADE Dynkin diagram $\hat{\Lambda}$ with $M_0(\hat{\Lambda}) = \{2, 2, 2, 2, 2, 2\}$ and $M_1(\hat{\Lambda}) = \{1, 1, 2, 3, 3\}$.

7.3.4. *The case $\hat{E}_8 * \hat{A}$.* The component X of type \hat{E}_8 has a vertex v_6 with $\mathbf{v}_X(v_6) = 6$ and therefore it cannot be connected to anything by an edge of Δ , regardless of $\text{scf}(G)$.

7.3.5. *The case $\hat{E}_6 * \hat{D}$.* Let X be the component of type \hat{E}_6 and let Y be the component of type \hat{D} . The cases $\text{scf}(G) = (4, 1)$ or $\text{scf}(G) = (1, 4)$ are impossible. Indeed, if Y gets a scaling factor of 1, none of its vertices can be connected to the vertex v_3 of X with $\mathbf{v}_X(v_3) = 3$. If on the other hand Y gets scaling factor of 4, there is just not enough vertices in X of the same color to collect $\mathbf{v}_Y(u) \times 4 = 8$ for a vertex $u \in Y$ with $\mathbf{v}_Y(u) = 2$.

Thus $\text{scf}(G) = (2, 2)$ and $\text{descr}(G) = \text{descr}(G^*) = \hat{E}_6 \Leftrightarrow \hat{D}_8$. Label vertices of X with v_1 through v_7 , and label vertices of Y with u_1 through u_9 as shown in Figure 28.

Assume v_1 is white, and then it follows that u_1 is also white from looking at the multisets of values. By the same reason, v_3 is connected to u_3, u_5 and u_7 , which must be connected to v_1, v_5, v_7 . Without loss of generality we can assume that we have edges $(u_3, v_1), (u_5, v_7), (u_7, v_5)$. This determines the position of the blue component of type \hat{E}_6 from

FIGURE 28. Labeling the nodes of X and Y .

which we can uniquely reconstruct the edges of the blue component of type \hat{D}_8 by counting the corresponding red-blue paths: we get that v_2 is connected to u_1, u_2 , v_4 is connected to u_8, u_9 , and thus v_6 is connected to u_4, u_6 which are connected to v_2 and v_4 or vice versa, and we see that in any case we get a contradiction.

7.3.6. *The case $\hat{E}_7 * \hat{D}$.* Let X be the component of type \hat{E}_7 and let Y the the component of type \hat{D} . Our three possibilities by (4.4) are:

- $\hat{E}_7 \Leftrightarrow \hat{D}_{14}$;
- $\hat{E}_7 \Leftarrow \hat{D}_{50}$;
- $\hat{E}_7 \Rightarrow \hat{D}_5$;

Since $M_0(X) = \{1, 1, 3, 3\}$ and since there is no Dynkin diagram $\hat{\Lambda}$ for which the maximum of $\mathbf{v}(\hat{\Lambda})$ is greater than 2 and is achieved more than once, it follows that only the third case is possible. From looking at the multisets of values, we get that $\text{descr}(G) = \text{descr}(G^*) = \hat{E}_7 \Rightarrow \hat{D}_5$, and in fact all the edges of Δ can be immediately reconstructed from knowing the additive function for each component of Δ , yielding the bigraph #38.

7.3.7. *The case $\hat{E}_8 * \hat{D}$.* The cases $\hat{E}_8 \Leftrightarrow \hat{D}_{m+2}$ and $\hat{E}_8 \Leftarrow \hat{D}_{m+2}$ are impossible because the vertex in \hat{E}_8 with $\mathbf{v} = 6$ cannot be connected to any vertex in \hat{D}_{m+2} . The only possibility is the case $\hat{E}_8 \Rightarrow \hat{D}_m$ which is also impossible because by (4.4), m must satisfy $4 \times 4m = 120$, but 120 is not divisible by 16.

7.4. Affine \boxtimes affine double bindings involving type \hat{A} .

7.4.1. *The case $\hat{A} * \hat{A}$.* By (4.4), there are two possibilities:

- $\hat{A}_{2n-1} \Leftrightarrow \hat{A}_{2n-1}$, $n \geq 1$;

- $\hat{A}_{8n-1} \xrightarrow{\cong} \hat{A}_{2n-1}$, $n \geq 1$.

In the second case, the multisets of values tell us that the red components of G^* are $2n$ copies of \hat{D}_4 , and since G^* is also required to be a double binding, we get that $n = 1$, in which case there is only one possible double binding which already is listed in family #12.

In the first case, the multisets of values tell us that $\text{descr}(G) = \text{descr}(G^*) = \hat{A}_{2n-1} \Leftrightarrow \hat{A}_{2n-1}$. Label the vertices of X with v_1 through v_{2n} , and label the vertices of Y with u_1 through u_{2n} (we will be taking the indices modulo $2n$). Since the case $n = 1$ is trivial, we assume that Δ has no double edges.

Lemma 7.6. *Assume edges (v_i, u_j) and (v_{i+1}, u_{j+1}) are present. Then so are the edges (v_{i+2}, u_{j+2}) and (v_{i-1}, u_{j-1}) . Similarly, assume the edges (v_i, u_j) and (v_{i+1}, u_{j-1}) are present. Then so are edges (v_{i+2}, u_{j-2}) and (v_{i-1}, u_{j+1}) .*

Proof. Due to symmetry, it is enough to prove the first claim. Again due to symmetry, it is enough to argue (v_{i+2}, u_{j+2}) exists. Assume not. Counting blue-red and red-blue paths between v_{i+1} and u_{j+2} we see that the edge (v_i, u_{j+2}) must exist. Similarly the edge (u_j, v_{i+2}) exists. Counting blue-red and red-blue paths between u_{j+1} and v_i we see that the edge (v_{i-1}, u_{j+1}) exists. A similar logic gives us the edge (v_{i+1}, u_{j-1}) . Continuing this way we get edges between v_{i-k} and v_{j+k} and v_{j+k+2} for $k = 1, 2, \dots$. For $k = 2n - 2$ we see that v_{i+2} is connected to u_{j+2} after all – a contradiction to our assumption. \square

Now it is easy to see that all edges of Δ consist of two such families as in Lemma 7.6: each family consisting of all $v_i u_{i \pm k}$ for fixed k . Furthermore, if one family has a plus sign and the other has a minus sign, we would have a double edge. Therefore both families have the same sign, which without loss of generality we can assume to be plus. Thus, there are two fixed choices k, k' of residues modulo $2n$ such that the edges of Δ are $v_i u_{i+k}$ and $v_i u_{i+k'}$ for all i . Such a bigraph is therefore listed in family #3.

7.4.2. *The case $\hat{A} * \hat{D}$.* Since the component Y of type \hat{D}_{n+2} has a vertex v with $\mathbf{v}_Y(v) = 2$, we cannot have a bigraph of type $\hat{A}_{2n-1} \xrightarrow{\cong} \hat{D}_n$. Thus the only two possibilities that we have are:

- $\hat{A}_{4n-1} \Leftrightarrow \hat{D}_{n+2}$, $n \geq 2$;
- $\hat{A}_{2n-1} \xrightarrow{\cong} \hat{D}_{2n+2}$, $n \geq 1$.

In the first case, the multisets of values tell us the following. If $n = 2k + 2$ is even for $k \geq 0$, one blue component will have $2n = 4k + 4$ ones and k twos and the other component will have $2n + 4$ ones and

$k + 1$ twos. Thus the second component must be of type \hat{D} which implies that $n = 0$, a contradiction. Now if $n = 2k + 1$ is odd for $k \geq 1$, each blue component has $2n + 2 = 4k + 4$ ones and k twos which is also impossible.

For the case $\hat{A}_{2n-1} \Leftarrow \hat{D}_{2n+2}$, one blue component has $2n$ twos while the other blue component has 4 ones and $2n - 1$ twos. Thus the first component must be of type \hat{A}_{2n-1} and the second component must be of type \hat{D}_{2n+2} so we get $\text{descr}(G) = \text{descr}(G^*)$.

Let v_1 and v_2 be two vertices with $\mathbf{v}_X(v_1) = \mathbf{v}_X(v_2) = 1$ adjacent to a vertex v_3 in X with $\mathbf{v}_X(v_3) = 2$. Label the vertices of Y as u_1 through u_{2n} . Let v_2 be connected to $u_1 \in Y$. Without loss of generality we can assume v_3 is connected to u_2 . Counting red-blue and blue-red paths between v_1 and u_2 we see that there are **two options**: v_1 is either connected to u_1 , or to u_3 .

Assume v_1 is connected to u_3 . Counting the red-blue and blue-red paths between v_1 and u_4 we see that v_3 has to be connected to u_4 . Counting the red-blue and blue-red paths between v_2 and u_{2n} we see that v_3 has to be connected to u_{2n} . By (4.2) applied to v_3 we see that this is impossible unless $u_{2n} = u_4$, that is, $n = 2$. In this case v_4 has to be connected to u_1 and u_3 and now we uniquely recover another exceptional bigraph listed as #39 in our classification.

Assume now v_1 is connected to u_1 . Counting red-blue and blue-red paths between v_3 and u_1 we see that there are **two options** to consider: either v_3 is connected by a double edge to u_2 , or it is connected by a single edge to u_2 and a single edge to u_{2n} .

In the **former** case, we get a component of type \hat{A}_1 so $n = 1$ and we get the bigraph #40.

Consider now the **latter** case. Counting red-blue and blue-red paths between v_3 and u_3 and u_{2n-1} we see that again there are **two options**: either $2n - 1 = 3$ and v_4 is connected to it by a double edge, or not, in which case v_4 is connected to both u_3 and u_{2n-1} . Continuing in this manner we arrive to the moment when v_{n+2} is connected to u_{n+1} by a double edge. Thus, the **option** of a double edge does get realized sooner or later, with the only choice of how soon it comes to be. But for $n > 1$ this contradicts the assumption that G^* is a double binding.

7.5. Affine \boxtimes affine double bindings involving only type \hat{D} .
By (4.4), we have the following two possibilities:

- $\hat{D}_{n+2} \Leftrightarrow \hat{D}_{n+2}$, $n \geq 2$;
- $\hat{D}_{n+2} \Leftarrow \hat{D}_{4n+2}$, $n \geq 2$.

Let us start with the **second case**. **Assume** that $n = 2k$ is even for some $k \geq 1$. Without loss of generality we may assume that

$$\begin{aligned} M(X_0) &= \{2, 2, 2, 2, \underbrace{4, \dots, 4}_{k-1}\}, & M(X_1) &= \{\underbrace{4, \dots, 4}_k\}; \\ M(Y_0) &= \{1, 1, 1, 1, \underbrace{2, \dots, 2}_{4k-1}\}, & M(Y_1) &= \{\underbrace{2, \dots, 2}_{4k}\}. \end{aligned}$$

We see that if $k > 1$ then there is no way to combine $M(X_0)$ with either $M(Y_0)$ or $M(Y_1)$ to get $M(\hat{\Lambda})$ in the union for any affine ADE Dynkin diagram $\hat{\Lambda}$. For $k = 1$, the blue components are necessarily $X_0 \cup Y_0$ of type \hat{D}_{10} and $X_1 \cup Y_1$ of type \hat{D}_4 so we get $\text{descr}(G) = \text{descr}(G^*) = \hat{D}_4 \Leftarrow \hat{D}_{10}$. We would like to show that such a double binding does not exist. Let v be the unique vertex of X of degree 4 and suppose that it is black. Then it is connected to all four white vertices of Y , and each of them satisfies $\mathbf{v}_Y(u) = 2$. By repeatedly counting red-blue and blue-red paths, we recover the dual of #31 with $\text{descr}(G^*) = \hat{D}_6 \Rightarrow \hat{D}_4 \Rightarrow \hat{A}_3$. In particular, G^* has three red components so is not a double binding.

Assume now that $n = 2k + 1$ is odd for some $k \geq 1$. Then without loss of generality we get that

$$\begin{aligned} M(X_0) &= \{2, 2, \underbrace{4, \dots, 4}_k\}, & M(X_1) &= \{2, 2, \underbrace{4, \dots, 4}_k\}; \\ M(Y_0) &= \{1, 1, 1, 1, \underbrace{2, \dots, 2}_{4k+1}\}, & M(Y_1) &= \{\underbrace{2, \dots, 2}_{4k+2}\}. \end{aligned}$$

We see that there is no way to combine $M(Y_0)$ with either $M(X_0)$ or $M(X_1)$ to get $M(\hat{\Lambda})$ because if $1, 4 \in M(\hat{\Lambda})$ then we must also have $3 \in M(\hat{\Lambda})$.

For the **first case**, both blue components have to also have type \hat{D}_{n+2} so we get

$$\text{descr}(G) = \text{descr}(G^*) = \hat{D}_{n+2} \Leftrightarrow \hat{D}_{n+2}.$$

First, **assume** $n = 2$. Since the blue components are two copies of \hat{D}_4 , the unique way to get them is to connect the vertex of X of red degree 4 to all the leaves of Y and vice versa. We obtain a twist $\hat{D}_4 \times \hat{D}_4$.

Suppose now that $n \geq 3$. We would like to show that in this case we get family #19 or #2, i.e., $G = \hat{D}_{n+2} \rtimes_p \hat{D}_{n+2}$ for some $p \in [n - 1]$. Recall that the bigraphs $\hat{D}_{n+2} \rtimes_p \hat{D}_{n+2}$ and $\hat{D}_{n+2} \rtimes_{n-p} \hat{D}_{n+2}$ are isomorphic and $\hat{D}_{n+2} \rtimes_1 \hat{D}_{n+2}$ is isomorphic to the twist $\hat{D}_{n+2} \times \hat{D}_{n+2}$.

Let us label the vertices of X and Y as in Section 5.4. Thus the vertices of X are labeled by

$$u_0^+, u_0^-, u_1, u_2, \dots, u_{n-1}, u_n^+, u_n^-$$

so that the leaves u_0^+ and u_0^- are connected to u_1 and the leaves u_n^+ and u_n^- are connected to u_{n-1} . Similarly, the vertices of Y are labeled in a similar way by

$$v_0^+, v_0^-, v_1, v_2, \dots, v_{n-1}, v_n^+, v_n^-.$$

Since we know that the blue components have type \hat{D}_{n+2} , we get that the leaves of X are not connected to the leaves of Y by blue edges. Without loss of generality we can assume that u_0^+ is connected to some v_p , where $p \in [n-1]$. Counting red-blue and blue-red paths we see that u_1 is connected to a neighbor v' of v_p . Counting red-blue and blue-red paths between u_0^- and v' , we get **cases**: u_0^- has to be connected to either v_p or to another neighbor v'' of v' .

Consider the case when u_0^- is connected to v'' . Since u_0^- is a leaf of X , v'' cannot be a leaf of Y . Moreover, v' has two different neighbors v_p and v'' so it also cannot be a leaf of Y . Without loss of generality we can therefore assume that $p \leq n-3$, $v' = v_{p+1}$ and $v'' = v_{p+2}$. Hence there exists a path of length 5 in Y of the form $(v_{p-1}^{(+)}, v_p, v_{p+1}, v_{p+2}, v_{p+3}^{(+)})$, where $v_i^{(+)}$ is equal to v_i if $i \neq 0, n$ and to v_i^+ if $i = 0$ or $i = n$. Counting red-blue and blue-red paths between $v_{p-1}^{(+)}$ and u_0^+ we get that $v_{p-1}^{(+)}$ is connected to u_1 . Counting red-blue and blue-red paths between $v_{p+3}^{(+)}$ and u_0^- we get that $v_{p+3}^{(+)}$ is connected to u_1 as well. This contradicts (4.3) for u_1 .

Thus u_0^- is connected to v_p as well as u_0^+ . Since v_p is connected to a leaf u_0^+ by a blue edge, every red neighbor of v_p must be connected to u_1 . Thus u_1 is connected to $v_{p-1}^{(+)}$. **Then either** $p-1 = 0$ or $p-1 > 0$. **Similarly either** $p+1 = n$ or $p+1 < n$. **Assume** that $1 < p < n-1$. Note that v_p cannot be connected to u_2 since counting red-blue and blue-red paths between v_p and u_1 we would arrive at a contradiction. Then counting red-blue and blue-red paths between u_2 and v_{p-1}, v_{p+1} we conclude that $v_{p-2}^{(+)}$ and $v_{p+2}^{(+)}$ exist and are connected to u_2 . Again, **either** $p-2 = 0$ or $p-2 > 0$, and **either** $p+2 = n$ or $p+2 < n$. Also, again, $v_{p\pm 1}$ are not connected to u_3 , since otherwise we get a contradiction by counting red-blue and blue-red paths between $v_{p\pm 1}$ and u_2 , etc. Continuing this way we get u_i to be connected to $v_{p\pm i}$ for $i = 0, 1, \dots$.

Eventually we arrive at a situation when without loss of generality $p-i = 0$, that is, $i = p$. Thus, v_0^+ is connected to u_p , and so is v_{2p} . Counting red-blue and blue-red paths between v_0^+ and u_{p+1} we conclude that v_1 is connected to u_{p+1} . Counting red-blue and blue-red paths between v_0^- and u_{p+1} we conclude that v_0^- is connected to either

u_{p+2} or to u_p . The former case as before leads to a contradiction. In the latter case we proceed as before, with u -s and v -s swapped, concluding the existence of edges between v_j and $u_{p\pm j}$ for $1 \leq j \leq p$.

Counting blue-red and red-blue paths between u_{p+1} and v_{2p} , and taking into account that the edge (v_{2p-1}, u_{p+1}) does not exist in Δ since (v_{2p-2}, u_p) does not, we conclude that u_{p+1} is connected to v_{2p+1} , etc. Continuing in this manner we get edges connecting u_{p+j} to $v_{2p+j}^{(+)}$, and also edges connecting v_{p+j} to $u_{2p+j}^{(+)}$ for $1 \leq j \leq n - 2p$. Finally, in a symmetric way to the previous argument we obtain edges connecting u_{n-2p+j} to v_{n-j} , and also edges connecting v_{n-2p+j} to u_{n-j} for $1 \leq j \leq p$.

As a result we obtain precisely the pseudo twist $\hat{D}_{n+2} \times_p \hat{D}_{n+2}$. \square

8. TWISTS

In this section, we concentrate on the case when the bigraph $G = (\Gamma, \Delta)$ is a *twist* $\hat{\Lambda} \times \hat{\Lambda}$ for some affine *ADE* Dynkin diagram $\hat{\Lambda}$. First, we introduce a certain game one can play on any undirected graph that very much resembles the Kostant's *find the highest root game* which is due to Allen Knutson. We deduce a positivity result for this game from the theory of Kac-Moody algebras [21]. We then give a general construction of a twist for any quiver in Section 8.2. We prove a factorization theorem for any such twist in Section 8.3 thus directly generalizing [28, Proposition 2.4] where this was done for the *del Pezzo 3 quiver* which can be seen as a twist of a triangle with itself as we explain in Section 8.2. Finally, in Section 8.4 we apply these results to the case $\hat{\Lambda} \times \hat{\Lambda}$ where $\hat{\Lambda}$ is an affine *ADE* Dynkin diagram and deduce Conjecture 1.7 for such twists as a special case.

8.1. Reflections on undirected graphs. Let $G = (I, E)$ be a connected undirected graph with possibly multiple edges but no loops. We denote by $V = \{h : I \rightarrow \mathbb{R}\}$ the vector space of all functions from I to \mathbb{R} and for each $i \in I$, denote by $\alpha_i : I \rightarrow \mathbb{R}$ the i -th basis vector defined by $\alpha_i(j) = \delta_{ij}$.

Suppose that G has one distinguished vertex $\mathfrak{b} \in V$. For every vertex $i \in I$, we define two *reflections* $s_i, s_i^{(\mathfrak{b})} : V \rightarrow V$ as follows. Given a vector $h \in V$, put

$$(s_i h)(j) = \begin{cases} h(j), & \text{if } i \neq j; \\ -h(j) + \sum_{(j,k) \in E} h(k), & \text{if } i = j; \end{cases} \quad s_i^{(\mathfrak{b})} h = \begin{cases} s_i h, & \text{if } i \neq \mathfrak{b}; \\ s_i h + \alpha_{\mathfrak{b}}, & \text{if } i = \mathfrak{b}. \end{cases}$$

h	a	b	c	d
$s_2(h)$	a	$a + c - b$	c	d
$s_3 s_2(h)$	a	$a + c - b$	$a + d - b$	d
$s_2 s_3 s_2(h)$	a	$a + d - c$	$a + d - b$	d
h	a	b	c	d
$s_2^{(b)}(h)$	a	$a + c - b + 1$	c	d
$s_3^{(b)} s_2^{(b)}(h)$	a	$a + c - b + 1$	$a + d - b + 1$	d
$s_2^{(b)} s_3^{(b)} s_2^{(b)}(h)$	a	$a + d - c + 1$	$a + d - b + 1$	d

TABLE 1. An example of applying the operators s_i and $s_i^{(b)}$.

Example 8.1. Let $I = \{1, 2, 3, 4\}$ and let G be an undirected path with edges $E = \{(1, 2), (2, 3), (3, 4)\}$. Thus V can be identified with \mathbb{R}^4 . Let $\mathbf{b} = 2$ be the distinguished vertex. Suppose that $h = (a, b, c, d) \in V$, thus for example $h(2) = b$. The values of $s_2(h)$, $s_3 s_2(h)$, $s_2 s_3 s_2(h)$, as well as of $s_2^{(b)}(h)$, $s_3^{(b)} s_2^{(b)}(h)$, and $s_2^{(b)} s_3^{(b)} s_2^{(b)}(h)$ are given in Table 1.

For an element $h \in V$, we write $h \geq 0$ if for any $i \in I$, $h(i) \geq 0$. The rest of this section will be concentrated on showing the following result:

Proposition 8.2. *For any sequence $\mathbf{i} = (i_1, i_2, \dots, i_p)$ of vertices of G , we have*

$$(8.1) \quad s_{i_p}^{(b)} s_{i_{p-1}}^{(b)} \cdots s_{i_1}^{(b)}(0) \geq 0.$$

Proof. First, one easily checks (for example, using Table 1) that if the vertices i and j are connected by exactly one edge (resp., zero edges) in G , we have $(s_i^{(b)} s_j^{(b)})^{m_{ij}} = \text{id}$ for $m_{ij} = 3$ (resp., $m_{ij} = 2$). Thus the operators $s_i^{(b)}$ define a representation of the *Weyl group W of the Kac-Moody algebra* associated to the *generalized Cartan matrix* $A_G = (a_{ij})_{i,j \in I}$ of G defined by

$$(8.2) \quad a_{ij} = \begin{cases} 2, & \text{if } i = j; \\ -q_{ij}, & \text{otherwise,} \end{cases}$$

where q_{ij} is the number of edges in G connecting i to j . This follows from [21, Proposition 3.13]. Thus we may assume that the word \mathbf{i} is *reduced*, that is, the element $s_{i_p} s_{i_{p-1}} \cdots s_{i_1}$ cannot be represented as a product of less than p elements in W .

We prove (8.1) by induction on p . The case $p = 0$ is trivial so suppose that $p > 0$.

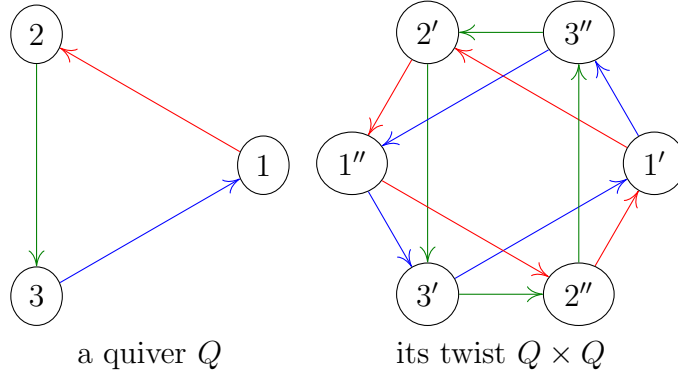


FIGURE 29. The del Pezzo 3 quiver is a twist.

Since $s_i(0) = 0$ for all $i \in I$, we may assume that $i_1 = \mathbf{b}$. One easily checks that in this case,

$$s_{i_p}^{(\mathbf{b})} s_{i_{p-1}}^{(\mathbf{b})} \cdots s_{i_1}^{(\mathbf{b})}(0) = s_{i_p}^{(\mathbf{b})} s_{i_{p-1}}^{(\mathbf{b})} \cdots s_{i_2}^{(\mathbf{b})}(0) + s_{i_p} s_{i_{p-1}} \cdots s_{i_2}(\alpha_{\mathbf{b}}).$$

This is true because for any $i \in I$ and $h_1, h_2 \in V$, we have

$$(8.3) \quad s_i^{(\mathbf{b})}(h_1 + h_2) = s_i(h_1) + s_i^{(\mathbf{b})}(h_2).$$

Since \mathbf{i} was reduced, the same is true for $\mathbf{i}' = (i_2, \dots, i_p)$, and thus the positivity of the first summand follows by induction. The positivity of the second summand is an immediate application of [21, Lemma 3.11(a)]. \square

8.2. Twists for arbitrary quivers. Let Q be a quiver, and let $I := \text{Vert}(Q)$ be the set of its vertices. Let G be the underlying undirected graph for Q with the same set I of vertices. We let $I' = \{i' \mid i \in I\}$ and $I'' = \{i'' \mid i \in I\}$. We are going to construct a new quiver $Q \times Q$ with vertex set $\text{Vert}(Q \times Q) = I' \cup I''$. For every edge $i \rightarrow j$ of Q , the quiver $Q \times Q$ contains edges

$$i' \rightarrow j', \quad i'' \rightarrow j'', \quad j'' \rightarrow i', \quad j' \rightarrow i''.$$

For example, when Q is a cycle with edges $1 \rightarrow 2 \rightarrow 3 \rightarrow 1$ then $Q \times Q$ is the well studied del Pezzo 3 quiver, see Figure 29.

For each $i \in I$, we define a new quiver $\tau_i(Q \times Q)$ to be $\sigma_i \circ \mu_{i'} \circ \mu_{i''}(Q \times Q)$, where $\mu_{i'}$ is the usual quiver mutation (see Definition 2.14) and σ_i is the operation that swaps the vertices i' and i'' in the quiver. We introduced this operation in [12], however, for the del Pezzo 3 quiver it already appeared in [28] under the name τ -mutation.

Lemma 8.3. *We have $\tau_i(Q \times Q) = Q \times Q$.*

Proof. Suppose that $u \rightarrow i' \rightarrow w$ is a path of length 2 in $Q \times Q$. We then therefore have a path $w \rightarrow i'' \rightarrow u$ of length 2 as well. The mutation $\mu_{i'}$ introduces an edge $u \rightarrow w$, but then the mutation $\mu_{i''}$ introduces an edge $w \rightarrow u$ so these edges cancel each other out.

For any edge $u \rightarrow i'$, there is an edge $i'' \rightarrow u$ so reversing both of these edges and swapping the vertices i' and i'' preserves both of these edges. We get that any edge of $Q \times Q$ is preserved by τ_i and no new edges are introduced. We are done with the proof. \square

Corollary 8.4. *If G is bipartite then Q is a bipartite recurrent quiver.*

For each $i \in I$, we introduce two variables x'_i and x''_i corresponding to the vertices i' and i'' of Q respectively, and thus the set of vertex variables for $Q \times Q$ is $\mathbf{x}' \cup \mathbf{x}''$ where $\mathbf{x}' = \{x'_i\}_{i \in I}$ and $\mathbf{x}'' = \{x''_i\}_{i \in I}$.

Consider a map $T : \text{Vert}(Q \times Q) \rightarrow \mathbb{Z}[(\mathbf{x}')^{\pm 1}, (\mathbf{x}'')^{\pm 1}]$ assigning a Laurent polynomial to each vertex of $Q \times Q$. The operation τ_i for $i \in I$ can be lifted to an operation on such maps T . More specifically, it is defined as follows: for $j \neq i \in I$, we set

$$(\tau_i T)(j') = T(j'), \quad (\tau_i T)(j'') = T(j'').$$

For the remaining two vertices, we put

$$(8.4) \quad \begin{aligned} (\tau_i T)(i') &= \frac{\prod_{u \rightarrow i''} T(u) + \prod_{i'' \rightarrow v} T(v)}{T(i'')}, \\ (\tau_i T)(i'') &= \frac{\prod_{u \rightarrow i'} T(u) + \prod_{i' \rightarrow v} T(v)}{T(i')}. \end{aligned}$$

Here $u, v \in I' \cup I''$ are the vertices of $Q \times Q$. Thus the operation τ_i can be viewed as a composition of two quiver mutations $\tau_{i'} \circ \tau_{i''}$ followed by swapping the values of T at i' and i'' .

8.3. A product formula for any τ -mutation sequence. We let $T_0 : \text{Vert}(G) \rightarrow \mathbb{Z}[\mathbf{x}', \mathbf{x}'']$ be the *initial seed*, that is, $T_0(i') = x'_i$ and $T_0(i'') = x''_i$ for all $i \in I$. Consider a sequence $\mathbf{i} = (i_1, i_2, \dots, i_p)$ of elements of I and let

$$(8.5) \quad T_1 = \tau_{i_1} T_0, \quad T_2 = \tau_{i_2} T_1, \quad \dots, \quad T_p = \tau_{i_p} T_{p-1}.$$

We are interested in giving a formula for $T_p(j)$ for any $j \in I$. For each $i \in I$, define $X_i \in \mathbb{Z}[(\mathbf{x}')^{\pm 1}, (\mathbf{x}'')^{\pm 1}]$ by

$$(8.6) \quad X_i = \frac{\prod_{j \rightarrow i} x'_j \prod_{i \rightarrow j} x''_j + \prod_{j \rightarrow i} x''_j \prod_{i \rightarrow j} x'_j}{x'_i x''_i}.$$

Just as in Section 8.1, we define the operators $s_i^{(j)}$ for each $i, j \in I$ to be the reflections $s_i^{(\mathbf{b})}$ for G with $\mathbf{b} = j$.

Proposition 8.5. *Let $\mathbf{i} = (i_1, i_2, \dots, i_p)$ and T_0, T_1, \dots, T_p be as in (8.5). Then there exists a matrix $A(\mathbf{i}) = (a_{ij}^{\mathbf{i}})_{i,j \in I}$ with nonnegative integer entries such that for any $i \in I$ we have*

$$(8.7) \quad T_p(i') = x'_i \prod_{j \in I} X_j^{a_{ij}^{\mathbf{i}}}; \quad T_p(i'') = x''_i \prod_{j \in I} X_j^{a_{ij}^{\mathbf{i}}}.$$

The j -th column $(a_{ij}^{\mathbf{i}})_{i \in I}$ of $A(\mathbf{i})$ is equal to

$$(8.8) \quad s_{i_p}^{(j)} s_{i_{p-1}}^{(j)} \cdots s_{i_1}^{(j)}(0).$$

Proof. We prove (8.7) and (8.8) by induction on p , the case $p = 0$ being trivial. Suppose that we already know the result for $p - 1$. The induction step is straightforward to check by substituting (8.6) into (8.4). The nonnegativity of the coefficients of $A(\mathbf{i})$ follows from Proposition 8.2 □

Corollary 8.6. *If Q is an orientation of a finite (resp., affine) ADE Dynkin diagram Λ (resp., $\hat{\Lambda}$) then the operators τ_i define a simply transitive action of the Weyl group W (resp., the affine Weyl group W_a) of Λ (resp., $\hat{\Lambda}$) on the clusters that can be obtained from the initial seed T_0 by applying τ -mutations. In particular, such clusters are in bijection with Weyl chambers of W (resp., with alcoves of W_a).*

Proof. This follows immediately from Proposition 8.5. We refer the reader to [3, Chapter V, §4] for the background on alcoves and Weyl chambers. □

8.4. Twists of ADE Dynkin diagrams. In this section, we return to the case when Q is a finite or affine ADE Dynkin diagram with every edge oriented towards a white vertex (see Definition 5.1). Let $I = \{0, 1, 2, \dots, n\}$ be the set of its vertices and suppose that the vertices $0, 1, 2, \dots, k - 1$ are white while the vertices k, \dots, n are black. We would like to apply the product formula (8.7) to the T -system associated with $Q \times Q$. Proposition 8.5 implies that we only need to analyze the left hand side of (8.1) for the specific mutation sequence $\mathbf{i} = (0, 1, 2, \dots, n, 0, 1, 2, \dots)$. Let us choose some distinguished vertex, say, $\mathbf{b} = 0$. Let V be a vector space with basis $\alpha_0, \alpha_1, \dots, \alpha_n$ as in Section 8.1 and a bilinear form B associated to the generalized Cartan matrix A_G of G from (8.2). In particular, for $h_1, h_2 \in V$, we have

$$B(h_1, h_2) = \langle h_1, h_2 \rangle := h_1^T A_G h_2.$$

Thus it is well known (see e.g. [38, Section 2.17]) that B is positive definite (resp., nonnegative definite) if and only if Q is an orientation

of a finite (resp., affine) *ADE* Dynkin diagram. The reflections s_i can be alternatively defined by

$$s_i(h) = h - \langle h, \alpha_i \rangle \alpha_i$$

for $i \in I$. Define the *Coxeter transformation* \mathbf{C} by

$$\mathbf{C} = \omega_2 \omega_1, \quad \text{where} \quad \omega_1 = s_{k-1} s_{k-2} \dots s_0, \quad \omega_2 = s_n s_{n-1} \dots s_k.$$

Let (h_0, h_1, \dots) be the sequence of elements of V associated with $\mathbf{i} = (0, 1, 2, \dots, n, 0, 1, 2, \dots)$ in the left hand side of (8.1). In other words, $h_0 = 0$ is the origin and $h_{k+1} = s_{i_k}^{(b)} h_k$ for $k \geq 0$. Here $i_k \in I$ is defined by $i_k \equiv k \pmod{n} + 1$ so that $\mathbf{i} = (i_0, i_1, \dots)$. The following lemma follows immediately from (8.3):

Lemma 8.7. *For any integer $m \geq 0$, we have*

$$(8.9) \quad h_{m(n+1)} = \mathbf{C}(h_{mn} + \alpha_0) = \sum_{k=1}^m \mathbf{C}^k \alpha_0.$$

Since the whole calculation amounts to computing the powers of the Coxeter transformation, it would be nice to find its Jordan normal form J which is actually well studied:

Proposition 8.8 ([38, Theorems 3.15 and 4.1]).

- (1) *If Q is an orientation of a finite *ADE* Dynkin diagram then J is diagonal and \mathbf{C} is periodic, and the eigenvalues of J are roots of unity not equal to 1;*
- (2) *If Q is an orientation of an affine *ADE* Dynkin diagram then J has one 2×2 block corresponding to the eigenvalue 1, the rest of its blocks are 1×1 and all the other eigenvalues of \mathbf{C} are roots of unity not equal to 1;*
- (3) *otherwise there is a simple maximal eigenvalue of \mathbf{C} that is greater than one.*

Theorem 8.9. *Let Q be a bipartite quiver.*

- (1) *If Q is an orientation of a finite *ADE* Dynkin diagram then the T -system associated with $Q \times Q$ is periodic;*
- (2) *If Q is an orientation of an affine *ADE* Dynkin diagram then the T -system associated with $Q \times Q$ grows quadratic exponentially;*
- (3) *otherwise the T -system associated with $Q \times Q$ grows doubly exponentially.*

Proof. Note that the first part follows from [12] while the third part follows from Theorem 1.5. However, it is easy to prove all the parts directly using (8.9) and Propositions 8.8 and 8.5. Let $\mathbf{C} = P^{-1}JP$ be

the Jordan normal form of \mathbf{C} and consider the vector $P\alpha_0$. Suppose that Q is an orientation of a finite ADE Dynkin diagram Λ . Then \mathbf{C} is periodic with some period h (the *Coxeter number*) so the sum of \mathbf{C}^k over the period will be zero. Indeed, the matrix J is diagonal and by Proposition 8.8, its entries are roots of unity that are not equal to 1. Thus the sequence h_k is periodic, and by Proposition 8.5, this sequence describes the degrees of the factors X_i in the values of the T -system associated with $Q \times Q$. This proves the first claim.

Suppose now that Q is an orientation of an affine ADE Dynkin diagram. Then the unique 2×2 block of J^k will have the form

$$\begin{pmatrix} 1 & k \\ 0 & 1 \end{pmatrix}.$$

Since all the other 1×1 blocks correspond to roots of unity that are not equal to 1, the corresponding entries of $J^1 + J^2 + \dots + J^m$ will be bounded while the unique 2×2 block of $J^1 + J^2 + \dots + J^m$ will have the form

$$\begin{pmatrix} m & \binom{m+1}{2} \\ 0 & m \end{pmatrix}.$$

This shows that the sequence $h_{m(n+1)}$ grows quadratically and thus the values of the T -system associated with $Q \times Q$ grow quadratic exponentially⁶ and we are done with the second claim.

Finally, suppose that the underlying graph G of Q is not a finite or affine ADE Dynkin diagram. Then there is a simple maximum eigenvalue λ in J and therefore we will have λ^k in J^k dominating all the other terms. Thus the sequence $h_{m(n+1)}$ grows exponentially which implies that the values of the T -system associated with $Q \times Q$ grow doubly exponentially and we are done with the third claim. \square

9. CONJECTURES

In addition to the main Conjecture 1.7 we make several other conjectures describing the behavior of T -systems in our affine \boxtimes affine classification. We prove some of them for twists.

9.1. Arnold-Liouville integrability. In this paper we worked with zero algebraic entropy, which is one of the ways to define integrability. An alternative way is to look for the *Arnold-Liouville integrability*, which means finding a non-degenerate Poisson bracket, and a number

⁶it may happen that even though some entries of J grow fast, the vector $P^{-1}JP\alpha_0$ is bounded. But then we can relabel the vertices and choose some other vertex \mathfrak{b} for which the growth will be quadratic exponential.

of algebraically independent conserved quantities in involution with respect to this Poisson bracket. We refer the reader to [1] for a classical account.

Conjecture 9.1. *Y*-systems associated with all the affine \boxtimes affine *ADE* bigraphs in our classification are integrable in Arnold-Liouville sense.

This conjecture has already been verified in the special case of our $\mathcal{T}(\hat{A}_{rd-1}, \exp(2\pi ip/r), n)$ family #3. Specifically, it is a special case of a theorem of Goncharov and Kenyon [17, Theorem 3.7]. It is also present in Ovsienko-Schwartz-Tabachnikov [33, Theorem 2] and Gekhtman-Shapiro-Tabachnikov-Vainshtein [14, Theorem 4.4]. The latter two sources prove it in a somewhat narrower generality than our family #3, however their methods extend easily to cover the whole family.

Note that all three of the above sources prove Arnold-Liouville integrability for the *Y*-variable dynamics. It remains to be understood if a similar claim can be made about the *T*-systems in our classification.

9.2. Devron property. Glick has introduced the *Devron property* in [15] as a counterpart to *singularity confinement*, often used to detect integrability. Roughly speaking, Devron property is a property of systems where time flow is reversible. Assume that going backward in time one fails due to a really bad singular behavior, i.e. a Devron singularity. Then the system has Devron property if this implies similar failure after a number of steps when going forward in time.

For a *T*-system associated with an affine \boxtimes affine *ADE* bigraph from our classification, let us say that the initial values $T_v(t)$ for $t = 0, 1$ form a *backward Devron singularity* if for any v of color $\epsilon_v = 1$ we have $T_v(-1) = 0$. Let us say that for some time t_0 , the values of the *T*-system form a *forward Devron singularity* if for any v of color $\epsilon_v \not\equiv t_0 \pmod{2}$ we have $T_v(t_0 + 1) = 0$.

Conjecture 9.2. If the initial values of a *T*-system associated with an affine \boxtimes affine *ADE* bigraph from our classification form a backward Devron singularity, then after a finite number of steps t_0 , the *T*-system will reach a state that forms a forward Devron singularity.

We prove this conjecture for twists of arbitrary bipartite quivers.

Proposition 9.3. *Let Q be any bipartite quiver. Then the twist $Q \times Q$ has the Devron property with $t_0 = 2$.*

Proof. This follows immediately from Proposition 8.5. Indeed, having a backward Devron singularity at $t = 0$ means that $X_v = 0$ for any

$v \in \text{Vert}(Q)$ with $\epsilon_v = 1$. Since X_v appears in $T_v(3)$ with exponent equal to 1 by Proposition 8.5, we are done. \square

For the case when Q is a tensor product of type $\hat{A}_{2n-1} \otimes \hat{A}_{2m-1}$, our limited computer evidence suggests that we have

$$t_0 \in \{\max(2n, 2m), 2 \max(2n, 2m)\},$$

depending on the parity of n and m .

9.3. Time-dependent conserved quantities. A notion of time dependent conserved quantities is sometimes used when analysing integrability of dynamical systems, see [18] for an accessible introduction. Let $A(t)$ be a function of the system parameters evaluated at time t . We say that A is a *time-dependent conserved quantity* if there exist integers $m, t_0 \geq 1$ such that for any $t \in \mathbb{Z}$, we have $A(t + t_0) = A(t)B^m$, where $B = B(t)$ is a fixed genuine conserved quantity of the system, that is, $B(t + t_0) = B(t)$ for all $t \in \mathbb{Z}$.

Conjecture 9.4. The T -systems associated with affine \boxtimes affine ADE bigraphs from our classification possess non-trivial time-dependent conserved quantities.

We again prove this conjecture for twists, but now only of affine ADE Dynkin diagrams. In order to state the result, we need to associate one more integer $h_a(\hat{\Lambda})$ to each affine ADE Dynkin diagram $\hat{\Lambda}$ which is called the *affine Coxeter number* in [38], not to be confused with the McKay number $h^{(2)}(\hat{\Lambda})$ of $\hat{\Lambda}$ from Figure 3.

Definition 9.5. The *affine Coxeter number* of an affine ADE Dynkin diagram $\hat{\Lambda}$ is the smallest positive integer $m = h_a(\hat{\Lambda})$ such that $\lambda^m = 1$ for any eigenvalue λ of the Coxeter transformation associated to $\hat{\Lambda}$. The values of $h_a(\hat{\Lambda})$ are given in [38, Table 4.1]. Moreover, define the *Coxeter-McKay ratio* $g(\hat{\Lambda})$ by

$$g(\hat{\Lambda}) = \frac{4h_a(\hat{\Lambda})}{h^{(2)}(\hat{\Lambda})}.$$

The values of $h_a(\hat{\Lambda})$ and $g(\hat{\Lambda})$ are given in Table 2. In particular, $g(\hat{\Lambda})$ is always equal to either 1 or 2.

The Coxeter-McKay ratio is closely related to the *Dlab-Ringel defect*, see [5] or [38, Section 6.3.3].

Proposition 9.6. *Let $\hat{\Lambda}$ be an affine ADE Dynkin diagram with vertex set I , edge set E , additive function $\lambda : I \rightarrow \mathbb{Z}$, and affine Coxeter number $m = h_a(\hat{\Lambda})$. Consider the twist $\hat{\Lambda} \times \hat{\Lambda}$ with vertex set $I' \cup I''$.*

$\hat{\Lambda}$	\hat{A}_{2n-1}	$\hat{D}_n, n \text{ even}$	$\hat{D}_n, n \text{ odd}$	\hat{E}_6	\hat{E}_7	\hat{E}_8
$h_a(\hat{\Lambda})$	n	$n - 2$	$2(n - 2)$	6	12	30
$g(\hat{\Lambda})$	2	1	2	1	1	1

TABLE 2. The affine Coxeter number and the Coxeter-McKay ratio for affine ADE Dynkin diagrams.

Then for each vertex $i \in I$, there is a time-dependent conserved quantity $A_i(t)$ defined as follows: for $t \equiv \epsilon_i \pmod{2}$, we put

$$A_i(t) = \frac{T_{i'}(t)^2}{\prod_{(i,j) \in \hat{\Lambda}} T_{j'}(t-1)}.$$

These functions satisfy

$$(9.1) \quad A_i(t+2m) = A_i(t) B^{g(\hat{\Lambda})\lambda(i)},$$

where $B = B(t)$ is defined as follows. For t even, we put

$$B(t) = \prod_j X_j^{\lambda(j)}(t - \epsilon_j).$$

For odd t , one replaces ϵ_j by $1 - \epsilon_j$. Here $X_j(t)$ is defined analogously to (8.6), namely,

$$X_j(t) = \frac{\prod_{k \rightarrow j} T_{k'}(t) \prod_{j \rightarrow k} T_{k''}(t) + \prod_{k \rightarrow j} T_{k''}(t) \prod_{j \rightarrow k} T_{k'}(t)}{T_{j'}(t-1) T_{j''}(t-1)}.$$

The function $B(t)$ is a genuine conserved quantity: $B(t+m) = B(t)$ for all $t \in \mathbb{Z}$.

Proof. Let us fix some $j \in I$ with say $\epsilon_j = 0$ and look at the exponent $a_{i,j}^t$ of $X_j = X_j(0)$ from (8.6) in $T_i(t)$. By Lemma 8.7, this value equals to the i -th coordinate of

$$\delta_j(t) = \sum_{k=1}^t \mathbf{C}^k \alpha_j.$$

Now, the degree of X_j in $A_i(t)$ is therefore the value of $\langle \alpha_i, \delta_j(t) \rangle$. We would like to show (9.1), and the exponent of X_j in $A_i(t+m)/A_i(t)$ is given by $\langle \alpha_i, \delta_j(t+m) - \delta_j(t) \rangle$. Note that

$$\delta_j(t+m) - \delta_j(t) = \mathbf{C}^t \left(\sum_{k=1}^m \mathbf{C}^k \alpha_j \right).$$

From Proposition 8.8 it follows that the right hand side, written in the Jordan basis for \mathbf{C} , has nonzero coordinates corresponding only to the two eigenvectors of \mathbf{C} associated to the 2×2 Jordan block. One of

these vectors is exactly λ and $\langle \alpha_i, \lambda \rangle = 0$. The other vector ν satisfies $\mathbf{C}\nu = \nu + \lambda$ so its coefficient in $\delta_j(t+m) - \delta_j(t)$ is independent of t and is equal to mc_j , where c_j is the coefficient of ν in the expansion of α_j in the Jordan basis of \mathbf{C} . Let us calculate c_j explicitly. The vector ν is orthogonal to the other Jordan basis vectors of \mathbf{C} with respect to the scalar product (\cdot, \cdot) defined by $(\alpha_i, \alpha_j) = \delta_{ij}$, see [38, (6.47)]. Thus c_j equals to $\frac{(\alpha_j, \nu)}{(\nu, \nu)}$. For any $k \in I$, we have $\nu(k) = \frac{1}{4}(-1)^{\epsilon_k} \lambda(k)$. Therefore $(\nu, \nu) = \frac{1}{16}h^{(2)}(\hat{\Lambda})$. On the other hand, (α_j, ν) is equal up to sign to $\frac{1}{4}\lambda(j)$. Thus c_j equals to $\frac{4\lambda(j)}{h^{(2)}(\hat{\Lambda})}$. Multiplying this by m shows that the coefficient of ν in $\delta_j(t+m) - \delta_j(t)$ equals $g(\hat{\Lambda})\lambda(j)$. It remains to note that up to sign we have $\langle \alpha_i, \nu \rangle = \lambda(i)$ which yields the result. \square

Note that for the $\mathcal{T}(\hat{A}_{rd-1}, \exp(2\pi ip/r), n)$ family #3 one can use the topology of the torus embedding of the quiver to define conserved quantities, as it was done in a slightly different language by Goncharov and Kenyon in [17]. In [13] we performed this construction in our language for cylindric rather than toric quivers, resulting in what we called *Goncharov-Kenyon Hamiltonians*. However, as evident from the definition, the task of finding time-dependent conserved quantities is strictly harder than that of finding conserved quantities: if one knows $A(t)$, one can find the associated function $B(t) = \left(\frac{A(t+t_0)}{A(t)}\right)^{1/m}$, but there is no simple way to go in the other direction. Thus, even for the T -systems from family #3 we do not know of a construction of time-dependent conserved quantities in general.

REFERENCES

- [1] V. Arnold. *Les méthodes mathématiques de la mécanique classique*. Éditions Mir, Moscow, 1976. Traduit du russe par Djilali Embarek.
- [2] M. P. Bellon and C.-M. Viallet. Algebraic entropy. *Comm. Math. Phys.*, 204(2):425–437, 1999.
- [3] Nicolas Bourbaki. *Lie groups and Lie algebras. Chapters 4–6*. Elements of Mathematics (Berlin). Springer-Verlag, Berlin, 2002. Translated from the 1968 French original by Andrew Pressley.
- [4] J. Diller and C. Favre. Dynamics of bimeromorphic maps of surfaces. *Amer. J. Math.*, 123(6):1135–1169, 2001.
- [5] Vlastimil Dlab and Claus Michael Ringel. Indecomposable representations of graphs and algebras. *Mem. Amer. Math. Soc.*, 6(173):v+57, 1976.
- [6] G. Falqui and C.-M. Viallet. Singularity, complexity, and quasi-integrability of rational mappings. *Comm. Math. Phys.*, 154(1):111–125, 1993.
- [7] Sergey Fomin and Andrei Zelevinsky. Cluster algebras. I. Foundations. *J. Amer. Math. Soc.*, 15(2):497–529 (electronic), 2002.

- [8] Sergey Fomin and Andrei Zelevinsky. Y -systems and generalized associahedra. *Ann. of Math. (2)*, 158(3):977–1018, 2003.
- [9] Allan P. Fordy and Andrew Hone. Discrete integrable systems and Poisson algebras from cluster maps. *Comm. Math. Phys.*, 325(2):527–584, 2014.
- [10] Edward Frenkel and Nicolai Reshetikhin. The q -characters of representations of quantum affine algebras and deformations of W -algebras. In *Recent developments in quantum affine algebras and related topics (Raleigh, NC, 1998)*, volume 248 of *Contemp. Math.*, pages 163–205. Amer. Math. Soc., Providence, RI, 1999.
- [11] Shmuel Friedland and John Milnor. Dynamical properties of plane polynomial automorphisms. *Ergodic Theory Dynam. Systems*, 9(1):67–99, 1989.
- [12] Pavel Galashin and Pavlo Pylyavskyy. The classification of Zamolodchikov periodic quivers. *Amer. J. Math.*, to appear. arXiv:1603.03942.
- [13] Pavel Galashin and Pavlo Pylyavskyy. Quivers with subadditive labelings: classification and integrability. *arXiv:1606.04878*, 2016.
- [14] Michael Gekhtman, Michael Shapiro, Serge Tabachnikov, and Alek Vainshtein. Integrable cluster dynamics of directed networks and pentagram maps. *Adv. Math.*, 300:390–450, 2016.
- [15] Max Glick. The Devron property. *J. Geom. Phys.*, 87:161–189, 2015.
- [16] F. Gliozzi and R. Tateo. Thermodynamic Bethe ansatz and three-fold triangulations. *Internat. J. Modern Phys. A*, 11(22):4051–4064, 1996.
- [17] Alexander B. Goncharov and Richard Kenyon. Dimers and cluster integrable systems. *Ann. Sci. Éc. Norm. Supér. (4)*, 46(5):747–813, 2013.
- [18] Alain Goriely. *Integrability and nonintegrability of dynamical systems*, volume 19 of *Advanced Series in Nonlinear Dynamics*. World Scientific Publishing Co., Inc., River Edge, NJ, 2001.
- [19] David Hernandez. Drinfeld coproduct, quantum fusion tensor category and applications. *Proc. Lond. Math. Soc. (3)*, 95(3):567–608, 2007.
- [20] Jarmo Hietarinta and Claude Viallet. Singularity confinement and chaos in discrete systems. *Phys. Rev. Lett.*, 81:325–328, Jul 1998.
- [21] Victor G. Kac. *Infinite-dimensional Lie algebras*. Cambridge University Press, Cambridge, third edition, 1990.
- [22] Bernhard Keller. The periodicity conjecture for pairs of Dynkin diagrams. *Ann. of Math. (2)*, 177(1):111–170, 2013.
- [23] A. N. Kirillov and N. Yu. Reshetikhin. Exact solution of the XXZ Heisenberg model of spin S . *Zap. Nauchn. Sem. Leningrad. Otdel. Mat. Inst. Steklov. (LOMI)*, 145(Voprosy Kvant. Teor. Polya i Statist. Fiz. 5):109–133, 191, 195, 1985.
- [24] Harold Knight. Spectra of tensor products of finite-dimensional representations of Yangians. *J. Algebra*, 174(1):187–196, 1995.
- [25] A. Kuniba and T. Nakanishi. Spectra in conformal field theories from the Rogers dilogarithm. *Modern Phys. Lett. A*, 7(37):3487–3494, 1992.
- [26] Atsuo Kuniba, Tomoki Nakanishi, and Junji Suzuki. Functional relations in solvable lattice models. I. Functional relations and representation theory. *Internat. J. Modern Phys. A*, 9(30):5215–5266, 1994.
- [27] Atsuo Kuniba, Tomoki Nakanishi, and Junji Suzuki. T -systems and Y -systems in integrable systems. *J. Phys. A*, 44(10):103001, 146, 2011.

- [28] Megan Leoni, Gregg Musiker, Seth Neel, and Paxton Turner. Aztec castles and the dp3 quiver. *Journal of Physics A: Mathematical and Theoretical*, 47(47):474011, 2014.
- [29] Takafumi Mase. Investigation into the role of the Laurent property in integrability. *J. Math. Phys.*, 57(2):022703, 21, 2016.
- [30] John McKay. Graphs, singularities, and finite groups. In *The Santa Cruz Conference on Finite Groups (Univ. California, Santa Cruz, Calif., 1979)*, volume 37 of *Proc. Sympos. Pure Math.*, pages 183–186. Amer. Math. Soc., Providence, R.I., 1980.
- [31] Hiraku Nakajima. t -analogues of q -characters of Kirillov-Reshetikhin modules of quantum affine algebras. *Represent. Theory*, 7:259–274 (electronic), 2003.
- [32] E. Ogievetsky and P. Wiegmann. Factorized S -matrix and the Bethe ansatz for simple Lie groups. *Phys. Lett. B*, 168(4):360–366, 1986.
- [33] Valentin Ovsienko, Richard Evan Schwartz, and Serge Tabachnikov. Liouville-Arnold integrability of the pentagram map on closed polygons. *Duke Math. J.*, 162(12):2149–2196, 2013.
- [34] Pavlo Pylyavskyy. Zamolodchikov integrability via rings of invariants. *Journal of Integrable Systems*, 1(1):xyw010, 2015.
- [35] F. Ravanini, A. Valleriani, and R. Tateo. Dynkin TBAs. *Internat. J. Modern Phys. A*, 8(10):1707–1727, 1993.
- [36] N. Yu. Reshetikhin. The spectrum of the transfer matrices connected with Kac-Moody algebras. *Lett. Math. Phys.*, 14(3):235–246, 1987.
- [37] David E. Speyer. Perfect matchings and the octahedron recurrence. *J. Algebraic Combin.*, 25(3):309–348, 2007.
- [38] R. Stekolshchik. *Notes on Coxeter transformations and the McKay correspondence*. Springer Monographs in Mathematics. Springer-Verlag, Berlin, 2008.
- [39] John R. Stembridge. Admissible W -graphs and commuting Cartan matrices. *Adv. in Appl. Math.*, 44(3):203–224, 2010.
- [40] András Szenes. Periodicity of Y -systems and flat connections. *Lett. Math. Phys.*, 89(3):217–230, 2009.
- [41] È. B. Vinberg. Discrete linear groups that are generated by reflections. *Izv. Akad. Nauk SSSR Ser. Mat.*, 35:1072–1112, 1971.
- [42] Alexandre Yu. Volkov. On the periodicity conjecture for Y -systems. *Comm. Math. Phys.*, 276(2):509–517, 2007.
- [43] Al. B. Zamolodchikov. On the thermodynamic Bethe ansatz equations for reflectionless ADE scattering theories. *Phys. Lett. B*, 253(3-4):391–394, 1991.

DEPARTMENT OF MATHEMATICS, MASSACHUSETTS INSTITUTE OF TECHNOLOGY, CAMBRIDGE, MA 02139, USA

E-mail address: galashin@mit.edu

DEPARTMENT OF MATHEMATICS, UNIVERSITY OF MINNESOTA, MINNEAPOLIS, MN 55414, USA

E-mail address: ppylyavs@umn.edu